PETER PAN, A NEW LINK BETWEEN RIBOSOME BIOGENESIS AND CELL CYCLE CONTROL

A Thesis Submitted for the Degree of Doctor of Natural Sciences
At the Faculty of Biology,
Ludwig-Maximilians-Universität München

Anastassia Malamoussi
Munich, 20 October 2008

Completed at the Helmholtz Centre Munich
Institute for Clinical Molecular Biology and Tumour Genetics

First Examiner: Prof. Dr. Dirk Eick

Second Examiner: PD Dr. Angelika Böttger

Date of the oral examination: 15.12.2008

Ehrenwörtliche Versicherung

Ich versichere hiermit ehrenwörtlich, dass die vorgelegte Dissertation von mir selbständig und ohne unerlaubte Hilfe angefertigt ist.

Erklärung

Hiermit erkläre ich, dass die Dissertation nicht ganz oder in wesentlichen Teilen einer anderen Prüfungskomission vorgelegt worden ist.
Ich erkläre weiterhin, dass ich mich nicht anderweitig einer Doktorprüfung ohne Erfolg unterzogen habe.

München, im Oktober 2008

Anastassia Malamoussi

Summary

The nucleolus is the nuclear compartment for ribosome biogenesis in eukaryotes. Inhibition of ribosome biogenesis induces the tumor suppressor p53 and inhibits cell cycle progression. In this thesis the molecular linkage between ribosome biogenesis and cell cycle control was studied.

Recent work identified the PeBoW complex, composed of Pes1, Bop1, and WDR12, as an essential factor for the processing of the ribosomal 28S RNA and cell cycle progression. To further elucidate the function of PeBoW in cell cycle control, its cellular interaction partners were investigated.

In this work Ppan was identified as PeBoW binding factor. Knock-down of Ppan affected cell proliferation and processing of the large ribosomal subunit RNA. The cellular interactions and localization of Ppan and Ppan deletion mutants in response to various kinds of stress were studied in detail. The σ70 and coil-coil domains in Ppan are required for nucleolar targeting, while the N-terminal domain of Ppan can be masked and unmasked, depending on the stress conditions. Strikingly, while most nucleolar factors translocate to the nucleoplasm or into so-called nucleolar caps under stress, Ppan remains in the nucleolar core, possibly involved in the maintenance of a basal nucleolar structure. Finally, with co-immunoprecipitation experiments and the Bimolecular Fluorescence Complementation assay (BiFC) the binding of Hdm2, a p53 specific ubiquitin ligase, to Ppan could be demonstrated. This observation links Ppan to p53-dependent cell cycle checkpoints.

Zusammenfassung

Der Nukleolus ist das nukleäre Kompartiment für die Ribosomenbiogenese in Eukaryonten. Die Inhibition der Ribosomenbiogenese aktiviert den Tumorsuppressor p53 und inhibiert die Zellzyklusprogression. In dieser Arbeit wurde der molekulare Zusammenhang zwischen Ribosomenbiogenese und Zellzykluskontrolle studiert.
Frühere Arbeiten identifizierten den PeBoW Komplex, bestehend aus den Proteinen Pes1, Bop1 und WDR12, als einen essentiellen Faktor für die Prozessierung der ribosomalen 28S rRNA und die Zellzyklusprogression. Die zellulären Interaktionspartner von PeBoW wurden herangezogen, um die Funktion des Komplexes in der Zellzykluskontrolle zu untersuchen.
In dieser Arbeit wurde Ppan als ein PeBoW Interaktionspartner identifiziert. Knock-down von Ppan wirkte sich auf die Zellzyklusproliferation, sowie die Prozessierung der RNA der großen ribosomalen Untereinheit aus. Die zellulären Interaktionen und Lokalisation von Ppan und Ppan Deletionsmutanten wurden als Antwort auf verschiedene Stresssituationen untersucht. Die σ70 und coil-coil Domänen in Ppan werden für die nukleoläre Lokalisation gebraucht, die N-terminale Domäne wird Stress-abhängig maskiert und demaskiert. Während die meisten nukleolären Faktoren nach Stress ins Nukleoplasma oder die so genannten nukleolären Caps delokalisieren, bleibt Ppan im nukleolären Zentrum und ist möglicherweise an der Erhaltung der nukleolären Struktur beteiligt. Mit Co-Immunopräzipitations-Experimenten und dem Bimolekularen Fluoreszenz Komplementationsassay (BiFC) konnte die Bindung von Hdm2, einer p53 spezifischen Ubiquitin-Ligase, an Ppan demonstriert werden. Diese Beobachtung verbindet Ppan mit p53-abhängigen Zellzyklus-Kontrollstellen.

Table of contents

Methods

List of abbreviations

A	adenine
α	(alpha) anti
aa	amino acids
ActD	actinomycin D
Arf	alternative reading frame
ATM	ataxia telangiectasia mutated
BiFC	bimolecular fluorescence complementation assay
Bop1	Block of proliferation 1
bp	base pairs
Brix	Biogenesis of ribosomes in *Xenopus*
C	cytosine
cDNA	complementary DNA
CMV	cytomegaly virus
Co-IP	co-immunoprecipitation
C-	carboxy-
DAPI	4,6-diamidino-2-phenylindole
DEPC	diethyl pyrocarbonate
DFC	dense fibrillar component
D. melanogaster	*Drosophila melanogaster*
DMSO	dimethyl sulfoxide
DNA	2'-deoxyribonucleic acid
DNAse I	deoxyribonuclease I
dnPes	dominant negative form of Pes1
dNTP	3'-deoxyribonucleoside-5'-triphosphate
DTT	dithiothreitol
E. coli	*Escherichia coli*
EDTA	ethylene diamine tetra-acetic acid
eGFP	enhanced green fluorescent protein
EGTA	ethylene glycol-bis(2-aminoethylether)-N,N,N',N'-tetra-acetic acid
EtBr	ethidium bromide
ETS	external transcribed spacer
FC	fibrillar centre
FCS	foetal calf serum
Fib	fibrillarin
Fig.	figure
5-FU	5-Fluorouracil
G	guanine
G1	gap-phase 1
G2	gap-phase 2
GC	granular component
HA	haemagglutinin
Hdm2	human Mdm2
HIV	human immunodeficiency virus
HRP	horseradish peroxidase
H. sapiens	*Homo sapiens*

ITS	internal transcribed spacer
K	lysine
kb	kilobases
kDa	kilodalton
M	mitosis
Mdm2	murine double minute 2
M. musculus	*Mus musculus*
MOPS	3-(N-Morpholino)-propansulfonsäure
mRNA	messenger RNA
NDF	nucleolar-derived foci
N-	amino-
NLS	nuclear localization signal
NORs	nucleolar organizing regions
NPM	nucleophosmin
NST	nucleostemin
OD	optical density
PCR	polymerase chain reaction
PEG	polyethylenglycol
Pes1	Pescadillo 1
PFA	paraformaldehyde
PML	promyelocytic leukemia
PMSF	phenylmethylsulfonylfluorid
PNB	pre-nucleolar body
Pol I	RNA polymerase I
Pol II	RNA polymerase II
Ppan	Peter pan
PR	perichromosomal region
r-gene	ribosomal gene
RNA	ribonucleic acid
RNAse A	ribonuclease A
R. norvegicus	*Rattus norvegicus*
r-protein	ribosomal protein
rRNA	ribosomal RNA
rpm	revolutions per minute
RT	reverse transcriptase
S. cerevisiae	*Saccharomyces cerevisiae*
SDS	sodium dodecylsulphate
siRNA	small interfering RNA
snoRNA	small nucleolar RNA
SRP	signal recognition particle
T	thymine
TEMED	N,N,N',N'-tetramethylethylenediamine
t-RNA	transfer-RNA
Tub	tubulin
WDR12	WD40-repeat protein 12
YFP	yellow fluorescent protein

1. Introduction

1.1 From tumor suppressors to oncogenes

The precise control of cell growth and cell cycle activity is critical for determining the size and shape of specific tissues in multicellular organisms. A complex network of signalling pathways integrating extracellular signals and intracellular cues controls cell proliferation. The ability of cells to arrest at cell cycle checkpoints as a consequence of cellular stress ensures genomic stability. Two categories of genes are involved in cell cycle and growth control and play a central role in the development of cancer: tumor suppressor genes protect from and oncogenes contribute to the development of cancer.

1.2 Tumor suppressor genes

Tumor suppressor genes control cell division, apoptosis and repair of damaged DNA (reviewed by Sherr, 2004). When tumor suppressor genes are mutated and inactivated, cells grow uncontrolled, which can lead to tumors. About 30 tumor suppressor genes have been identified so far. These can be classified as genes that control cell division, like the retinoblastoma tumor suppressor gene, or as genes that repair DNA, like the HNPCC gene (hereditary nonpolyposis colon cancer), or cell "suicide" genes, like p53. Because tumor suppressor genes are recessive, cells that contain one normal and one mutated gene still behave normally. Several mechanisms can lead to loss of the normal gene. For example, this may result from "loss of heterozygosity" or LOH. LOH applies to most abnormalities in tumor suppressor genes and can be provoked by either the deletion of the normal allele, the whole chromosome arm or even the deletion of the entire chromosome containing the normal allele. Furthermore, loss of a chromosome containing the normal allele followed by a duplication of a chromosome containing a mutated allele can occur. Another mechanism for inactivation of tumor suppressor genes is epigenetic methylation of the promoter as described e.g. for p14 Arf (Iida *et al.,* 2000).

1.3 Oncogenes

Oncogenes are mutated forms of genes that cause cells to proliferate and to become cancerous. Mutations can cause a change in the protein structure, leading to increased activity or expression or loss of regulation of the oncogene. Chromosomal translocations can also be the cause for increased gene expression in the wrong cell type or at wrong times. Furthermore deregulated hybrid proteins can occur after chromosomal translocation, as described for adult leukemias. Mutation of microRNAs can additionally lead to activation of oncogenes (Esquela-Kerscher and Slack, 2006; Zhang *et al.*, 2007). When proto-oncogenes mutate to oncogenes, they become permanently activated and the cell cycle runs out of control. Oncogenes can be growth factors, growth factor receptors, signal transducers, transcription factors or programmed cell death regulators.

1.4 c-Myc

The proto-oncogene *c-myc* is part of a transcription factor network that regulates cellular proliferation, replication, growth, differentiation and apoptosis. Generally, c-Myc expression closely correlates with the proliferation status of a cell: in quiescent cells, c-Myc is almost undetectable, whereas upon mitogen stimulation, mRNA and protein levels are rapidly induced (Henriksson and Luscher, 1996). c-Myc is down-regulated during differentiation. Deregulated expression of *c-myc* has been found through genomic aberrations in a wide array of B-cell-specific malignancies and several other types of neoplasias (Boxer and Dang, 2001). c-Myc is a transcription factor controlling the expression of many genes associated with progression through the cell cycle and synthesis of cellular components preparing cells for division. c-Myc directly regulates ribosome biosynthesis through the transcription of genes coding for factors involved in ribosome maturation and assembly (Schuhmacher *et al.*, 2001; Schlosser *et al.*, 2003). c-Myc associates with ribosomal DNA and stimulates RNA polymerase I transcription in response to mitogenic signals (Arabi *et al.*, 2005; Grandori *et al.*, 2005).

The aim of this thesis is the functional analysis of c-Myc target genes with nucleolar function. The focus will be on the linkage of ribosome biogenesis and cell cycle control and particular on the mechanism and factors coupling these two processes.

1.5 Conventional roles of the nucleolus

The nucleolus is a distinct sub-nuclear compartment where all eukaryotes synthesize their ribosomes (reviewed by: Leary and Huang, 2001; Shaw and Doonan, 2005; Raska *et al.*, 2006; Boisvert *et al.*, 2007). It has been estimated that a growing HeLa cell produces about 7.500 ribosomal subunits per minute, which requires approximately 300.000 ribosomal proteins and numerous associations and dissociations with trans-acting factors, putting an immense demand on the cellular machinery (Lewis and Tollervey, 2000). The nucleolus is formed around genetic loci on the chromosomes called nucleolar organizing regions (NORs), which consist of tandemly repeated genes for rRNA. Human cells have NORs on the short arms of the five acrocentric chromosomes (13, 14, 15, 21 and 22). They contain about 400 ribosomal genes (r-genes). Each r-gene repeat forms the 47S pre-rRNA precursor and consists of 18S, 5.8S and 28S rRNA coding sequences, transcribed internal and external spacers (ITS and ETS) and non-transcribed intergenic spacers (Fig. 1).

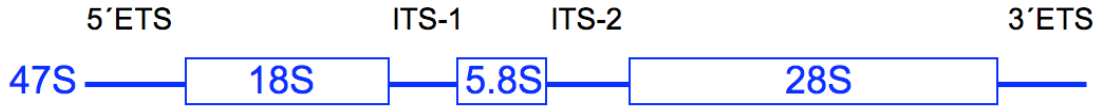

Fig. 1. Mammalian 47S pre-rRNA precursor. The 18S, 5.8S and 28S rRNAs are separated by two internal transcribed sequences (ITS-1 and -2) and flanked by two external transcribed sequences (5´ETS and 3´ETS).

The coordinated activity of RNA polymerases I, II and III is required for ribosome biogenesis. The RNA polymerase I transcribes ribosomal DNA for the 18S, 5.8S and 28S rRNA, the RNA polymerase II transcribes the genes for ribosomal proteins and accessory factors and the RNA polymerase III is important for transcription of 5S rDNA.

Although the nucleolus in not enclosed in a membrane, it does exhibit three distinct compartments, namely fibrillar centres (FC), the dense fibrillar component (DFC) and the granular component (GC). The most important step of ribosome biosynthesis is the transcription of rDNA by RNA polymerase I (RNA pol I), which takes place at the border between the fibrillar centre and dense fibrillar component. The product of RNA pol I transcription is a long rRNA precursor (pre-rRNA), which is modified by 200

nucleotide methylations and pseudouridylations. The three mature rRNAs are produced through sequential cleavage by endo- and exonucleases in the dense fibrillar component of the nucleolus. Recent evidence was given for the coordinated action of rDNA transcription and processing of the ribosomal RNAs (Gallagher *et al.*, 2004; Granneman and Baserga, 2005; Kopp *et al*., 2007). The assembly of 5.8S with 28S and 5S rRNA into the 60S subunit occurs in the granular component, as well as the assembly of 18S into the 40S ribosomal subunit. Both subunits are then exported to the cytoplasm to form mature ribosomes.

1.6 The nucleolus during the cell cycle

The nucleolus is a dynamic structure: it disassembles when cells enter mitosis and reassembles during the G1 phase of the cell cycle. At the beginning of the prophase components of the rDNA transcription machinery are hyperphosphorylated and transcription is downregulated. The RNA pol I transcription machinery remains associated with the active NORs (Roussel *et al.*, 1996), whereas the rRNA processing machinery leaves the nucleoli (Leung *et al.*, 2004). Some processing factors are released into the cytoplasm, whereas others become attached to the surface of condensed chromosomes, which is called the perichromosomal region (PR) (Gautier *et al*., 1992). This PR consists of rRNA processing components, the small nucleolar RNA U3 (U3 snoRNA), pre-rRNA, fibrillarin and non-nucleolar proteins. In anaphase, rRNA-processing components are either associated with the chromosomes or are packaged in the cytoplasm into nucleolar-derived foci (NDF) (Dundr and Olson, 1998). NDF contain early and late rRNA-processing factors, the U3 snoRNA and partially processed pre-rRNAs. In the late anaphase and early telophase, the rDNA transcription is reactivated (Sirri *et al.,* 2000). Small particles dissociate from the NDF and pass into the nucleus through the newly formed nuclear membrane. The number of NDFs decreases until they completely disappear at the end of the G1 phase (Dundr *et al.*, 2000). Most of the components of the NDF are transferred to newly formed structures, the pre-nucleolar bodies (PNBs), which are associated with the chromosomes. The PNBs contain, similar to the NDF, processing proteins, snoRNAs and partially processed pre-rRNAs (Savino *et al.*, 2001). The perichromosomal region breaks down and most components are incorporated into the PNBs, whereas other processing components are distributed in the nucleoplasm

(Hernandez-Verdun, 2006). During the G1 phase nucleoli are reassembled. Processing components of the PNB are subsequently released in a defined order and recruited to nucleoli. First, components, which have early roles in the pre-rRNA processing are recruited, like fibrillarin, and later, proteins involved in late steps of rRNA processing move from the PNBs to the nucleoli (Sirri *et al.*, 2002). Finally the rRNA transcription machinery and rRNA processing machinery reassemble on the rDNA and the NORs move together in the nucleoplasm and fusion to new functional nucleoli.

1.7 PeBoW and the connection to Ppan

Pes1, Bop1 and WDR12 are members of the previously characterized human PeBoW complex (Hölzel *et al.*, 2005; Rohrmoser *et al.*, 2007) with nucleolar function, and are essential for ribosome biogenesis. All three factors are encoded by c-Myc target genes. The PeBoW complex is required for the processing and maturation of the ribosomal large subunit 28S rRNA (Hölzel *et al.*, 2005, Grimm *et al.*, 2006). The connection between ribosome biogenesis and cell cycle control was the reason to study this complex in detail. In particular, interaction partners of PeBoW were investigated for further characterization. Since nothing was known about mammalian interaction partners, examination of binding partners of the homologous complex in yeast was performed. Nop7, Erb1 and Ytm1 are homologues of mammalian Pes1, Bop1 and WDR12. For Nop7 230 interactions have been described, 164 for Erb1 and 125 for Ytm1 (www.yeastgenome.org; www.thebiogrid.org). Nop7, Erb1 and Ytm1 have 35 common interaction partners in yeast. Thirteen of the thirty-five interaction partners attracted my attention, because they have homologues in human and are described as c-Myc targets (Guo *et al.*, 2000; Schlosser *et al.*, 2002; Li *et al.*, 2003; Marinkovic *et al.*, 2004) (Tab. 1).

Table 1 contains several interesting candidate factors. In this work we decided to work with Ppan for two reasons. Firstly, the function of Ssf1 in yeast is well described and secondly, interesting preliminary observations were made for Ppan in the fruit-fly and a human cancer cell line, ascribing Ppan tumor suppressor gene functions.

Tab. 1. Common yeast interaction partners of Nop7, Erb1 and Ytm1 and their homologues in human, described as c-Myc targets.

yeast	function	human	function
Dbp10	DEAD box RNA helicase (Burger *et al.*, 2000)	**DDX54**	unknown
Ebp2	required for 60S subunit synthesis (Tsujii *et al.*, 2000)	**EBP2**	interacts with the EBV nuclear antigen 1 (Shire *et al.*, 1999)
Glc7	catalytic subunit of type 1 serine/threonine protein phosphatase, involved in many processes (Feng *et al.*, 1991)	**PPP1CC**	regulates an enormous variety of cellular functions (Cohen, 2002)
Has1	helicase, required for snoRNA release from pre-rRNA (Liang and Fournier, 2006)	**DDX18**	helicase; important for cell proliferation (Dubaele and Chène, 2007)
Mak21	required for 60S ribosomal subunit biogenesis (Edskes *et al.*, 1998)	**CBF**	involved in cell proliferation and differentiation (Ramji and Foka, 2002)
Nop1	associated with snoRNA; required for rRNA processing (Schimmang *et al.*, 1989)	**fibrillarin**	binds U3, U8 and U13 snoRNA; required for pre-rRNA processing (Kass *et al.*, 1990)
Nog1	required for 60S ribosomal subunit biogenesis (Kallstrom *et al.*, 2003)	**Nog1**	assembly of pre-60S subunits, processing of pre-rRNA intermediates (Lapik *et al.*, 2007)
Nop2	60S subunit synthesis (Hong *et al.*, 1997)	**p120**	proliferation marker, binds rRNA (Gustafson *et al.*, 1998)
Nug1	associates with pre-60S ribosomal particles (Bassler *et al.*, 2006)	**NST**	controls cell proliferation in stem cells and cancer cells (Tsai and McKay, 2002)
Rpf1	Brix-domain containing protein	**BXDC5**	unknown
Rrp1	involved in 60S subunit synthesis (Horsey *et al.*, 2004)	**Nop52**	predicted role in generation of 28S rRNA (Savino *et al.*, 1999)
Rrp5	40S and 60S subunit synthesis (Venema and Tollervey, 1996)	**NFBP**	processing of rRNA (Sweet *et al.*, 2008)
Ssf1	prevents premature processing of pre-rRNA, involved in maturation of 25S (Fatica *et al.*, 2002)	**Ppan**	functions as a tumor suppressor (Welch *et al.*, 2000)

1.8 Yeast Ssf1

Yeast Ssf1 was originally identified in a screen for altered sensitivity in the response to mating pheromone (Yu and Hirsch, 1995; Kim and Hirsch 1998). However, in these studies Ssf1 localized to the nucleolus, suggesting an alternative or additional role for the protein in ribosome synthesis in yeast. Ssf1 and Ssf2 form a gene pair with 94% identity. Cells containing null alleles of either Ssf1 or Ssf2 show no obvious phenotype, but disruption of both genes is lethal (Yu and Hirsch, 1998). Yeast Ssf1 is 34% identical and 58% similar to human Ppan, indicating its evolutionary conservation. Ssf1 is a member of a conserved gene family, including Ssf2, Imp4, Rpf1, Rpf2 and Brx1 (Fatica *et al.*, 2002; Eisenhaber *et al.*, 2001). All proteins of this family are implicated in ribosome biogenesis and contain a conserved domain, the Brix domain (Biogenesis of ribosomes in Xenopus). In yeast Ssf1 is involved in the synthesis of the large subunit rRNAs (Fatica *et al.*, 2002).

1.9 The function of Ssf1 in ribosome biogenesis

In yeast, ribosome biogenesis is initiated by the transcription of the 35S pre-rRNA precursor and multiple coordinated processing steps to form the mature 18S, 5.8S and 25S rRNA (Fig. 2). The yeast 35S pre-rRNA precursor contains the sequences for the mature rRNAs, two internal transcribed sequences 1 and 2 (ITS-1 and ITS-2) and two external transcribed spacers (5' ETS and 3' ETS). The processing of the pre-rRNA precursor occurs sequentially at specific cleavage sites (Fig. 2 and 3). Normally, the 35S pre-rRNA precursor is cleaved to produce the 32S pre-RNA, which in turn is processed to give the 20S and 27SA pre-rRNA forms (Fig. 3). The 27SA pre-rRNA is converted to 27SB and then to 25S rRNA and 5.8S rRNA, whilst the 20S pre-rRNA is converted to 18S rRNA. A detailed description of the complicated cleavage sequence is described in figure 3.

The depletion of factors involved in ribosome biogenesis leads to abnormal rRNA processing, with accumulation of different rRNA precursor forms (Venema and Tollervey, 1999). For instance, the depletion of Ssf1 leads to an abnormal pre-rRNA processing and formation of aberrant rRNA precursors (Fatica *et al.*, 2002). In Ssf1-depleted cells the kinetics of 18S rRNA are not changed, instead the pathway leading

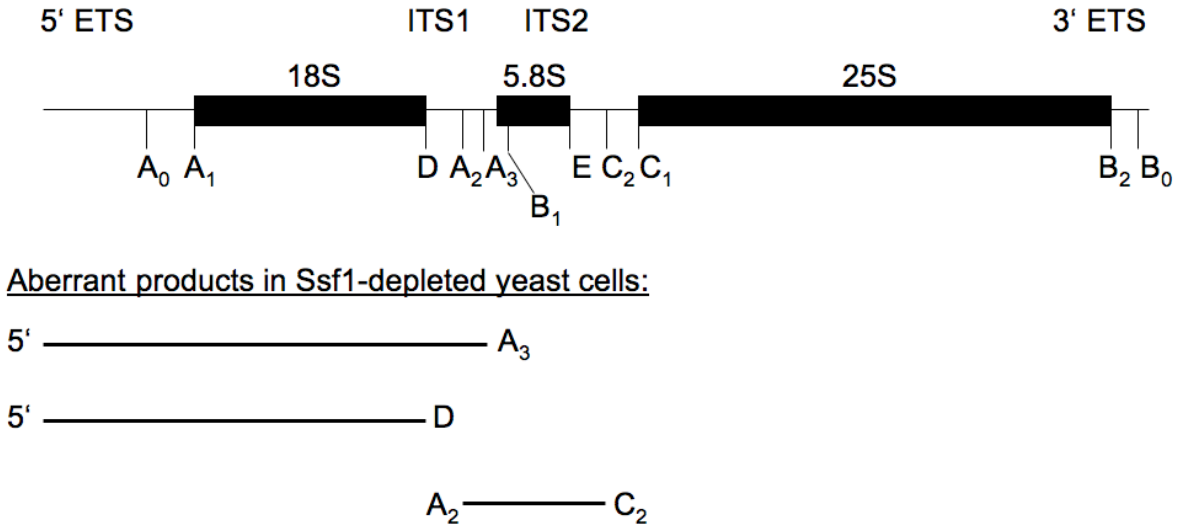

Fig. 2. Structure and processing sites of the *Saccharomyces cerevisiae* 35S pre-rRNA. The cleavage sites are described by letters and numbers. Ssf1-depleted cells accumulate aberrant RNA products, which extend from the 5’ end to cleavage site A_3 (23S) or D, or accumulate a fragment spanning between the cleavage sites A_2 and C_2.

to 5.8S and 25S is affected. An aberrant product of 23S appears, which originates from cleavage of the 35S pre-rRNA at site A_3, when the cleavages at sites A_0, A_1 and A_2 are delayed (Fig. 2 and 3). The delay in cleavage at sites A_0 to A_2 is probably secondary to the defect of the large subunit synthesis. Similar defects have also been described for other factors involved in 60S subunit biogenesis (Venema and Tollervey, 1999). As a consequence the 35S rRNA precursor accumulates, while the 32S and 27SA pre-rRNAs is less abundant and the mature 25S rRNA is greatly reduced. Furthermore, an aberrant RNA fragment also accumulates, which extends from the end of the 5’ ETS to site D. In addition an RNA species that extends from A_2 to C_2 is accumulated in Ssf1 depleted cells. It has therefore been concluded that Ssf1 is necessary to prevent premature processing at site C_2 and to maintain the normal order of pre-rRNA processing.

1.10 Known interaction partners of Ssf1

Ssf1 associates with 27S pre-rRNA in a preribosomal particle containing additionally twenty-three non-ribosomal nucleolar proteins, among them Nop7, Erb1 and Ytm1 (Fatica *et al*., 2002). The list of interaction partners of Ssf1 currently contains 51

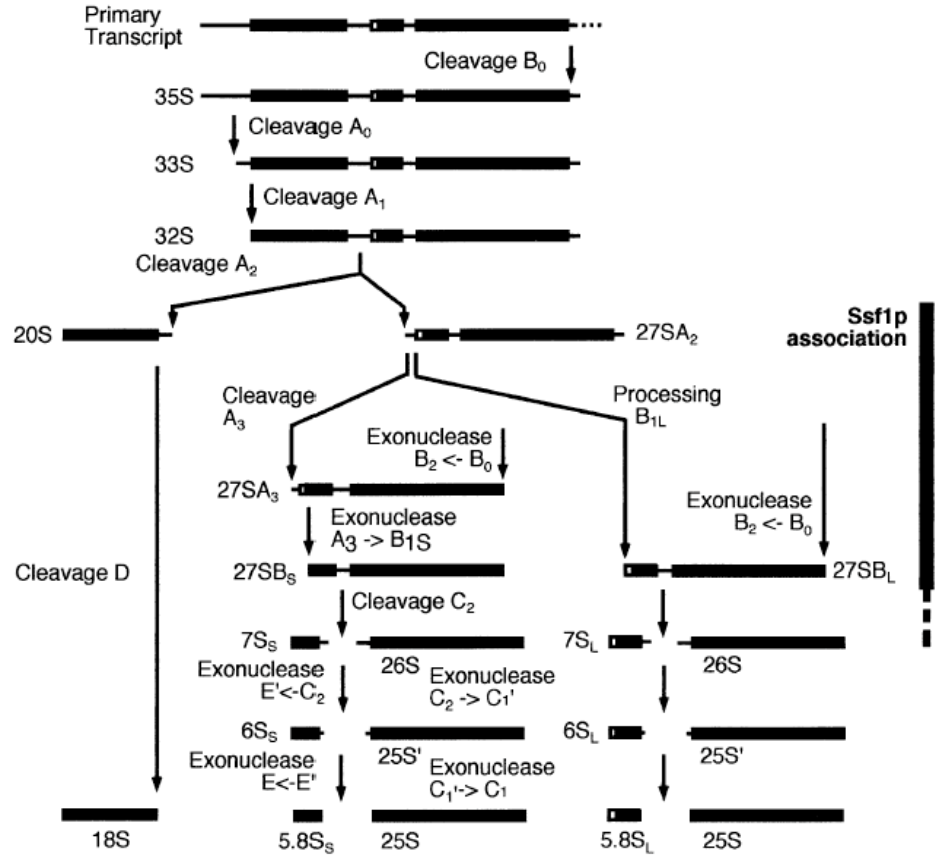

Fig. 3. Pre-rRNA processing pathway in *Saccharomyces cerevisiae* (adapted from Fatica *et al.*, 2002). In wild-type cells, the 35S pre-rRNA is first cleaved at site A_0, producing the 33S pre-rRNA; this molecule is rapidly cleaved at site A_1 to produce the intermediate 32S. 32S is cleaved at site A_2, releasing 20S and $27SA_2$. $27SA_2$ is then processed via two alternative pathways. It is either cut at site A_3 to produce $27SA_3$, which is then trimmed to site B_{1S}, producing $27SB_S$, or it can be processed to $27SB_L$ by an as yet unknown mechanism. $27SB_S$ and $27SB_L$ are matured to the 5.8S and 25S following identical pathways. Cleavage at site C_2 generates the 7S and 26S pre-rRNAs. The 7S pre-rRNA is digested 3' to 5' to 6S pre-rRNA and then to the mature 5.8S rRNA. The 26S pre-rRNA is digested 5' to 3' to the 25S pre-rRNA and then to the mature 25S rRNA. (For a review of pre-rRNA processing and the known processing enzymes, see Venema and Tollervey, 1999.) The vertical thick line indicates strong associations between the Ssf1p protein and RNA species and the dashed line shows weak associations.

factors (Gavin *et al.*, 2002; Ho *et al.*, 2002; Krogan *et al.*, 2006; Lebreton *et al.*, 2006). Of these factors, 31 are directly involved in biogenesis of the large ribosomal subunit, 7 are ribosomal proteins, 1 has unknown functions and the remaining 12 have other functions in the cell.

1.11 Peter Pan in *Drosophila*

The gene *peter pan* (*ppan*) was identified in a screen for larval growth-defective mutants of the fruit-fly *Drosophila melanogaster*. *Ppan* mutant larvae did not grow, like Peter Pan, the homonymous boy who never wanted to grow up in the story of James M. Barrie. The same larvae showed minimal DNA replication but could survive well after their heterozygotic siblings had pupariated (Migeon *et al.*, 1999). It was the first evidence that Ppan is required for some aspects of cell differentiation as well as for cellular growth.

1.12 Human Ppan

Ppan attracted attention in a study showing that it plays a role in tumor suppression. Welch and his colleagues used a library of hairpin ribozymes to identify genes involved in anchorage-dependent growth (Welch *et al.*, 2000). Human HF cells, a non-transformed revertant of HeLa cells, have lost the ability to grow in soft agar, probably due to the activation of a tumor suppressor (Boylan *et al.*, 1996). Nevertheless, HF cells could grow again in soft agar, when Ppan was depleted by application of the specific ribozyme. The authors proposed that Ppan is part of a pathway that provides a cell with information about its substrate contact and may be involved in the metastatic potential of transformed cells. Overexpression of Ppan induced toxicity in HeLa cells, suggesting that overproduction could possibly lead to tumor-specific cell death.

Communi *et al.* (2001) isolated during a screen of a human placenta library a chimeric transcript consisting of Ppan and P2Y11 (SSF1-P2Y11). The P2Y11 gene is adjacent to *ppan* at chromosome 19p13.2 and codes for a receptor belonging to the P2Y family of G-protein-coupled nucleotide receptors. The functional significance of the chimera remains unclear. The presence of chimeric messengers resulting from intergenic splicing is not commonly observed in normal mammalian cells. The authors postulated that intergenic splicing could be a mechanism for generating new multidomain proteins and could therefore have major evolutionary implications.

In the year 2004, Ppan was placed on the list of c-Myc target genes with a potential role in lymphomagenesis (Marinkovic *et al.*, 2004). In this study the authors searched

for direct Myc target genes using different mouse T and B cell lymphoma cell lines transformed by a conditional Myc-allele. Ppan was found to be upregulated by c-Myc.

1.13 Structure of the human Ppan protein

The major characteristic in the Ppan protein is the occurrence of a large globular Brix domain, spanning between amino acids 30-300 (Fig. 4). The Brix domain contains a RNA-binding motif, called σ70 like motif, which is a short sequence highly related to a DNA binding motif of the *E. coli* σ70 transcription factors. The σ70 like motif of the Brix domain is unique to a superfamily of proteins from yeast to human required for ribosome biogenesis and confers RNA binding (Wehner and Baserga, 2002). The N-terminal part of the Brix domain contains 2 putative nuclear localization sites (NLS) (amino acids 51-67 and 113-129) and the C-terminal part harbours the σ70-like motif (amino acids 270 to 285). The Brix domain is followed by a coil-coil domain (amino acids 304-342), which is known to mediate protein-protein interactions and subunit oligomerization (Burkard *et al.*, 2001). At the C-terminus of Ppan two predicted AT-hook domains (amino acids 425-435 and 460-470) are located. These domains are present in proteins preferentially binding to the minor groove of stretches of A-T-rich sequences (Reeves and Nissen, 1990). A third putative NLS (amino acids 449-465) is embedded between the two AT-hook domains. Ppan has four phosphorylated residues: S238, S240, T370 (Dephoure *et al.*, 2008) and S359 (Beausoleil *et al.*, 2004). According to the SUMOplot™ prediction database, Ppan possesses 4 putative sumoylation sites at lysine-residues at position K413 with high probability and positions K217, K336 and K435 with low probability.

1.14 Ppan' s homology across different species

Protein database searches revealed Ppan homologs in four different species (Tab. 2). All of these contain a Brix domain.

The major difference between human Ppan and yeast Ssf1 are the two predicted AT-hook domains at the far C-terminus of the human Ppan protein. Most probably these evolutionary younger domains enable Ppan to have additional functions in mammalian cells.

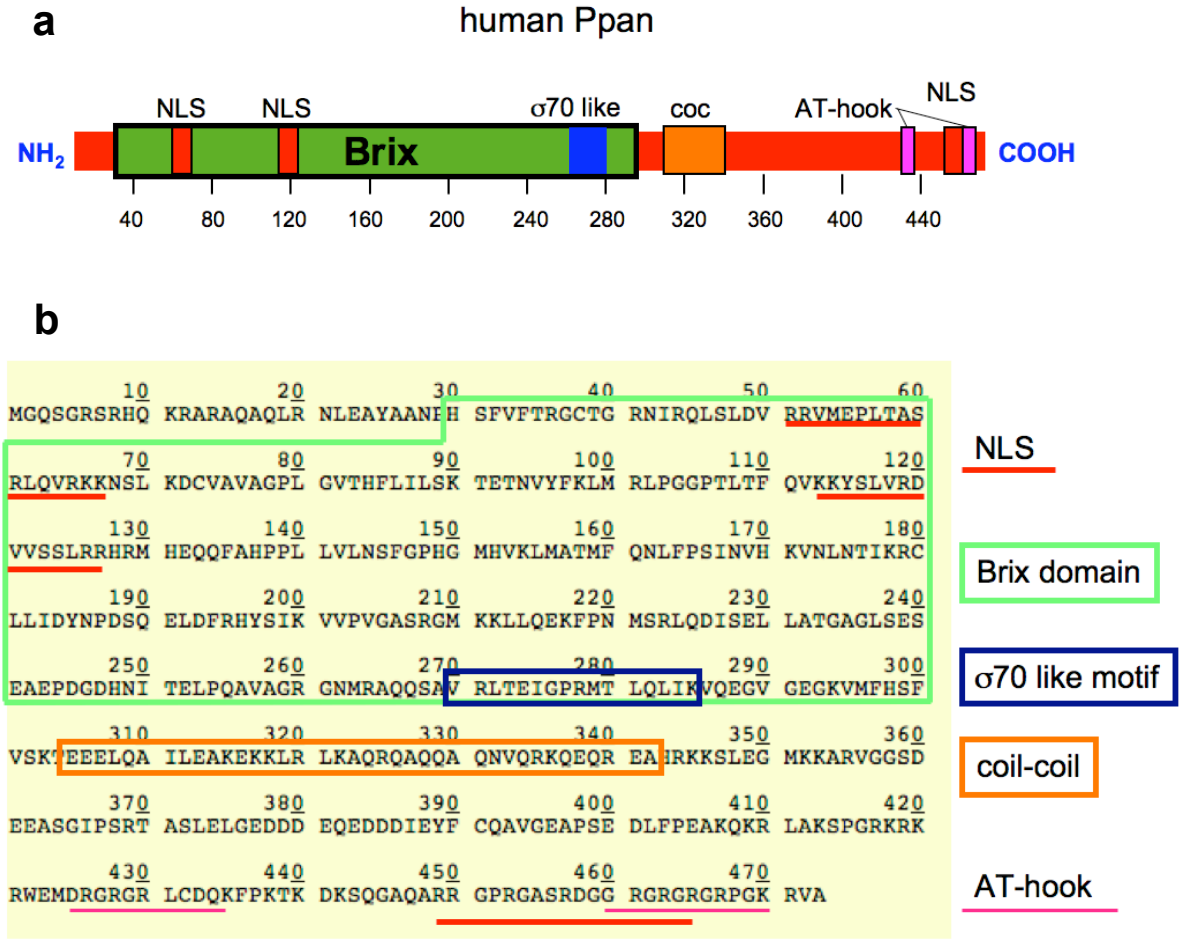

Fig. 4. (a) Schematic model and (b) amino acid sequence of human Ppan with characteristic features. According to UniProt (http://expasy.proteome.org.au/uniprot) there are two isoforms of Ppan: Q9NQ55-1 (473 amino acids) and Q9NQ55-2 (460 amino acids). In isoform Q9NQ55-2 amino acids at positions 444 to 456 are missing. There is no experimental evidence for the existence of the isoform 2. Only the isoform Q9NQ55-1 (full length) of Ppan was studied in this thesis. (adapted and modified from www.expasy.org).

Tab. 2. Ppan homologues in different species

Species	Reference protein	Protein accession number	Identity %	Length (aa)
R. norvegicus	Ppan homolog	NP_001011980.1	88.1	463
M. musculus	Ppan homolog	NP_663585.1	84.8	468
D. melanogaster	Ppan CG5786-PA	NP_476979.1	46.1	406
S. cerevisiae	Ssf1	NP_011933	34.5	455

1.15 Non-conventional roles of the nucleolus

In addition to ribosome biogenesis the nucleolus is involved in many other aspects of cellular activities, like signal recognition particle assembly, modulation of telomerase function, modification of small nuclear RNAs and cell cycle regulation (Olson *et al.*, 2002). The nucleolus is not a static structure and its components move constantly and exchange with the surrounding nucleoplasm (Phair and Misteli, 2000; Olson and Dundr, 2005). Nucleoli respond to changes in cellular growth rate and metabolic activity, which indicates that they constantly receive and respond to signalling events. It is therefore not surprising that many nucleolar proteins are regulated by c-Myc (Schlosser *et al.*, 2003).

Signal recognition particle (SRP) is a translational arrest machine that binds to the N-terminal signal peptide sequence of nascent secretory and membrane proteins, and blocks the peptidyl-transferase activity of 28S rRNA. The SRP of higher eukaryotes contains an essential RNA component and 6 proteins. The SRP RNA is localized and processed in the nucleolus (Jacobson and Pederson, 1998).

The telomerase is a reverse transcriptase ribonucleoprotein enzyme that synthesizes telomeric DNA repeats at the ends of eukaryotic chromosomes. The localization of telomerase is dynamic throughout the cell cycle. In early S-phase the key components of telomerase localize in nucleoli (Tomlinson *et al.*, 2006). The reason for this localization is not known at the moment. The nucleolus also serves for processing of other small nuclear RNAs (snoRNAs), including tRNA. The small nuclear RNA U6, normally localizing in nucleoplasmic foci, was found to be associated in nucleoli with fibrillarin, which directs the methylation of the U6 snoRNA (Pederson, 1998). Furthermore it was shown that nucleolar trafficking is essential for nuclear export of intronless herpesvirus mRNA (Boyne and Whitehouse, 2006).

Recent studies regarding proteins involved in cell cycle regulation suggest that the nucleolus might function as a “prison”. Sequestration in the nucleolus prevents proteins from reaching their targets in other regions of the cell (Visintin and Amon, 2000). For example, the phosphatase Cdc14 localizes during mitotic interphase and metaphase in nucleoli of yeast cells, whereas at anaphase it spreads to the nucleus and cytoplasm, where it inactivates mitotic kinases, leading to exit from mitosis (Visintin *et al.*, 1998).

1.16 Nucleolus and the tumor suppressor p53

In a hallmark study, Rubbi and Milner (2003) proposed that the nucleolus is a major stress sensor that transmits signals for regulation of activity of the tumor suppressor p53. The tumor suppressor and transcription factor p53, termed the “guardian of the genome”, can induce cell-cycle arrest or apoptosis in response to a variety of cellular stress signals. These properties are exploited in anti-cancer therapy, mainly by triggering a p53 response through genotoxic stress (Weinstein *et al.*, 1997). The importance of p53 is underlined by the fact that the protein has been shown not to function properly in most human cancers. Approximately 50% of sporadic human tumors harbour somatic mutations in the p53 gene locus. p53 is inactivated most frequently by mutation in the DNA binding domain. Furthermore, mislocalization of the protein can block its proper function. Viral infections can cause an inactivation of p53, when viral oncogenes bind and inactivate p53 or stimulate its degradation (reviewed in Vogelstein *et al.*, 2000).

p53 is a short-lived protein that is present in cells at a barely detectable level. Although it is continuously synthesized, p53 is subjected to fast degradation, in order to maintain low levels of the protein in the cell. Upon exposure of cells to various forms of exogenous or endogenous stress, the cellular amount of p53 rapidly increases by blocking its degradation. Activated p53 binds to promoters of target genes and activates the transcription of e.g. *p21*, *mdm2* and *BAX* (Levine, 1997; Vogelstein *et al.*, 2000; Zhao *et al.*, 2000). Depending on the cellular stress p53 induces cell cycle arrest or apoptosis. This is thought to be possible through differences in its binding affinity to the promoters of target genes. When damage is repairable, p53 binds preferably to genes promoting cell cycle arrest, like p21. Is the damage more severe, p53 targets promoters of genes responsible for apoptosis (Chen *et al.*, 1996; Ludwig *et al.*, 1996).

The degradation of the p53 protein is promoted by Hdm2 (Mdm2 in mouse), which is an E3 ubiquitin ligase and mono-ubiquitinates p53. Ubiquitination of p53 marks it for export and degradation in the cytoplasm. Stabilization of p53 can be achieved when the formation of the Hdm2-p53 complex is blocked for example by posttranslational mechanisms. The p53 protein is targeted by modifying kinases and acetyl-transferases. Different types of cellular stress activate distinct kinases and acetyl-transferases (reviewed by Ljungman, 2000), to modify p53 at different residues,

which might explain the different p53 response to each stress situation (Zhao *et al.*, 2000). For example, ionizing radiation induces on p53 phosphorylation on serine residues Ser15 and Ser37 by the kinase ATM, which blocks Hdm2 binding (Sakaguchi *et al.*, 1998). The acetyltransferase p300 functions in the apoptotic response to ionizing radiation and acetylates lysine at amino acid position 382 of p53, leading to increased stability of p53 (Gu and Roeder, 1997).

Disruption of the nucleolus and aberrant ribosome biogenesis results in an increase of p53 and cell-cycle arrest (Rubbi and Milner, 2003). But how is a disruption of the nucleoli transmitted to p53? Several models for the stabilization of p53 in response to nucleolar perturbation are discussed.

One model suggests that the nucleolus is required for the export of the p53-Hdm2 complex into the cytoplasm for degradation and that disruption of the nucleolus inhibits the export (Tao and Levine, 1999; Sherr and Weber, 2000). The model of Hdm2-p53 complexes „riding the ribosome“ (Sherr and Weber, 2000) is supported by the observation that p53 can be covalently linked to 5.8S rRNA and associates with a subset of ribosomes (Fontoura *et al.*, 1992 and 1997). Furthermore, the activity of p53 is regulated by several nucleolar proteins (Fig. 5):

- p14Arf binds to Hdm2 and sequesters it to the nucleolus, liberating thereby p53 in the nucleoplasm, which then becomes activated (Weber *et al.*, 1999 and 2000). p14Arf also translocates from the nucleolus into the nucleoplasm when cells are treated with inhibitors of cyclin-dependent protein kinases with concomitant increase in levels of p53 (David-Pfeuty and Nouvian-Dooghe, 2002).
- Nucleophosmin (NPM) is a multifunctional protein involved in ribosome biogenesis and regulates the stability and transcriptional activity of p53 (Colombo *et al.*, 2002). Nucleophosmin interacts with Hdm2 and inhibits its activity preventing the ubiquitination of p53 (Kurki *et al.*, 2004).
- Nucleolin, is mobilized from the nucleolus to the nucleoplasm under stress conditions, where it interacts directly with p53 (Daniely and Borowiec, 2000).
- Nucleostemin (NST), a GTP-binding protein, shuttles between the nucleolus and nucleoplasm and seems also to be involved in regulating p53 activity (Tsai and McKay, 2002).
- The ribosomal proteins S7 (Chen *et al.*, 2007), L5 (Marechal *et al.*, 1994), L11 (Lohrum *et al.*, 2003, Zhang *et al.*, 2003) and L23 (Jin *et al.*, 2004) interact

with Hdm2 after ribosomal perturbation resulting in accumulation of p53 and cell cycle arrest.

- Recent evidence demonstrates the nuclear protein PML regulating p53 stability after DNA damage through sequestration of Hdm2 to the nucleoli (Bernardi *et al.*, 2004).

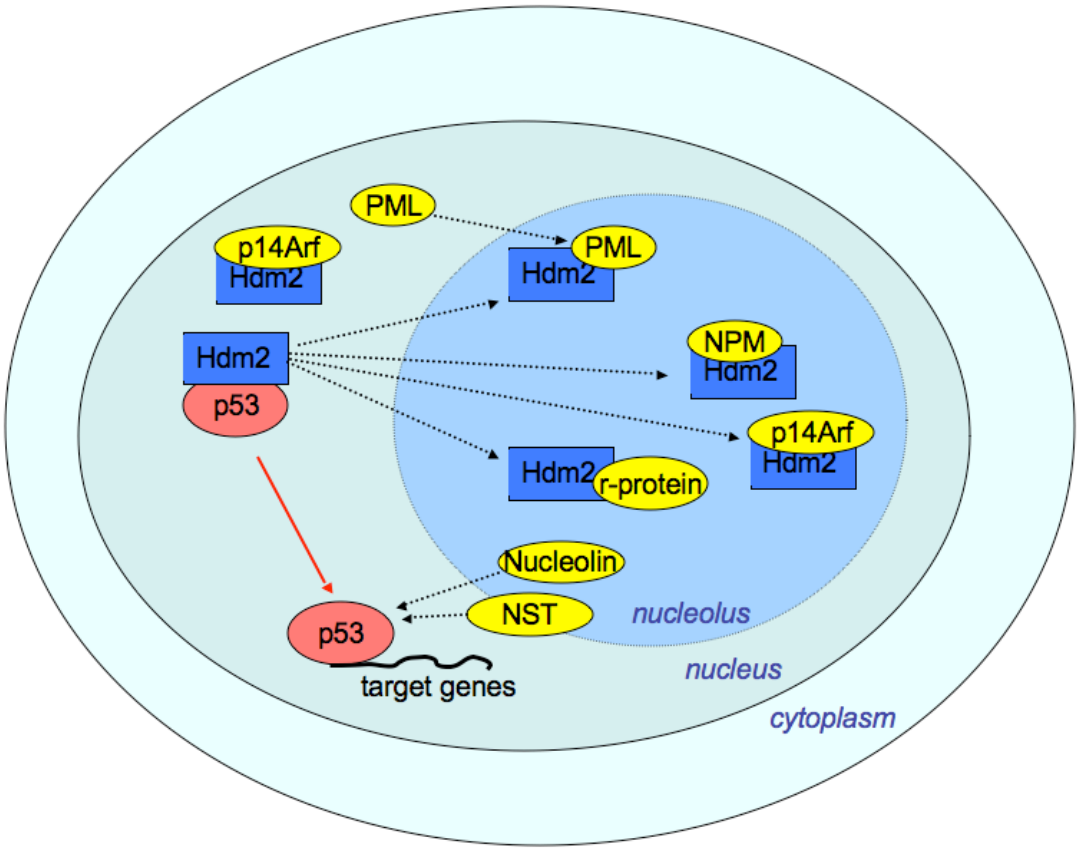

Fig. 5. Binding of Hdm2 by several nucleolar factors activates p53. p14Arf, nucleophosmin, ribosomal proteins (r-proteins) S7, L5, L11 and L23, and PML sequester Hdm2 to the nucleolus after nucleolar perturbation. Nucleolin and NST bind to p53 in the nucleoplasm and regulate its activity. p53, which is no longer interacting with Hdm2, binds subsequently to target genes implicated in apoptosis of cell cycle arrest.

The cross talk between the p53 pathway and the nucleolus has been tried to be explained by several models. Many proteins seem to regulate Hdm2, which indicates a high complexity of the nucleolar stress response machinery. The exact mechanism how the nucleolus is linked to the cell cycle control remains unknown and speculative. Other nuclear and nucleolar factors could probably be involved in the regulation of p53 in response to nucleolar stress.

1.17 The goal of this work

The previously characterized PeBoW complex consisting of Pes1, Bop1 and WDR12 has been shown to play a crucial role in ribosome biogenesis as well as cell cycle progression. Imbalanced levels of these proteins impair ribosome biogenesis and activate a p53-dependent checkpoint, leading to a reversible block of proliferation. Aiming to understand the connection between ribosome biogenesis and cell cycle regulation, Ppan was chosen to further elucidate this checkpoint. Studies in fruit-fly and human indicated a role of Ppan in cell differentiation and growth as well as tumor suppression. These characteristics, together with the finding that the yeast homologue of Ppan, Ssf1, interacts with the trimeric yeast complex of Nop7, Erb1, and Ytm1, which is the homologue of PeBoW, prompted us to investigate the function of Ppan in human cells in detail. In particular, a possible role of Ppan for the linkage of impaired ribosome biogenesis and p53-mediated cell cycle arrest should be investigated.

2. Material and Methods

Material

2.1 Reagents

1-kb-DNA Ladder	Invitrogen, Karlsruhe
β-Mercaptoethanol	Sigma-Aldrich, Hamburg
[γ-^{32}P] dATP, 3000 µCi/mmol	Hartmann-Analytik, Braunschweig
[α-^{32}P] dCTP, 3000 µCi/mmol	Hartmann-Analytik, Braunschweig
Acrylamid Rotiphorese® Gel 30 (37, 5:1)	Carl Roth, Karlsruhe
Actinomycin D	Sigma-Aldrich, Hamburg
Agar	Gibco™, Invitrogen, Karlsruhe
Agarose	Invitrogen, Karlsruhe
Ampicillin	Carl Roth, Karlsruhe
Ammoniumperoxodisulfat (APS)	Carl Roth, Karlsruhe
Bovine serum albumin Fraktion V	Carl Roth, Karlsruhe
Bromophenol blue	Sigma-Aldrich, Hamburg
Calf Intestine Alkaline Phosphatase (CIAP)	MBI Fermentas, St. Leon-Rot
Cycloheximide	Sigma-Aldrich, Hamburg
DAPI	Sigma-Aldrich, Hamburg
Diethyl Pyrocarbonate (DEPC)	Sigma-Aldrich, Hamburg
Dimethyl sulfoxide (DMSO)	Sigma-Aldrich, Hamburg
Dithiothreitol (DTT)	Carl Roth, Karlsruhe
DNAse I	Roche, Mannheim
DMEM	Invitrogen, Karlsruhe
dNTP	Promega, Mannheim
Doxycycline	Sigma-Aldrich, Hamburg
ECL™ Plus Western Blotting Detection Reagent	GE-Healthcare, München
ECL™ Western Blot Detection Reagent	GE-Healthcare, München
EDTA	Carl Roth, Karlsruhe
EGTA	Carl Roth, Karlsruhe
Ethanol p.A.	Merck, Darmstadt
Ethidium bromide	Sigma-Aldrich, Hamburg
Fetal calf serum (FCS)	PAA, Invitrogen, Karlsruhe
Fluorescent Mounting Medium	DakoCytomation, Hamburg
5-Fluorouracil	Sigma-Aldrich, Hamburg
Formaldehyde 37 %	Carl Roth, Karlsruhe

Formamide	Carl Roth, Karlsruhe
FuGene transfection reagent	Roche, Mannheim
L-Glutamine	PAA, Invitrogen, Karlsruhe
Glycerin 87 %	Carl Roth, Karlsruhe
Glycine	Carl Roth, Karlsruhe
HEPES	Merck, Darmstadt
HCl	Merck, Darmstadt
Hygromycin B	Invitrogen, Karlsruhe
Immersion oil „Immersol“ 518F fluorescence free	Carl Zeiss, Göttingen
Isopropanol p.A.	Carl Roth, Karlsruhe
Kanamycin	Sigma-Aldrich, Hamburg
Magnesium chloride	Merck, Darmstadt
Manganese chloride	Merck, Darmstadt
Methanol p.A.	Merck, Darmstadt
MG-132	Sigma-Aldrich, Hamburg
Milk powder	Carl Roth, Karlsruhe
MOPS 3-(N-Morpholino)-propansulfonsäure	Sigma-Aldrich, Hamburg
Oligofectamin	Invitrogen, Karlsruhe
Oligo-dT primer	MBI Fermentas, St.Leon-Rot
Oligonucleotids for PCR	Metabion, Martinsried
	Sigma-Aldrich, Hamburg
OptiMEM	Invitrogen, Karlsruhe
Paraformaldehyde	Sigma-Aldrich, Hamburg
Penicillin/streptomycin	PAA, Invitrogen, Karlsruhe
Pfu DNA Polymerase	Promega, Mannheim
Phenylmethylsulfonylfluorid (PMSF)	Carl Roth, Karlsruhe
Taq DNA Polymerase	Invitrogen, Karlsruhe
PIPES	Merck, Darmstadt
Platinum® Pfx Polymerase	Invitrogen, Karlsruhe
PMSF	Carl Roth, Karlsruhe
Polyethylenglycol (PEG) 6000	MBI Fermentas, St. Leon-Rot
Polyfect	Qiagen, Hilden
T4-Polynucleotidekinase	MBI Fermentas, St. Leon-Rot
Potasium chloride	Merck, Darmstadt
Potasium hydroxide	Merck, Darmstadt
Protein G-Agarose	GE-Healthcare, München
Proteinase inhibitor cocktail	Roche, Mannheim
Puromycine	Sigma-Aldrich, Hamburg
Restriction enzymes	MBI Fermentas, St. Leon-Rot
	New England Biolabs, Frankfurt

RNAse A	Roche, Mannheim
RNAsin RNAse inhibitor	MBI Fermentas, St. Leon-Rot
Rubidium chloride	Merck, Darmstadt
SDS	Carl Roth, Karlsruhe
Sodium acetate	Carl Roth, Karlsruhe
Sodium chloride	Merck, Darmstadt
Sodium hydroxide	Carl Roth, Karlsruhe
Sodium phosphate dibasic anhydrous	Merck, Darmstadt
Sodium molybdate	Carl Roth, Karlsruhe
Sodium orthovanadate	Carl Roth, Karlsruhe
Sodium phosphate monobasic monohydrate	Merk, Darmstadt
Sparfloxacine	Sigma Aldrich, Hamburg
Sucrose	ICN, Northeim
T4 DNA Ligase	Invitrogen, Karlsruhe
TEMED	Carl Roth, Karlsruhe
TriFast	Peqlab, Erlangen
Tris Base	Carl Roth, Karlsruhe
Triton X-100	Sigma-Aldrich, Hamburg
Trypsin-EDTA	Gibco™, Invitrogen, Karlsruhe
Tween® 20	Sigma-Aldrich, Hamburg
Xylencyanol	Sigma-Aldrich, Hamburg

2.2 Material and Kits

Blotting paper GB003	Schleicher & Schuell, Dassel
Coverslips	Menzel-Gläser, Braunschweig
Cryotube™	Nunc, Wiesbaden
Electroporation cuvettes 2mm	Peqlab, Erlangen
Endofree® Plasmid Maxi kit (10)	Qiagen, Hilden
Eppendorf tubes	Eppendorf, Hamburg
Filter 0.22µm	Millipore, Schwalbach
High-Prime-Kit	Roche, Mannheim
Hybond-N nylon membrane	GE-Healthcare, München
Hybond™ ECL™ nitrocellulose membrane	GE-Healthcare, München
Hyperfilm ECL high performance	GE-Healthcare, München
Hyperfilm MP	GE-Healthcare, München
Microcentrifuge tube (1.5 ml)	Eppendorf, Hamburg
Microscope slides	Menzel-Gläser, Braunschweig
MicroSpin S-200HR columns	GE-Healthcare, München

MinElute Gel Extraction Kit	Qiagen, Hilden; Peqlab, Erlangen
Mitsubishi thermal papervideo-printer	Mitsubishi, Hatfield, UK
PCR cleanup kit	Qiagen, Hilden
Plastic ware for cell culture	Greiner, Frickenhausen; Nunc, Wiesbaden
Polypropylene conical tubes	Becton Dickinson, Heidelberg
RNeasy Mini Kit	Qiagen, Hilden
Qiashredder™ columns	Qiagen, Hilden

2.3 Equipment

AxioCam HR digital camera	Carl Zeiss, Göttingen
Axioplan 2 Imaging microscope	Carl Zeiss, Göttingen
Axiovert 200M microscope	Carl Zeiss, Göttingen
BioPhotometer 6131	Eppendorf, Hamburg
Centrifuge 5417 R	Eppendorf, Hamburg
Centrifuge RC5B Plus	Thermo Scientific Kendro, Schwerte
Dounce tissue grinder set	Sigma-Aldrich, Hamburg
Electroporator (Easyject Prima)	Peqlab, Erlangen
GS Gene Linker™ UV Chamber	BioRad Laboratories, Hercules, USA
Incubator for cell culture	Heraeus Instruments, Hanau
PCR system 2400	Perkin Elmer, Massachusetts, USA
Stereomicroscope	Leica Microsystems, Wetzlar
Stratalinker	Stratagene, Amsterdam
Thermomixer 5436	Eppendorf, Hamburg

2.4 Software

Openlab 3.08 (Improvision, Coventry, UK) and Leica-TCS 2.61 were used for visualizing and photographic documentation of cells. Pictures were processed with Openlab Demo 5.01 (Improvision, Coventry, UK) or ImageJ (Wayne Rasband, National Institutes of Health, USA) and worked on Microsoft Powerpoint 2004. Mac Vector™ 9.0 (Oxford Molecular Group) was used for sequence analysis and primers design. Microsoft Office 2004 for Mac (Microsoft Corporation, USA) was used for text editing, table calculations and graphic images, Adobe Reader 7.0 (Adobe Systems, Mountain View, U.S.A) was used to convert documents into PDF format.

2.5 Buffers and Solutions

All buffers and solution were prepared with deionized H_2O (ddH_2O) or H_2O treated with diethyl pyrocarbonate (DEPC) when working with RNA.

Buffer A (for nuclei preparation)	10 mM 10 mM 1.5 mM 0.5 mM	HEPES pH 7.9 KCl $MgCl_2$ DTT
Church Buffer	0.5 M 7 % 1 mM	Sodium Phosphate Buffer pH 7.2 SDS EDTA
Co-IP Buffer	Co-IP Lysis Buffer 200 mM	 NaCl
Co-IP Lysis Buffer	10 mM 1 mM 1 mM 2 % 1 mM 1 mM 0.1 %	Tris/HCl pH 7.4 EDTA DTT protease inhibitor coctail Na_2MoO_4 $NaVO_3$ SDS
Co-IP wash buffer	50 mM 200 mM 0.1 % 1 mM	Tris/HCl pH 8.0 NaCl Triton-X100 PMSF
DEPC-H_2O	0.01 % mixed well, incubated over night at 37°C and autoclaved	diethyl pyrocarbonate (DEPC) in ddH_2O
DNA loading buffer 6x	0.03 % 0.03 % 10 mM 50 mM 30 %	bromophenolblue xylencyanol Tris/HCl pH 7.5 EDTA pH 8.0 glycerol
Doxycycline	1 mg/ml in ddH_2O stored at 4°C, protected from light; used as 1 µg/ml	

electrophoresis buffer 10x	30 g Tris 144 g glycine 1 % SDS
Hygromycine	50 mg/ml solution stored at 4°C, protected from light; used as 100 µg/ml
Laemmli loading buffer 2x	100 mM Tris/HCl pH 6.8 200 mM DTT 4 % SDS 0.2 % bromophenolblue 20 % glycerol 5 mM EDTA
Luria Bertani Medium (LB Medium)	25 g Luria Broth Base (Invitrogen) 1 l dH_2O, autoclaved
MOPS RNA running buffer 10x	2 M MOPS 500 mM NaAc 10 mM EDTA adjusted to pH 7.0, stored at RT protected from light
paraformaldehyde (PFA) 3,7 %	1.85 g paraformaldehyde 3.5 ml ddH_2O 10 µl 10 M KOH mixed together in a 50 µl Falcon tube. Boiled water in a 250 ml-glass bottle and put tube in it with cap loose, swirling frequently to mix, for no longer than 5 min. added: 20 ml ddH_2O and 25 ml 2X PHEM buffer stored at 4°C for 1 month
PBS	80 g NaCl 14.4 g Na_2HPO_4 2.4 g NaH_2PO_4 2 g KCl pH 7.4, adjusted to 1l and autoclaved
PHEM buffer 2x	18.14 g PIPES 6.5 g HEPES 3.8 g EGTA 0.99 g $MgSO_4$ pH 7.0 with 10 M KOH, adjusted to 500 ml with ddH_2O, filtered and stored in frozen aliquots or at 4°C

Ponceau S solution	0.1%	Ponceau S
	5 %	acetic acid
protease inhibitor coctail	1 tablet in 1 ml H_2O	
Puromycine	10 mg/ml in ddH_2O	
	stored in aliquots at -20°C, used as 1 µg/ml	
RNA sample buffer	50 %	formamide
	15 %	formaldehyde (37%)
	1x	MOPS pH 7.0
	0.1 %	bromophenolblue
	10 µg/ml	ethidiumbromide
S1 solution	0.25 M	sucrose
	10 mM	$MgCl_2$
S2 solution	0.35 M	sucrose
	0.5 mM	$MgCl_2$
S3 solution	0.88 M	sucrose
	0.5 mM	$MgCl_2$
SDS 10 %	10 % (w/v)	sodium dodecylsulfate
SDS running buffer 10x	1.92 M	glycine
	250 mM	Tris base
	1 %	SDS
Sodium phosphate buffer	684 ml	1 M Na_2HPO_4
pH 7.2	316 ml	1 M NaH_2PO_4
	pH 7.2	
Sparfloxacine	20 mg/ml in 0.1 N NaOH	
	stored at 4°C, protected from light; used as 1 µg/ml	
SSC 20x	3 M	NaCl
	0.3 M	sodium citrate
	pH 7.0, autoclaved	
TBF1	30 mM	potassium acetate
	10 mM	$CaCl_2$
	50 mM	$MnCl_2$
	100 mM	RbCl
	15 %	glycerol
	adjusted to pH 5.8 with 1 M acetic acid and filtered	

TBF2	10 mM	PIPES pH 6.5
	75 mM	$CaCl_2$
	10 mM	RbCl
	15 %	Glycerol
	adjusted to pH 6.5 with 1 M KOH and filtered	
TBS 1x	10 mM	Tris/HCl pH 8.0
	150 mM	NaCl
TBST washing buffer 1x	1X TBS	
	0.1 %	Tween® 20
TE buffer 10x	100 mM	Tris/HCl pH 8.0
	10 mM	EDTA
Transfer buffer	3 g	Tris
	14.4 g	glycine
	20 %	methanol
Transfer buffer	1X	Western blot buffer
	20 %	methanol
Tris/SDS pH 6.8	250 mM	Tris base
	0.2 %	SDS
	adjusted to pH 6.8 with HCl	
Tris/SDS pH 8.8	750 mM	Tris base
	0.2 %	SDS
	adjusted to pH 8.8 with HCl	
Western blot buffer 10x	1.92 M	glycine
	250 mM	Tris base

2.6. Culture media

2.6.1 Culture medium for bacteria

Luria Bertani (LB) medium was prepared with H_2O and autoclaved. For LB agar plates 1.5 % agar was used. In order to select transformed cells ampicilline or kanamycine was added to the medium at final concentration of 100 µg/ml and 50 µg/ml, respectively. LB-agar medium with antibiotic was poured onto petri dishes and stored at 4° C.

2.6.2 Cell culture medium

All cell culture media and solutions were handled under sterile conditions and stored at 4°C. Dulbecco´s Modified Eagle medium (DMEM), was supplemented with 10% (v/v) fetal calf serum (FCS), penicillin/streptomycin and L-Glutamine. For transfections of mammalian cells OptiMEM (Invitrogen) was used. For cell preservation, cells were resuspended in 90% FCS and 10% DMSO.

2.7 Cell lines and strains

2.7.1. Bacterial strains

Strain	Genotype
DH10B (*Invitrogen*)	F- *mcr*A ∆(*mrr-hsd*RMS-*mcr*BC) φ80*lac*Z∆M15 ∆*lac*X74 *rec*A1 *end*A1 *ara*D139 ∆(*ara, leu*)7697 *gal*U *gal*K λ- *rps*L *nup*G
XL1-BLUE (*Stratagene*)	*recA1 endA1 gyrA96 thi-1 hsdR17 supE44 relA1 lac* [F' *proAB laclqZDM15* Tn10 (*Tetr*)

2.7.2. Mammalian cell lines

Name	Cell type/origin
HeLa	human cervix carcinoma
U2OS	human osteogenic sarcoma, p53 wild type
HepG2	human , p53 wild type
T98G	human glioblastoma multiform
TGR-1	rat, fibroblast
$HCT^{-/-\ p53}$, $HCT^{+/+\ p53}$ *	human colon carcinoma p53 null or wild type

* kindly gift from Dr. Harald Gerhard (AGV Apoposis, Helmholtz Centre Munich)

2.8. Plasmids

Name	short description
pUC18-HA *	provides a COOH-terminal HA tag
pSfiExpress-HA *	provides a COOH-terminal HA tag
pRTS-1*	Doxycycline inducuble bidirectional promoter controls simultaneously the expression of both eGFP and the gene of interest (Bornkamm *et al*., 2005)
pBiFC-YN (1-154) ‡	provides a N-terminal FLAG tag and the first 154 amino acids from YFP to the C-terminus, (Hu *et al*., 2002)
pBiFC-YC (155-238) ‡	provides a N-terminal HA tag and the amino acids 155 to 238 from C-terminus of YFP (Hu *et al*., 2002)
p80-GFP*	provides p80 (coilin)-GFP tagged for immunofluorescence
pEGFP-C1**	provides N-terminal GFP
pEGFP-N1*	provides C-terminal GFP

‡ provided by Dr. Andreas Thomae, Helmholtz Centre Munich

* provided by Dr. Michael Hölzel, Helmholtz Centre Munich

**provided by Dr. Rob Chapman, Helmholtz Centre Munich

2.9. Oligonucleotides

All nucleotides were synthesized by Metabion at the concentration of 100 pmol/µl.

Oligonucleotide	Sequence 5'-3'	Tm °C
BglII fwd	GAT CAG ATC TAT GGG ACA GTC AGG	54
Ppan Seq middle	CAC CAT CAA GCG CTG CCT CCT C	65.8
Ppan-Sfimut-fwd2	Pho-CAG GCT CAG CAG GCT CAG AAT G	65.9
Ppan-Sfimut-rev3	Pho-CCT CTG CGC CTT CAG CCG CAG	69.1
Pp-start	GCC ACC ATG GGA CAG TCA GGG	67.2
Pp-end	GGC CAC TCT CTT CCC TGG G	63.8
Pp-delN-for	GCC ACC ATG TCG TTC GTG TTC AC	66.4
Pp-delBrixA-for	GTG AAC CTG AAC ACC ATC AAG CGC	66.9
Pp-delBrixA-rev	GTG CGG GTT CGC GGC ATA G	63.8
Pp-delBrixB-for	AGC AAG ACG GAG GAG GAG CTG C	67.7

Oligonucelotides (continued)

Oligonucleotide	Sequence 5'-3'	Tm °C
Pp-delBrixB-rev	GTG CAC GTT GAT GGA GGG GAA C	65.9
Pp-delcoc-for	CTG GAG GGC ATG AAG AAG GCA C	65.9
Pp-delcoc-rev	CTT GCT CAC AAA ACT GTG GAA CAT CAC	66.8
Pp-delC-rev	GCT CTT CTT TCT GTG GGC CTC C	65.9
pRTS_Sfi+55bp rev	AAT CAA GGG TCC CCA AAC TC	55
SalI rev	GCA AGT CGA CGG CCA CTC TCT	54
YN EcoRV fwd	ATC ATA TCG GTA CCA GTC GAC TCT AGA GGA TCC	66.3
YN EcoRV rev	ATC TAT CGA TGA ATT CGC GGC CG	62.2
YC EcoRV fwd	GAT ATC TCT CGA GGT ACC GCG GCC	67.1
YC EcoRV rev	GGT CGA CCG AAT TCG GGC C	66.7
YN col fwd	CTT GCG GCC GCG AAT TC	60.9
YC col fwd	CAT GTA CCC ATA CGA TGT TCC AG	59.1
YN 1094 (rev)	CGT CCA GCT CGA CCA GGA TG	70.5
YC781 (fwd)	GTG TTA CTT CTG CTC TAA AAG CTG CG	66.8
YC998 (rev)	TTC ACC TTG ATG CCG TTC	62.3

2.10 Antibodies

2.10.1 Primary antibodies

Name (alphabetically)	Company	species	Dilution
α-Bop1 (6H11)	Helmholtz-Centre, Munich*	rat	1:10
α-fibrillarin	Abcam ab5821, Cambridge	rabbit	1:1.000
α-FLAG (M2)	Sigma-Aldrich F1804, Hamburg	mouse	1:5.000 (WB) 1:1.000 (IF)
α-HA (3F10)	Roche, Mannheim	rat	1:1.000
α-HA (12CA5)	Roche, Mannheim	mouse	1:1.000
α-Hdm2 (D-12)	Santa Cruz Biotechnology, Heidelberg	mouse	1:1.000
α-Hdm2 (SMP-14)	Santa Cruz Biotechnology, Heidelberg	mouse	1:1.000

primary antibodies (continued)

Name (alphabetically)	Company	species	Dilution
α-hRrp6 (PM-Scl, Exosc10)	Sigma-Aldrich P4124, Hamburg	rabbit	1:1.000
α-nucleophosmin (FC-6)	Sigma-Aldrich B0556, Hamburg	mouse	1:12.000 (WB) 1:1.000 (IF)
α-p53 (DO-1)	Santa Cruz Biotechnology, Heidelberg	mouse	1:2.000 (WB) 1:200 (IF)
α-Pes1 (8E9)	Helmholtz-Centre, Munich*	rat	1:10 (WB) 1:100 (IF)
α-PML (PG-M3) sc-966	Santa Cruz Biotechnology, Heidelberg	mouse	1:1.000
α-Ppan (1C3)	Helmholtz-Centre Munich*	rat	1:500
α-splicing factor sc-35	Sigma S4045	mouse	1:1.000
α-alpha-tubulin (DM1A)	Sigma T6199	mouse	1:40.000
α-WDR12 (1B8)	Helmholtz-Centre Munich*	rat	1:10

WB: Western blot, IF: Immunofluorescence

*Service unit monoclonal antibodies, Helmholtz-Centre Munich-mAb

2.10.2 Secondary antibodies

Name	Company	species	Dilution
α-rat HRP	Dianova, 112-035-062, Hamburg	goat	1:5.000
α-mouse HRP	Promega W402B, Mannheim	goat	1:5.000
α-rabbit HRP	Promega W401B, Mannheim	goat	1:5.000
α-rat Alexa 488	Invitrogen, Karlsruhe	goat	1:400
α-mouse Alexa 488	Invitrogen, Karlsruhe	goat	1:400
α-rat Cy3	Dianova, 112-165-167, Hamburg	goat	1:300
α-mouse Cy3	Dianova, 115-165-062, Hamburg	goat	1:300
α-mouse Cy5	Dianova, 115-175-166, Hamburg	goat	1:500
α-rabbit Cy3	Dianova, 111-165-045, Hamburg	mouse	1:300

Methods

2.11 Working with DNA

2.11.1 Mini preparation of plasmid DNA (miniprep)

For mini preparation buffers of the Qiagen plasmid maxi kit were used. First, single *E. coli* colonies were inoculated in 2 ml of LB medium plus selective antibiotics and incubated overnight with vigorous shaking at 37°C. Each culture was centrifuged for 10 min at 10.000 rpm and the supernatant removed. The bacterial pellet was resuspended in 300 µl of P1 resuspension buffer and cells were lysed by adding 300 µl P2 lysis buffer followed by 5 min incubation at RT. 300 µl of P3 neutralization buffer was added to the lysate, gently mixed and the reaction was centrifuged for 10 min at 14.000 rpm. The supernatant containing the plasmid DNA was transferred to a fresh 1.5ml tube. DNA was purified by precipitation with 0.7 vol of isopropanol followed by 10 min incubation on ice and 30 min centrifugation at 4°C (14.000 rpm). The DNA pellet was washed with 1 ml 70 % ethanol (10 min; 14.000 rpm, 4°C), air dried and dissolved in 30 µl ddH_2O. DNA was stored at 4°C.

2.11.2 Maxi preparation of plasmid DNA (maxiprep)

For maxi preparation of DNA the Qiagen plasmid maxi kit was used. The bacterial cells of a 200 ml-overnight culture were harvested by centrifugation at 3.000 rpm for 10 min at 4°C. The pellet was resuspended with 10 ml P1 buffer and the instructions of the kit were followed. The DNA was resuspended in buffer TE and stored at 4°C.

2.11.3 Determination of nucleic acid concentration

Concentration of DNA and RNA was determined in an UV spectrophotometer (BioPhotometer 6131, Eppendorf, Hamburg). 2 µl of sample were diluted in 198 µl H_2O and measured by absorption at 260 nm and 280 nm. The concentration was calculated according to the ratio A_{260}/A_{280}. 1 A_{260} unit of double-stranded DNA = 50 µg/ml and of RNA = 40 µg/ml.

2.11.4 DNA digestion

For preparative restrictions 4 µg plasmid-DNA were digested with 10 U of the appropriate enzyme in recommended buffer and optimal temperature in a volume of 20 µl. Reactions were incubated for 2 hours to overnight. For control restrictions 1 µg plasmid DNA or 10 µl from a mini-prepared DNA were digested with 5-10 U enzyme in 20 µl volume for 1-2 hours.

2.11.5 Polymerase Chain Reaction (PCR)

2.11.5.1 PCR for cloning

The human *ppan* sequence NM_020230 was used to design primers flanking the *ppan* open reading frame. A 1419 bp *ppan* cDNA fragment was amplified by RT-PCR from EREB 2.5 RNA (gift from Dr. M. Schlee) using previously phosphorylated *ppan start* and *ppan end* primer pair. To phosphorylate the primers 2 µl of each primer (10 µM) was incubated with 1 µl ligase buffer and 1 µl T4-Polynucleotidkinase in 10 µl reaction volume at 37°C for one hour. The mixture containing phosphorylated primers was used for the PCR reaction with the Platinum *Pfx* Polymerase under following conditions:

10x *Pfx* amplification buffer	5 µl
50 mM $MgSO_4$	1 µl
dNTP mixture (10 mM each)	1.5 µl
primer mix	10 µl
cDNA (10 pmol/µl)	3 µl
10X PCR_x Enhancer Solution	1 µl
Platinum *Pfx* DNA Polymerase	1 µl
autoclaved, distilled water	27.5 µl

PCR program

94°C (denaturation)	2 min	
94°C (denaturation)	15 sec	30x
58°C (annealing)	30 sec	
68°C (extension)	2 min	
72°C (final extension)	10 min	

2.11.5.2 PCR for site directed mutagenesis

Site directed mutagenesis was used to make point mutations and delete DNA sequences coding for protein domains. In addition the internal *SfiI* restriction site of *ppan* was silently mutated (from GCC to GCT).

10x Pfu buffer	5 µl
dNTP mixture (10 µM each)	1.5 µl
primer mix (10 µM each)	3 µl
pUC18-Ppan HA 10 ng/µl	1 µl
Pfu Polymerase	1 µl
autoclaved, distilled water	38.5 µl

PCR program

94°C	2 min	
94°C	30 sec	25x
63°C	30 sec	
72°C	8.5 min	
72°C	10 min	

The template DNA was eliminated by over night enzymatic digestion with *DpnI*, a restriction enzyme, which cleaves only bacterial methylated DNA (by Dam methylase). The mutated plasmid is preserved because it was generated *in vitro* and is unmethylated as a result.

2.11.5.3 PCR for controlling (colony PCR)

Colony PCR was performed to investigate the existence and orientation of the cloned sequences in newly generated plasmids. Bacterial colonies were picked with sterile pipette tips and each released in 20 µl of reaction mix. In parallel a copy of the colony was saved on a new agar plate with appropriate antibiotic and incubated at 37°C.
The reaction mix for PCR contained for one reaction:

10X Taq Polymerase Buffer	2 µl
50 mM $MgCl_2$	1 µl
dNTP mix (each 10 µM)	0.4 µl
foreward primer	0.05 µl
reverse primer	0.05 µl
Taq polymerase (5 u/µl)	0.2 µl
autoclaved, distilled water	16.3 µl

PCR program

94°C	10 min	
94°C	15 sec	30x
Tm-3°C	30 sec	
72°C	1 kb/min	
72°C	10 min	

2.11.6 DNA Ligation

For ligating restricted fragments both vector and insert were cut to have compatible ends. Prior to ligation blunt end cut vectors were dephosphorylated to avoid undesired religation. For this, appropriate amount of the vector was incubated with 1 µl Calf Intestine Alcaline Phosphatase (CIAP) with 1 µl CIAP buffer in 10 µl reaction volume at 37°C for 1 hour. The CIAP was then removed using the PCR cleanup kit (Qiagen). Vector and insert were used at proportion 3:1 in the ligation reaction in a 10 µl volume. Blunt end ligations of PCR products were performed in presence of 5% PEG-6000. The reactions were incubated at 16°C over night.

2.11.7 Transformation of *E.coli*

Chemically competent cells (100 µl aliquot) were mixed with 1 µl plasmid DNA (50-100 ng) or 10 µl ligation reaction. Reaction was incubated for 30 min on ice, heat shocked for 45 sec at 42°C and placed on ice for 2 more min. 900 µl LB medium was added to the reaction, which was incubated for 60 min shaking at 37°C. Cells were subsequently plated onto LB agar containing appropriate selective antibiotics. Plates were incubated overnight at 37°C.
Alternatively, electrocompetent cells (40 µl aliquot) were mixed with 1 µl plasmid DNA (50-100 ng) or 5 µl ligation reaction (the ligase was prior inactivated at 70°C for 10 min) incubated for 1 min on ice and transferred to a previously cooled electroporation cuvette. The cuvette was placed in the electroporator and cells were electroporated at 1.8 kV. After electroporation, 900 µl LB medium was immediately added to the cells, the suspension was transferred to a fresh 15 ml tube and incubated for 1 hr with vigorous shaking at 37°C. Cells were harvested by brief centrifugation (15 sec, at 14. 000 rpm), resuspended in 200 µl LB medium and plated onto LB agar plates containing the appropriate selective antibiotic. Plates were incubated overnight at 37°C.

2.11.8 Preparation of chemocompetent cells

An overnight culture of *E.coli* strain DH10b was diluted 1:100 in LB medium supplemented with 20 mM $MgSO_4$ and incubated at 37°C until an OD_{600} of 0.4-0.6 was reached. The bacterial cells were centrifuged for 5 min at 4.500 rpm and 4°C and washed in 20% of the primary culture volume icecold TBF1. Afterwards the cells were resuspended in 2% of the primary culture volume icecold TBF2 and incubated on ice for 60 min. Cells were split in 100 µl-aliquots, quickly frozen in liquid nitrogen and stored at -80°C.

2.11.9 Preparation of electrocompetent cells

An overnight culture of *E.coli* XL1-blue was diluted into 400 ml LB medium and incubated for approx. 2-3 hours until culture had reached an OD_{600} of 0.5-0.6.

Bacterial suspension was cooled on ice and cells were harvested by centrifugation for 5 min at 4.500 rpm and 4°C. Pelleted cells were washed twice with 400 ml ice cold 10% glycerol, twice with 40 ml ice cold 10 % glycerol and finally resuspended in 800 µl of the same solution. Cells were aliquoted (40 µl vol) in sterile 1.5 ml tubes, quickly frozen in liquid nitrogen and stored at -80°C.

2.11.10 DNA electrophoresis and isolation of fragments

Agarose gels from 0.8 % to 2 %, dependent on the DNA fragment, were prepared by boiling the desired amount of agarose in 0.5x TAE in the microwave. For visualizing DNA in the gel, 1 µg/ml ethidium bromide was added. If desired, DNA fragments were cut out of the gel under UV light (312 nm) with a sterile scalpel and transferred to a sterile 1.5 ml tube. Gel extraction was performed with the MiniElute Gel Extraction Kit (Qiagen).

2.11.11 Cloning into pUC18 HA

The RT-PCR product described under 3.1.5.1 was cloned blunt end into the *EcoRV* site of the pUC18-HA vector (gift from Dr. M. Hölzel) in order to get a C-terminal fused HA-tag sequence and fully sequenced with primers M13 for and M13 rev (provided by Sequiserve).

2.11.12 Cloning into pRTS

Cloning in this vector was useful for stable transfections of human cells (Bornkamm *et al.*, 2005). First of all, *ppan* was mutated by inverse PCR using primers *Sfi mut fwd* and *Sfi mut rev* in plasmid pUC18-PpanHA in order to eliminate the internal *SfiI* restriction site, considering the human codon usage. *PpanHA* in pUC18-PpanHA was digested with *SfiI* and cloned between the *SfiI* sites of the vector pRTS-SVH-GL, replacing the gene for Luciferase resulting in pRTS-PpanHA (Fig. 6). The correct direction of cloned *ppan* was confirmed by bacterial colony PCR, using primers *pRTS_Sfi+55bp rev* and *Pp-delcoc-for* and restriction enzyme analysis after isolation of the plasmid DNA. pRTS is carrying genes coding for ampicilline resistance to select positive bacterial clones and hygromycine

resistance to select positive human cell clones. Production of PpanHA in stably transfected cells was tested by Western blot analysis.

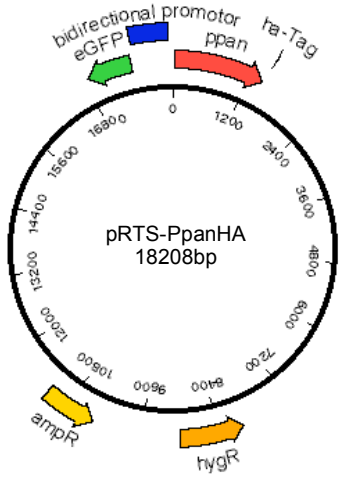

Fig. 6. Model of pRTS-PpanHA (simplified). The bidirectional promoter (in blue) controls simultaneously the expression of both e*gfp* (in green) and *ppan* (in red) and is activated by doxycycline. The plasmid carries a hygromycine resistance gene for selection of stable mammalian cells and an ampicilline resistance cassette for selection of transformed bacteria.

2.11.13 Cloning into pSfiExpress HA

Cloning in this vector is useful for transient transfections of human cells, because the expression of the gene of interest is controlled by the cytomegaly virus (CMV) promoter, which is constitutively active in mammalian cells. The *ppan* cDNA fragment (see under "cloning into vector pUC18 PpanHA") was cloned blunt end in the *Eco*RV digested pSfiExpressHA vector (gift from Dr. Michael Hölzel), which was primarily dephosposphorylated. The right direction of cloned *ppan* in ligated plasmids was tested by bacterial colony PCR and confirmed by sequencing using primers *CMV profor* (provided by Sequiserve) and *PP-delBrixB-for*. pSfiExpress carries a gene coding for kanamycine resistance in *E.coli*.

2.11.14 Cloning into pEGFP-N1

Prior having a functional Ppan specific antibody, the subcellular localization of Ppan was monitored with a Ppan-GFP fusion protein. A plasmid expressing the green fluorescent protein (*gfp*) as a C-terminal fusion to *ppan* under control of the CMV promoter was constructed. For this, full-length *ppan* was cut out from plasmid pUC18-PpanHA with *SacI* and *BstEII* restriction enzymes and cloned in frame with the gene coding for green

fluorescent protein into the pEGFP-N1 vector (gift from Dr. Michael Hölzel). The *ppan*-gfp gene fusion of the plasmid was fully sequenced with primers *CMV profor* (provided by Sequiserve) and *PP-delBrixB-for*. For generation of a PpanΔσ70-GFP fusion, *ppan*Δσ70 was cut out from plasmid pUC18- PpanΔσ70HA with *SacI* and *BstEII* restriction enzymes and cloned in frame with *gfp* as already described for *ppan*.

2.11.15 Cloning into pEGFP-C1

For construction of a GFP-Ppan fusion protein, the primers *BglII fwd* and *SalI rev* were used to amplify *ppan* with the restriction sites *BglII* and *SalI* on the 5' and 3' end respectively. After digestion of the vector pEGFP-C1 (gift from Dr. Rob Chapman, Helmholtz Centre Munich) with the appropriate enzymes and the following ligation with the *BglII-ppan-SalI* fragment, the newly formed plasmids were tested in colony PCR reactions. A pEGFP-C1-Ppan plasmid was sequenced with primers *EGFP-Cfor* and *SV40-pArev* (provided by Sequiserve).

2.11.16 Cloning into vectors for BiFC analysis

Cloning in the vectors pBiFC-YN(1-154) and pBiFC-YC(155-238) (provided by Dr. Tom Kerppola, Howard Hughes Medical Institute, University of Michigan, USA and gift from Dr. Andreas Thomae, Helmholtz Centre, Munich) was useful for performing BiFC analysis in human cells. The principle of BiFC assay function is described in the results of this thesis. A scheme of pBiFC plasmids is shown in figure 7.

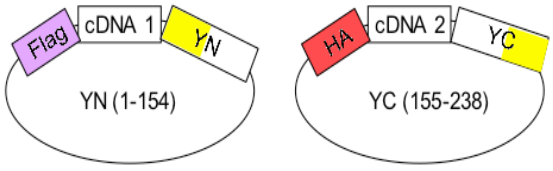

Fig. 7. Plasmids used for BiFC. Models of plasmids YN (1-154) (pBiFC-YN(1-154)) and YC (155-238) (pBiFC-YC(155-238)).

2.11.17 Cloning into vector pBiFC-YN(1-154)

First of all, the original pBiFC-YN155 vector was mutated at the multiple cloning site with inverse PCR using primers *YN EcoRV fwd* and *YN EcoRV rev* in order to get a new

*Eco*RV (GAT ATC) site (Fig. 8). This new *Eco*RV restriction site in pBiFC-YN(1-154)* allows in frame blunt end ligation of any cDNA sequence starting with ATG and ending just prior to the stop codon, because following *yfp* should be successfully transcribed. The old *Eco*RV site was destroyed by the PCR reaction.

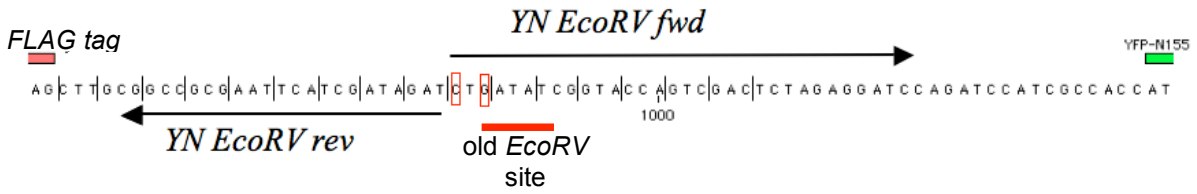

Fig. 8. DNA sequence of the multiple cloning site of the original plasmid pBiFC-YN(1-154). Mutagenesis with primers *YN EcoRV fwd* (ATC ATA..) and *YN EcoRV rev* resulting in substitution of CTG (in red boxes) with ATC by forward primer and formation of a new *Eco*RV site (GAT ATC) for in-frame cloning of every cDNA starting with ATG and ending one triplet just before stop codon to allow following *yfp* to be translated. The old *Eco*RV site is underlined in red.

The *ppan* cDNA fragment (see under "cloning into vector pUC18 PpanHA") was cloned blunt end into the *Eco*RV digested pBiFC-YN(1-154)* vector which was primarily dephosphorylated. Ligated new plasmids were controlled by bacterial colony PCR to confirm the successful cloning and simultaneously the direction of cloned *ppan* with primers *YN col fwd* and *Pp-delcoc-rev*. A plasmid carrying *ppan* in the right direction was sequenced with primers *CMV profor* (provided by Sequiserve) and *YN 1094 (rev)* and used for BiFC analysis. For the sake of simplicity this plasmid is decribed as YN Ppan in this work.

2.11.18 Cloning into vector pBiFC-YC(155-238)

Cloning in this vector was useful for performing BiFC analysis in human cells. As done with the original pBiFC-YN155 vector, the original pBiFC-YC(155-238) vector was mutated at the multiple cloning site with inverse PCR using primers *YC EcoRV fwd* and *YC EcoRV rev* in order to generate a new *Eco*RV (GAT ATC) site (Fig. 9). This new *Eco*RV restriction site in pBiFC-YC(155-238)* allows, similar to pBiFC-YN(1-154)*, in frame blunt end ligation of any cDNA sequence starting with ATG and ending just prior to the stop codon, to allow the carboxy-terminal part of *yfp* to be successfully translated.

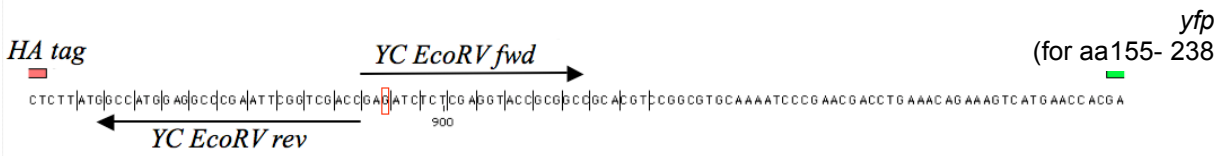

Fig. 9. DNA sequence of multiple cloning site of the original plasmid pBiFC-YC(155-238). Mutagenesis with primers *YC EcoRV fwd* (GAT ATC..) and *YC EcoRV rev* resulting in substitution of GA**G** (in red box) with GA**T** by forward primer and formation of a new *Eco*RV site (GAT ATC) for in-frame cloning of every cDNA starting with ATG and ending one triplet just before stop codon to allow following *yfp* to be translated.

The *ppan* cDNA fragment (see under "cloning into vector pUC18 PpanHA") was cloned blunt end into the *Eco*RV digested pBiFC-YC(155-238)* as described for pBiFC-YN(1-154)*. The colony PCR was performed using the primers *YC col fwd* and *Pp-delcoc-rev*. The new plasmid was sequenced with primers *YC781 (fwd)* and *YC998 (rev)* and used for BiFC analysis. The plasmid coding for the Ppan-YFP fusion in pBiFC-YC(155-238)* is named YC Ppan in this work.

2.11.19 Cloning of *pes1*, *bop1*, *wdr12* and *hdm2* into vector pBiFC-YC155

cDNA fragments of *pes1* (NM_ 014303.2), *bop1* (NM_013481.1), *wdr12* (NM_018256.2) and *hdm2* (NM_002392.2) were amplified from total cDNA of U2OS cells. Cloning into the pBiFC-YC(155-238)* plasmid was similar to that described for YC Ppan (amplification PCR and cloning were done by Dr. Michaela Rohrmoser, Helmholtz Centre Munich). Resulting plasmids were named for simplicity YC Pes1, YC Bop1, YC WDR12 and YC Hdm2.

2.11.20 Mutagenesis of human *ppan*

The mutagenesis of *ppan* was done by inverse PCR in pUC18-Ppan HA with specific flanking primers as indicated at Tab. 3. The genes encoding the new truncated forms of Ppan were subcloned into pSfiExpress and pRTS-SVH-GL, as already described for *ppan*.

Tab. 3. Mutagenesis of *ppan* for generation of new Ppan forms.

ppan mutagenesis (deletion of nucleotides)	Primers for mutagenesis of cDNA	new Ppan forms (deletion of amino acids)
Δ 1-87	*Pp-delN-for* *Pp-end*	Ppan ΔN (1-29)
Δ 511-903	*Pp-delBrixB-for* *Pp-delBrixB-rev*	Ppan Δσ70 (172-301)
Δ 91-513	*Pp-delBrixA-for* *Pp-delBrixA-rev*	Ppan ΔBrixA (31-171)
Δ 904-1041	*Pp-delcoc-for* *Pp-delcoc-rev*	Ppan Δcoc (304-342)
Δ 1019-1419	*Pp-start* *Pp-delC-rev*	Ppan ΔC (343-473)

2.12 Working with RNA

2.12.1 Preparation of RNAse free solutions

For RNAse free water and solutions diethyl pyrocarbonate (DEPC) was added in a final concentration of 0.1% and after incubation at 37°C over night, autoclaved.

2.12.2 Isolation of RNA

Total RNA from adherent cell lines was isolated using the RNeasy® Mini Kit (Qiagen). For extraction from cultured cell lines, cells of two six-wells of a six-well-plate were lysed by the addition of 350 µl RLT buffer. For further homogenization, samples were passed through a QIAshredder spin column placed in a 2 ml collection tube (2 min at 14.000 rpm). 1 vol of 70 % ethanol was added to the homogenized lysate and mixed thoroughly by pipetting. The lysate was applied to a RNeasy mini column placed in a 2 ml collection tube and centrifuged for 15 sec at 10.000 rpm. The flow-through was discarded and the total RNA bound to the column was washed once with 700 µl RW1 buffer and twice with 500 µl RPE buffer. The first and second centrifugation steps were carried out for 15 sec and the third for 2 min at 10.000 rpm, the flow-through was discarded after each washing step. Finally, to elute the RNA from the RNeasy column (placed in a fresh 1.5 ml tube), 30 µl RNase-free H_2O was applied to the column and incubated for 1 min at room temperature. RNA was

collected by centrifugation (1 min at 10.000 rpm). RNA concentration was determined photometrically. The isolated total RNA was stored at -20°C.

2.12.3 Electrophoresis of RNA and Northern Blot

RNA was electrophoretically separated in 1 % agarose-formaldehyde gels, containing 1x MOPS buffer and 6.2 % Formaldehyde. Equal amounts of RNA were 1:1 mixed with 2x RNA sample buffer and denatured for 10 min at 65°C, with subsequent placing on ice. Electrophoresis was performed at 90-120 V and gels were photographed.

For Northern Blot, RNA was blotted on Nylon Membranes (Hybond N^+, Amersham) in 10x SSC Buffer in a capillary transfer system over night. First the RNA gel was placed with gel slots down onto a pile of blotting paper GB003 having its ends in a 10x SSC-containing reservoir. The membrane was soaked in 10x SSC and placed blebfree onto the gel and covered by 2 more layers of G003 blotting paper. Free surface around the membrane was sealed by Saran transparent foil. An 8 cm-thick block of paper towels was placed onto the blotting paper, covered by a leveled weight glass to ensure equal distribution of pressure on the blot. Finally, a 500 g weight was distributed on the glass plate. Transfer was performed over night at room temperature. Next day, after briefly drying the membrane at room temperature, the RNA was UV-cross-linked with the Stratalinker (program: auto cross link).

2.12.4 Hybridisation with phospho-labeled probes

For detecting the *ppan* mRNA expression in T98G cells, a probe for *ppan* was labelled with α^{32}P-dCTP (3.000 Ci/mmol) using the High-Prime-Kit (Roche). Briefly, 1 µl of 1 pmol/µl *Sfi*I-Fragment of pUC18-PpanHA containing *ppan* was mixed with 8 µl H_2O and incubated for 5 min at 95°C with subsequent placing on ice. 4 µl High-Prime reaction mixture, 3 µl dATP, dGTP, dTTP mixture (prepared by making a 1+1+1 mixture of provided solutions) and 5 µl of α^{32}P-dCTP (50 µCi) were added to the probe and the reaction was incubated at 37°C for 10 min. 2 µl 0.2M EDTA were added and probes were purified with MicroSpin S-200HR columns.

In order to visualize pre-rRNA precursors probes were used, which are specific for

the internal transcribed spacers 1 and 2 (ITS-1). The sequences of the probes were:

ITS-1 5'-CCT CCG CGC CGG AAC GCG CTA GGT ACC TGG ACG GCG GGG GGG CGG ACG-3'

ITS-2 5'- GCG GCG GCA AGA GGA GGG CGG ACG CCG CCG GGT CTG CGC TTA GGG GGA-3'

For the labelling reaction 1 µl of the 10 µM DNA-oligonucleotide was mixed with 2 µl H_2O and heated at 95°C for 3 min, with subsequent cooling on ice. 1 µl T4 polynucleotide kinase (PNK), 1 µl PNK buffer A and 5 µl (50 µCi) γ^{32}P-ATP were added and the reaction was performed at 37°C for 30 min. After addition of 40 µl H_2O probes were purified with MicroSpin S-200HR columns.

For the Northern Blot analysis, the nylon membranes with the cross-linked RNA (2.12.3) were prehybridized in hybridization tubes (DNA inwards) in 20 ml Church Buffer for 60 min at 65°C. The labelled probes were denatured for 5 min at 95°C, cooled in ice and resuspended in 10 ml Church Buffer. Northern blot hybridization occurred at 65°C over night in a roller oven. The next day probes were collected and membranes were washed at 65°C for 10 min with 2x SSC/0.1 % SDS and afterwards for 10 min with 0.2x SSC/0.5% SDS. Finally membranes were air dried, wrapped in a transparent membrane and placed in a x-ray cassette. For film exposure (1-5 days) the cassette was kept at -80°C.

2.12.5 Synthesis of cDNA

Total RNA was isolated from U2OS cells grown at 80 % confluency on a 15 cm culture dish as described in 2.12.2 2 µl of isolated RNA were incubated with 1 µl oligo-dT primer (500 µg/ml), 1 µl dNTP mix (10 mM each) in 10 µl volume at 65°C for 5 min and subsequent chilled on ice. The RNA mixture was collected by brief centrifugation and 4 µl RT-Buffer (5x), 2 µl 0.1 M DTT and 1 µl RNAsin 40 U/µl (RNAse Inhibitor) were added, gently mixed and incubated for 2 min at 42°C. For reverse transcription 1 µl of Superscript II (Invitrogen) was used. Reaction took place at 42°C for 50 min. The enzyme was inactivated at 70°C for 15 min and cDNA was kept at -20°C. 1.5 µl of cDNA was used for subsequent PCR reaction.

2.12.6 Knock-down with siRNA

H1299 and U2OS were seeded at a density of 200.000 cells in 6-well plates the day before transfection. 5 μl of 20 μM control, *ppan* or *hrrp6*-specific siRNA were diluted in 150 μl OptiMEM (Invitrogen). 150 μl OptiMEM containing 4 μl Oligofectamine (Invitrogen) was added and the mixture was incubated for 15 min at room temperature. 600 μl OptiMEM was added and applied to cells after aspiration of the culture medium. Cells were incubated with the transfection mixture for 5–6 h. The following sequences were used (sense):

control UUC UCC GAA CGU GUC ACG UdTdT

ppan (3'UTR) CUC GGU UUC CUU UCA UAA AdTdT

2.13 Working with proteins

2.13.1 Production of a monoclonal antibody directed against human Ppan

A panel of monoclonal antibodies raised against the Ppan protein was generated in cooperation with Dr. Elisabeth Kremmer from the Institute of Molecular Immunology, Helmholtz Centre Munich. A synthetic peptide identical to the N-terminal tail of Ppan with the sequence MGQSGRSRHQKRA was used to immunize rats. Many clones were tested for reactivity to endogenous and overproduced Ppan in Western blot analysis and immunofluorescence and clone 1C3 was elected for further studies.

2.13.2 Lysis under denaturing conditions

Adherent cells of a 6 well were washed once with PBS and lysed when 80% confluent with 50 µl 2x Laemmli loading buffer and collected in 1.5 ml tubes. Lysates were boiled for 5 min at 95°C, then sonicated for 15 sec (output 4, duty cycle 50%). Lysates were kept at -20°C until use. Just prior use lysates were again boiled for 5 min at 95°C and spun down for 2 min at 14.000 rpm to precipitate insoluble material. 5-10µl of lysates were applied to every gel slot.

2.13.3 Denaturing Polyacrylamide Gel Electrophoresis (PAGE)

SDS-Polyacrylamide (SDS-PAGE) Gel Electrophoresis was used for separation of proteins under denaturing conditions. The concentration of the gels used was determined according to the effective range of separation of SDS-PAGE shown below:

Acrylamide concentration (%)	Linear range of separation (kDa)
15	12-43
10	22-68
8	31-97

For the resolving gel the following components were mixed together:

Components (10 ml)	8 %	10 %	15 %
30 % Acrylamide mix	2.6 ml	3.3 ml	5 ml
H_2O	2.3 ml	1.6 ml	-
Tris/SDS pH 8.8	5 ml	5 ml	5 ml
10 % APS	85 µl	85 µl	85 µl
TEMED	10 µl	10 µl	10 µl

Stacking gel was prepared by mixing the following components:

Components (3.8 ml)	stacking gel 4 %
30 % Acrylamide mix	0.5 ml
H_2O	1.35 ml
Tris/SDS pH 6.8	1.88 ml
10 % APS	22.5 µl
TEMED	5 µl

Proteins were separated at 30 mA.

2.13.4 Western Blot

Cellular lysates were electrophoresed on 8-15 % SDS-PAGE gels and transferred to a nitrocellulose membrane using the wet system. Membranes were pre-wet in transfer buffer. Transfer of protein from the gel to the membrane occurred under electric current from the negative to the positive pole at 0.45 A for 1.5 hours. The membranes were shortly dried and stained with Ponceau S solution to verify equal loading. After extensive washes with TBST, membranes were blocked for non-specific binding sites with 5 % nonfat dried milk for 0.5 hour at room temperature. Immunoblotting was carried out with specific antibodies diluted in 5 % nonfat dried milk or 5 % BSA in TBST at optimal concentration. Incubation with primary antibody was carried out in most cases overnight at 8°C followed by three 5 min washing steps with TBST. Secondary antibodies conjugated with horseradish peroxidase (HPR) were used for detection of the primary antibody. Incubation was carried out for 1 hour at room temperature followed by extensive washing steps as described above. Finally, the proteins were detected by incubating the membrane with enhanced or super enhanced chemiluminescent reagent for 5 min at room temperature. The membrane was then wrapped in foil and placed in a x-ray film cassette. Exposition of the film varied between 30 sec and 4 min.

2.13.5 Lysis under native conditions for immunoprecipitations

For every immunoprecipitation reaction adherent cells of two 15 cm cell culture dishes were washed once with cold PBS and lysed directly on the plate with each 0.5 ml Co-IP Lysis Buffer. Cells were released with a cell scraper and placed in a 1.5 ml tube for 10 min at room temperature. Lysates were sonicated twice for 15 sec (output 4, duty cycle 50%) with inbetween 1 min pause on ice and spun down for 15 min at 14.000 rpm and 4°C to precipitate insoluble material. 50 µl of the lysate were mixed with 50 µl 2x Laemmli loading buffer and used as input control. 900 µl of lysates were applied to Protein G beads pre-coupled with antibody. For this 25 µl Protein G bead slurry (in 20 % ethanol) was washed twice in Co-IP wash buffer at 6.000 rpm for 1 min and incubated with 500 µl antibody supernatant or 1 µl of concentrated antibodies in 500 µl Co-IP buffer for 1 hour at 8°C on a roller. After 3 washes with Co-IP wash buffer, beads were incubated with cell lysates overnight at 8°C on a roller.

Next day beads were washed 5 times with Co-IP buffer supplemented freshly with PMSF and resuspended in 50 µl of Co-IP wash buffer plus 50 µl of 2x Laemmli loading buffer. Lysates were kept at -20°C until use. Just prior use they were boiled for 5 min at 95°C with subsequent cooling on ice and briefly spun down.

2.13.6 Isolation of nucleoli

Nucleoli of HepG2 cells were prepared according to Andersen *et al*. (2002). All centrifugations steps were done in a HS-4 rotor, Sorvall centrifuge, at 4°C. Briefly, cells were plated on ten tissue culture dishes with a diameter of 14 cm until >90% confluence. Cells were harvested by trypsinization. The harvested cells were pooled into 50 ml Falcon tubes and washed 3 times with ice-cold PBS at 218 g (1.000 rpm). After the final PBS wash, cells were resuspended in 5 ml of Buffer A and incubated on ice for 5 min. Swallen but not burst cells were observed under the microscope. The cell suspension was transferred to a pre-cooled 7 ml Dounce tissue homogenizer tissue grinder with pestle B (clearance 0.0008-0.00022 in) and homogenized with 10 strokes on ice. Homogenized cells were centrifuged at 218 g (1.000 rpm) for 5 min. The pellet was resuspended with 3 ml S1 solution and layered carefully over 3 ml of S2 solution, keeping the two layers cleanly separated. After centrifugation at 1.430 g (2.700 rpm) for 5 min, the nuclear pellet was resuspended in 1 ml of S2 solution by pipetting up and down and 50 µl were mixed with 2x Laemmli loading buffer for western blot analysis. 2 ml of S2 solution were added and nuclei were sonicated on ice for 6 x 10 second bursts (with 10 second intervals between each burst) at power setting 4 and output control 50%. Sonicated suspension was layered carefully on 3 ml of S3 solution keeping the two layers cleanly separated. Probe was then centrifuged at 3.000 g (4.000 rpm) for 10 min. The pellet contained the nucleoli, which were washed in 0.5 ml S2 solution and centrifuged at 1.430 g (2.700 rpm) for 5 min. Finally the pellet containing purified nucleoli was resolved in 100 µl S2 solution plus 100 µl 2x Laemmli loading buffer.

2.13.7 Immunofluorescence

For immunofluorescence microscopy experiments approximately 80.000 cells were plated on 18 mm round and sterile (90 s, program STR, GS Gene Linker^{TM} UV

Chamber) cover slips in 12 well slots. For staining overproduced proteins approximately 50.000 cells were seeded per slip and induced 24 hours with 1 µg/ml doxycycline. The cells were washed with PBS, fixed with 3.7% paraformaldehyde for 5 min at room temperature, washed again with PBS, permeabilized with 0.5 % Triton X-100 in PBS for 10 min at room temperature and subsequent blocked in 10 % FBS in PBS for at least 30 min at room temperature (alternatively over night at 4°C). Primary (and secondary) antibodies were diluted in 1.5 % FBS in PBS and incubated from 1 hour (α-HA, α-FLAG) to overnight (antiserum supernatant, α-p53, α-NPM, α-Fibrillarin) at 8°C in a humidified chamber. Unbound antibody was released with three 5 min-washes in 0.1 % Triton X-100 in PBS and cells were incubated with species specific secondary antibody, conjugated with Cy3, Cy5 (1:300) or Alexa488 (1:400) at room temperature for 1 hour in a dark humidified chamber. After three 5 min-washes in a solution of Triton X-100 0.1 % (in PBS) and DNA was counterstained with 0.1 µg/ml DAPI for 2 min. Cells were mounted in Dako mounting medium, placed on microscope slides and sealed with nail polish to avoid run dry. Microscope slides were kept at 4°C and dark.
For RNAseA or DNAseI in-cell-digestion experiments, cells were permeabilized with 0.1% Triton-X-100 in PBS for 15 min at room temperature and incubated with 15 µg/ml RNAseA or DNAseI (in PBS) for 30 min at 37°C, before they were fixed with paraformaldehyde. After the fixation, the protocol described above was used.

2.14 Cell culture

Mammalian cells were cultured in Dulbecco's modified Eagle Medium supplemented with 10% fetal bovine serum and antibiotics at 37°C and 8% CO_2. Split ratio varied between 1:4 and 1:10. To exclude mycobacterial infections of adherent cells sparfloxacine (1 µg/ml) was added to the medium. To avoid bacterial resistance to this component, it was used only periodically. For cell preservation, cells were resuspended in 90% FBS, 10% DMSO, subsequently freezed at -80°C and for long term keeping transferred to liquid nitrogen.

2.14.1 Transfection of mammalian cells

Twenty-four hours before transfection, mammalian cells were subcultured and seeded in a 6-well plate at the density of $2x10^5$ cells per well. Transfection experiments were carried out using 2 µg plasmid DNA and 5 µl of Polyfect (Qiagen) in the presence of serum, according to the manufacturer's instructions. An exception was the transfection of HepG2 cells for the BiFC analysis where 0.5 µg plasmid DNA was mixed with 1.5 µg pUC18 Ppan HA and complexed by 5 µl of FuGene HD transfection reagent (Roche). Briefly, formation of DNA-carrier complexes was performed in 100 µl serum-free OptiMEM (Invitrogen). 15 min later 500 µl DMEM was added and DNA complexes were dropped carefully to the cells. Selection of cells was started with hygromycine (100 µg/ml) or puromycine (1 µg/ml) containing medium 24 hours after transfection. To obtain stable transfected cells the selective antibiotics were applied for at least 10-14 days.

2.15 Microscopy

2.15.1 Fluorescence microscope

Cells were observed under an automated Axiovert 200M microscope (Carl Zeiss, Jena, Germany) equipped with single-band pass filter sets for visualization of DAPI, Texas red (cy3) and Alexa 488 (GFP of FITC) fluorescence. Images were recorded using the Openlab 3.08 software (Improvision, Coventry, UK) and processed with Openlab Demo (free software) or Image J (version 10.2, (http://rsb.info.nih.gov/ij/)).

2.15.2 Confocal laser scanning microscope

The confocal laser scanning microscope Leica LSCM SP2 with software Leica-TCS 2.61 was used in order to obtain high-resolution optical images, for BiFC analysis and co-localization studies. Images were taken with objective HCX PL APO 63x 1.4 at 400 Hz scan speed, with an average scan of 4 pictures. The argon laser was set at

minimum level. For YFP monitoring of BiFC analysis the Alexa 488 channel (529-560 nm) and photomultiplier PMT 2 at 750 mV was used.
Three-dimensional pictures were taken by defining end and start point of scanning and 0.25 µm thick sections. The average for each picture was set at 1 and a sequential modus with the different laser “between frames” was chosen.

For detection of different stainings following settings were preferred:

Detection of:	Excitation (laser)	Emission	Laserpower
DAPI	405 nm (UV)	420-470 nm	50%
Cy3 (PMT 3)	543 nm (Ar/HeNe)	588-617 nm	40%
Cy5 (PMT 3)	633 nm (Ar/HeNe)	660-694 nm	40%
Alexa488 (PMT 2)	488 nm (Ar/HeNe)	529-560 nm	40%
ITC (interference contrast)	405 nm (UV)		40%

The YFP signal of BiFC analysis was monitored at the Alexa 488 channel (529-560 nm). The photomultiplier PMT 2 was adjusted to 750 mV.

3. Results

3.1 Generation of a Ppan specific monoclonal antibody

Monoclonal antibodies are a key tool for identification and characterization of proteins, since they recognize only a single epitope of interest. A synthetic peptide with the sequence MGQSGRSRHQKRA, corresponding to amino acids 1-13 of the N-terminus of Ppan, was used to immunize rats (E. Kremmer, Helmholtz Centre Munich). Several hybridoma supernatants were tested in Western blot analysis. Monoclonal antibodies of hybridoma clone 1C3 detected the endogenous Ppan protein (approx. 62 kDa) in U2OS cells. In cells transfected with a specific small interfering RNA (siRNA) for *ppan*, the signal intensity of the Ppan protein decreased significantly, supporting the specificity of the antibody (Fig. 10a). U2OS cells were also stably transfected with an expression vector for Ppan, pRTS-Ppan. Antibody 1C3 recognized the overexpressed protein with a molecular weight of about 64 kDa (Fig. 10b). The recombinant Ppan has additionally a C-terminally fused HA-tag, which explains the slower migration in polyacrylamid gels.

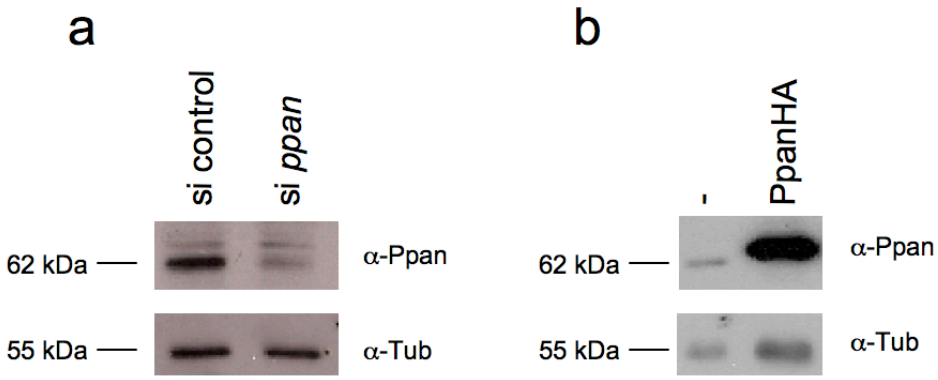

Fig. 10. The Ppan antibody produced by hybridoma clone 1C3 recognizes specifically Ppan. (a) U2OS cells were transfected with control- or *ppan*-specific siRNA. (b) Stably transfected U2OS cells with pRTS-Ppan were treated with 1 μg/ml doxycycline to induce the expression of PpanHA for 24 hours. Total cell lysates were analysed by Western blot using the Ppan-specific antibody 1C3. Tubulin was used as loading control.

The antibody was only stable for approximately two months at 4°C and therefore this work was done with several charges of freshly made hybridoma supernatant, which

differed in antibody titer. The antibody was used always in excess and incubated for at least 48 hours with antigen to allow reproducible results.

3.2 Expression and localization of Ppan

Expression of *ppan*

Normally, cells require growth factors for proliferation in culture. The fetal calf serum (FCS) is usually provided as a growth factor supplier in the medium of cultured cells. In the absence of serum many cells entry a non-dividing state, the G_0 phase, which is characterized by low metabolic activity. The addition of FCS induces the proliferation of cultured cells and is accompanied by changes in gene expression (Iyer *et al*., 1999). The cellular response to serum involves the induction of genes for transcription factors, like c-Myc, and reduced expression of transcription regulators involved in maintaining the cells in the G_0 phase. Since *ppan* has been described as a target gene of the transcription factor c-Myc, its response to growth factor stimulation was studied. The human glioblastoma T98G cell line can be synchronized by serum starvation without activation of apoptotic pathways. Serum deprived T98G cells were incubated with medium containing FCS and the total RNA was isolated at different time points following restimulation. Northern blot analysis with a *ppan* specific probe showed an induction of *ppan* expression four hours after restimulation (Fig. 11). The hybridization with the *ppan* specific probe revealed a single detectable transcript of approximately 1.4 kb.

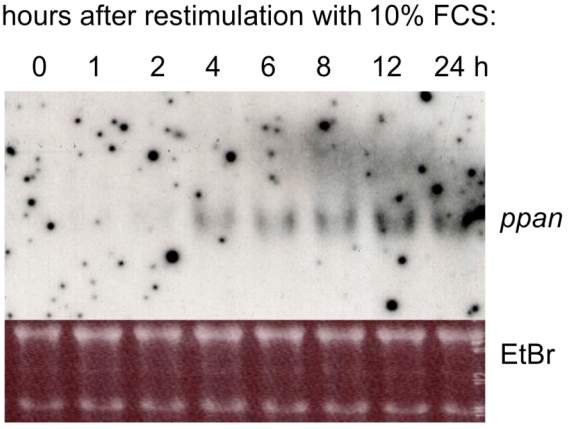

Fig. 11. Expression of *ppan* increases in restimulated T98G cells after serum starvation. T98G cells were serum-starved for seventy-two hours and restimulated in medium containing fetal calf serum. Total RNA was isolated at indicated time points. Northern blot analysis was performed with a specific probe for *ppan*.

Thus, the expression of the *ppan* gene is associated with proliferation of T98G cells.

The expression of *ppan* was studied in a panel of different cell lines. Whole protein lysates of a proliferating lung cancer cell line (H1299), a cervical adenocarcinoma cancer cell line (HeLa), a human leukemic cell line (J6), Burkitt's lymphoma cell lines (Mutu (-), Mutu I and III, EBV 1.25, Raji, BL60, BL70, Namalwa, CHEP, ww2, DG-75 and Akata) and a B-lymphoblastoid cell line (721) were analyzed by Western blot analysis (Fig. 12)

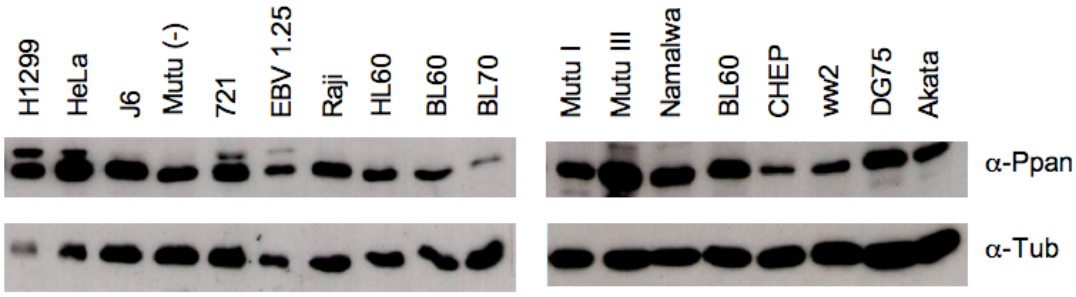

Fig. 12. Expression of Ppan protein in different proliferating cell types. Western blot analysis of proteins from distinct cancer cell lines using the specific Ppan antibody. Tubulin was used as a loading control.

The Ppan protein was expressed at comparable levels in all studied cell lines. Only the BL70 cell line showed reduced Ppan protein levels, when comparing with the levels of the other cell lines and the loading control tubulin. Furthermore, the antibody against Ppan recognized an additional slower migrating form in the cell lines H1299, HeLa, 721 and EBV 1.25. This could indicate a modification of the protein or the existence of an isoform of Ppan. In conclusion, Ppan is expressed in a broad range of cells, probably in a proliferation associated manner.

Localization of Ppan

The yeast homologue of Ppan, Ssf1, localizes to nucleoli (Kim and Hirsch, 1998) and proteomic analysis of the human nucleolus revealed that human Ppan is a component of purified nucleoli (Andersen *et al*., 2002). In order to study the cellular distribution of Ppan, the human hepatocellular carcinoma cell line HepG2 was used for the immunostaining, because it is very suitable for microscopic imaging due to its

large nuclei and nucleoli. In asynchronously growing HepG2 cells, Ppan localized in all cells at a first glance nuclear (Fig. 13). In the majority of the cells Ppan stained more strongly the nucleoli, whereas the nucleolar protein Pes1 localized in all cells predominantly nucleolar. To quantify the nucleolar localization more precisely, two hundred cells were carefully examined for localization of Ppan or Pes1. The percentage of cells showing a protruding nucleolar staining of Ppan was found to be 77 %. All cells showed a predominant nucleolar staining of Pes1.

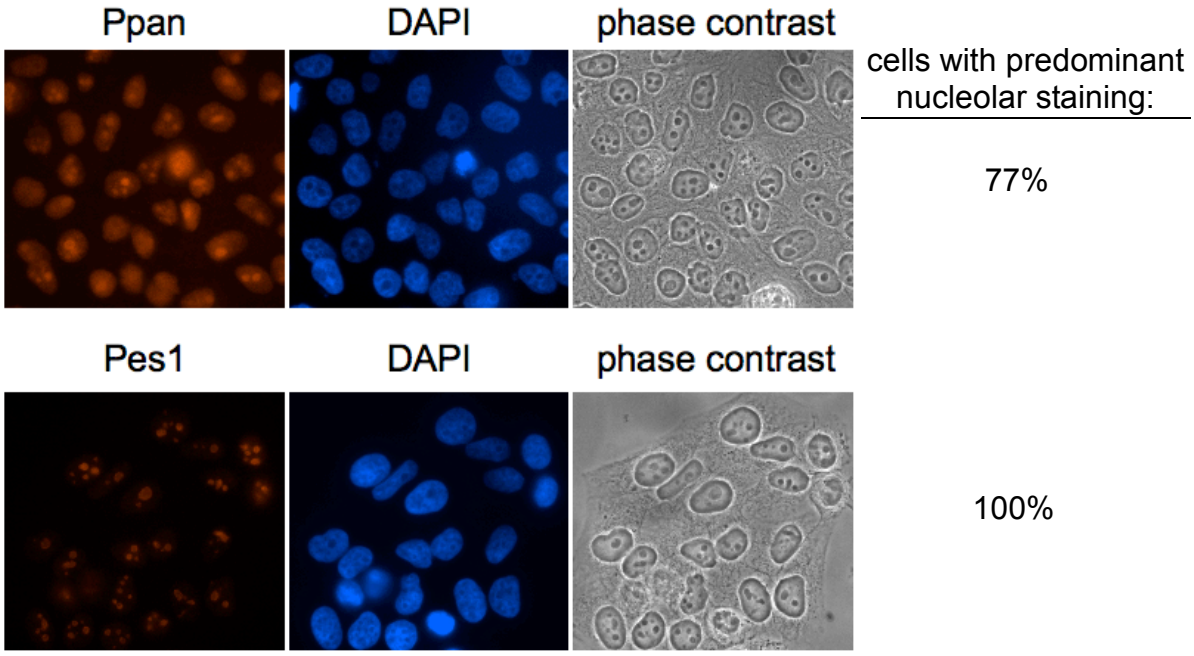

Fig. 13. Immunofluorescence analysis of endogenous Ppan and Pes1. An asynchronous culture of HepG2 cells was fixed with paraformaldehyde and incubated with specific antibodies for Ppan (1C3) and Pes1 (8E9). DNA was counterstained with DAPI.

To confirm the cellular localization of Ppan, two fusion proteins with the green fluorescent protein (GFP) at the N- or C-terminus of Ppan (GFP-Ppan and Ppan-GFP, respectively) were constructed. U2OS cells were used for this approach, because they are very suitable for transient transfections. Ppan-GFP, as well as GFP-Ppan localized in transfected U2OS cells in nuclei and prominently nucleolar, indicating that the N- or C-terminal fusion of GFP to Ppan did not alter the localization behaviour of Ppan (Fig. 14).

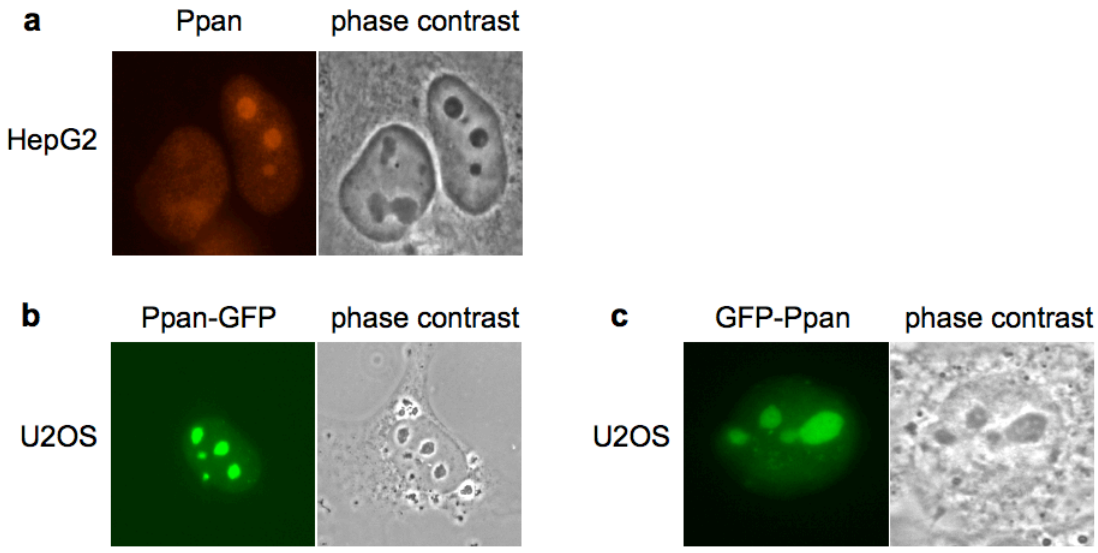

Fig. 14. Localization of the Ppan protein fused to the green fluorescent protein (GFP). (a) Endogenous Ppan in HepG2 cells stained with monoclonal antibody 1C3. (b) Localization of Ppan-GFP and (c) GFP-Ppan fusion proteins in transiently transfected U2OS cells.

In interphase cells Ppan localizes in the nucleus and nucleoli. To analyze the localization of Ppan during mitosis, HepG2 cells were examined in the metaphase. Ppan surrounded the condensed chromosomes in the metaphase plate, indicating that it is associated with the perichromosomal space during mitosis (Fig. 15).

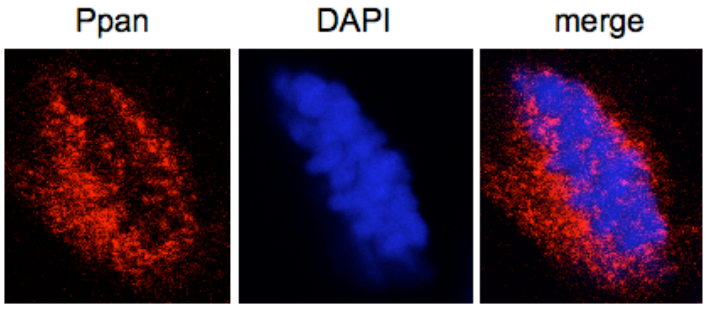

Fig. 15. Localization of Ppan during the metaphase of mitosis. Immunofluorescence microscopy of a single mitotic HepG2 cell, fixed with paraformaldehyde. Ppan was stained with 1C3 monoclonal antibody and DNA was counterstained with DAPI.

3.3 The nucleolar localization of Ppan is dependent on RNA but not DNA

Nuclear proteins can either be soluble or attached to nuclear structures. An example

is the tumor suppressor p53, which can be soluble in the nucleoplasm or be bound to nucleoplasmic complexes, like transcription complexes, or even be bound within the nucleolus (Rubbi and Milner, 2000; Klibanov *et al.*, 2001). To study whether Ppan is soluble or attached to nuclear structures, HepG2 cells were either directly fixed or permeabilized prior to fixation to remove any soluble proteins. The fixed cells were then incubated with the Ppan specific antibody 1C3. Non-permeabilized and permeabilized cells stained nucleoplasmic and some nucleolar for Ppan (Fig. 16a and b).

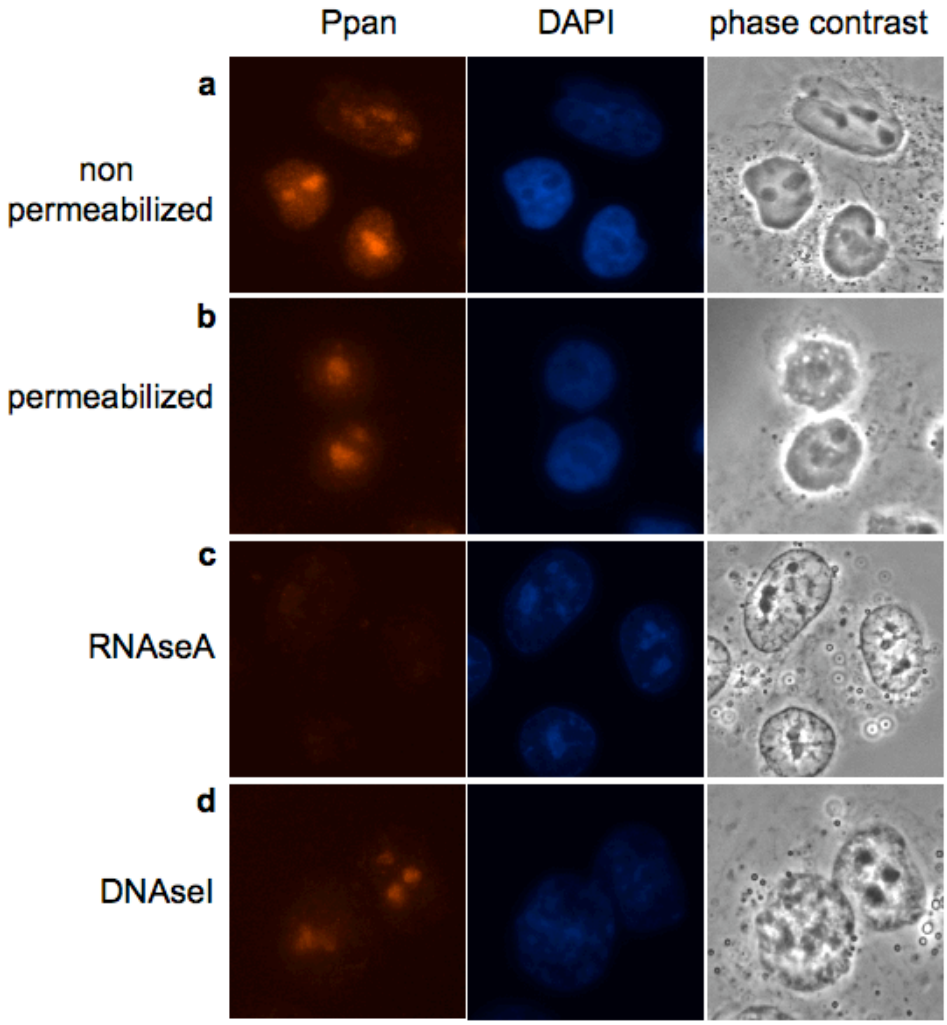

Fig. 16. Nucleolar localization of Ppan is dependent on RNA but not DNA. Immunofluorescence staining of Ppan. HepG2 cells were fixed with paraformaldehyde (a) or permeabilized (b,c,d) and treated with 15 μg/ml RNAseA (c) or 15 μg/ml DNAseI (d) for 30 min prior to fixation. Ppan was immunostained with the 1C3 monoclonal antibody. DNA was counterstained with DAPI.

The yeast homolog of Ppan, Ssf1, binds specifically to 27S pre-rRNA. To explore whether the localization of Ppan to the nucleolus involves binding to RNA, HepG2

cells were permeabilized and incubated with RNAseA for 30 min, followed by fixation and subsequent immunostaining with the specific Ppan antibody. Staining of Ppan was strongly diminished after treatment with RNAseA, suggesting that tethering of Ppan to the nucleoli is mediated by RNA-containing structures (Fig. 16c).
To study if Ppan is associated to DNA in the nucleoli, permeabilized cells were incubated with DNAseI. Immunostaining showed that the nucleolar localization of Ppan was independent of DNA (Fig. 16d).

In summary, the expression of Ppan is associated with cell proliferation, Ppan localizes nuclear and in 77 % of cells predominantly in nucleoli. Interestingly, the nucleolar localization of Ppan is dependent on RNA but not DNA. To shed light on the domain functions of Ppan and particularly on the domain(s) involved in nucleolar localization, several deletion mutants were generated.

3.4 Generation of deletion mutants of Ppan

The N-terminus, the left- and right-hand side of the Brix-domain, the coil-coil domain and the C-terminus with the two AT-hooks of Ppan were deleted (Fig. 17). *Ppan* wildtype and the mutants were cloned in the vector pRTS for conditional gene expression.

3.5 Expression and localization of mutant Ppan proteins

To verify that Ppan and the mutant Ppan proteins were correctly translated, human U2OS cells were stably transfected with pRTS coding for Ppan or the mutants. Gene expression was induced for twenty-four hours with doxycycline (Fig. 18). Whole cell lysates were separated electrophoretically and blotted for detection with antibodies recognizing the HA-tag.
PpanHA has an apparent molecular weight of 64 kDa, PpanΔBrixA of 48 kDa, PpanΔσ70 of 44 kDa, PpanΔcoc of 50 kDa, PpanΔN of 54 kDa, and PpanΔC of 36 kDa. Ppan and all deletion mutants were expressed and appeared to be stable in U2OS cells, since no degradation was seen. Furthermore, the proteins migrated at

expected positions and were present in equal levels when compared to the loading control tubulin.

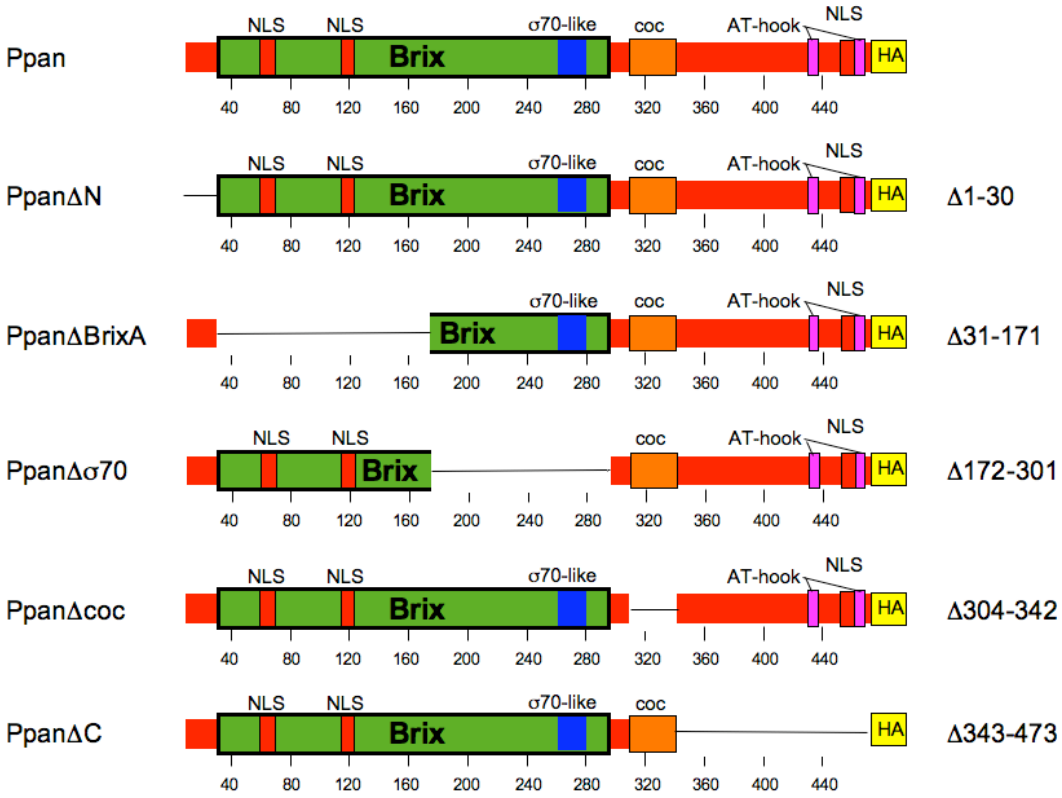

Fig. 17. Human Ppan and the deletion mutants. PpanΔN lacks the first 30 amino acids, PpanΔBrixA the amino acids 31-171, PpanΔσ70 the amino acids 172-301, PpanΔcoc the amino acids 304-342 and PpanΔC the amino acids 343-473. Ppan and the Ppan mutants were constructed with a C-terminal HA-tag.

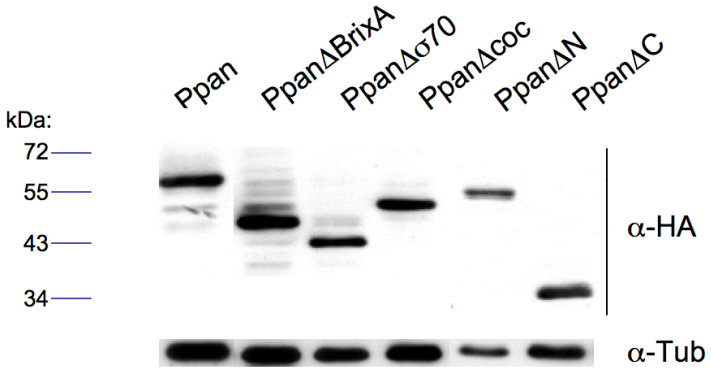

Fig. 18. Western blot analysis of Ppan and the Ppan deletion mutants. U2OS cells were stably transfected with pRTS coding for Ppan and the deletion mutants. Twenty-four hours after induction of gene expression with doxycycline, cell lysates were electrophoresed and immunoblotted for detection with α-HA and α-tubulin antibodies.

Next the localization of Ppan and its deletion mutants was investigated in order to identify domains responsible for localization of the protein. Rat TGR-1 fibroblasts were used, because they can be transfected with high efficiency and are good selectable with antibiotics. TGR-1 cells were stably transfected with pRTS coding for Ppan and the deletion mutants and the expression of the genes was induced for twenty-four hours with doxycycline. The recombinant Ppan localized in the nucleus and predominately in nucleoli of the cells (Fig. 19). PpanΔBrixA showed the same staining pattern like the wildtype protein, indicating that the N-terminal part of the Brix domain is not essential for nucleolar localization. Interestingly, PpanΔσ70 stained the nucleoplasm in spot-like structures, excluding the nucleoli. The RNA binding σ70-like motif seems to be therefore important for nucleolar localization of Ppan. This phenotype will be discussed later on. The Ppan mutant lacking the coil-coil domain, PpanΔcoc, localized diffusely in the nucleoplasm, excluding some nuclear regions. The coil-coil domain is important for protein-protein interactions or dimerization of a protein. This suggests that Ppan requires a binding partner for nucleolar localization. The Ppan mutant lacking the N-terminal first 30 amino acids (PpanΔN), as well as the PpanΔC protein localized diffusely in the cytoplasm, the nucleoplasm and the nucleoli, showing that these domains regulate also the localization behaviour of the wildtype protein.

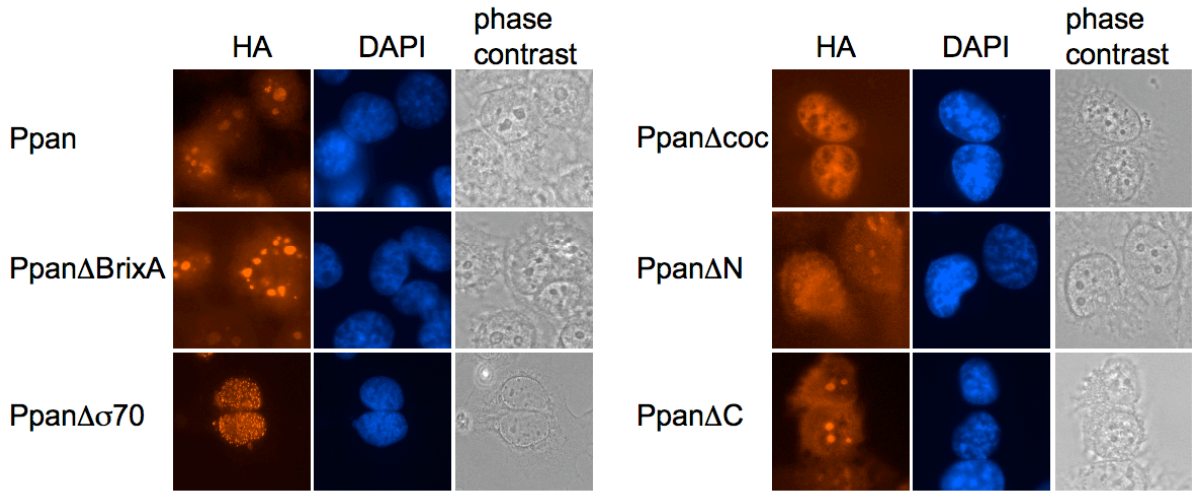

Fig. 19. Immunofluorescence studies for detection of localization of Ppan, and the deletion mutants. TGR-1 cells were stably transfected with pRTS coding for Ppan and the Ppan mutants. Twenty-four hours after induction of gene expression with doxycycline cells were fixed with methanol/aceton and stained with α-HA (3F10) antibody. Nuclear DNA was stained with DAPI.

Deletion of the RNA-binding σ70-like motif in PpanΔσ70 delocalized the

overexpressed protein from nucleoli to discrete foci in the nucleoplasm of TGR-1 cells (Fig. 19). The same delocalization was observed if PpanΔσ70 was expressed in HepG2 cells (Fig. 20)

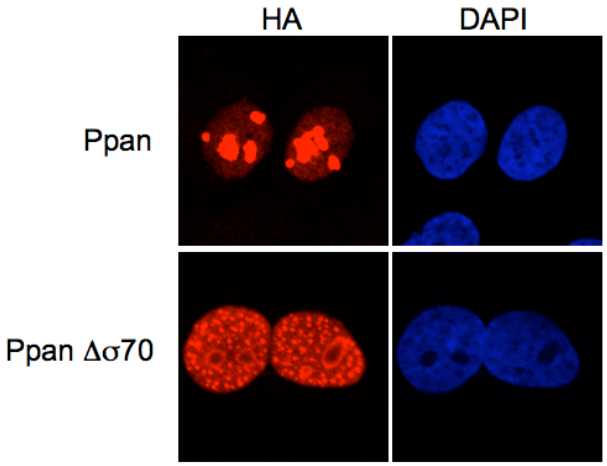

Fig. 20. The RNA binding σ70 like motif is crucial for nucleolar localization of Ppan. Ppan and PpanΔσ70 were expressed in HepG2 cells with doxycycline for 68h. After fixation with paraformaldehyde, cells were incubated with α-HA antibody (12CA5).

In this work only wildtype Ppan and the mutants PpanΔσ70 and PpanΔN were further studied for reasons explained later on.

3.6 PpanΔσ70 directs nucleophosmin, hRrp6 and Pes1, but not fibrillarin to discrete nuclear foci

The nucleolar localization of Ppan appears to be dependent on its binding to nucleolar RNA structures (Fig. 16). The Ppan protein with a deletion in the RNA binding σ70 like motif, PpanΔσ70, delocalized from the nucleoli to discrete nuclear foci (Fig. 19 and 20). To analyze the nucleoplasmic structures formed by overexpression of PpanΔσ70, co-stainings of Ppan with different nuclear proteins were performed. Firstly two nucleoplasmic proteins, the PML protein, which locates in the PML bodies, and the sc-35 protein, a component of the nuclear splicing speckles, were examined. U2OS cells were transiently transfected with PpanΔσ70-GFP expression vectors and cells were fixed 25 hours later (Fig. 21). The GFP-tagged PpanΔσ70 protein localized more prominently in nucleoli. Nevertheless, PpanΔσ70-GFP displayed the characteristic nucleoplasmic spots, outside of nucleoli, as seen for

the HA-tagged form (Fig. 21). These spots did not co-stain with PML bodies (Fig. 21a) or nuclear splicing speckles (Fig. 21b), suggesting that the spots formed by PpanΔσ70-GFP were not components of these nucleoplasmic structures.

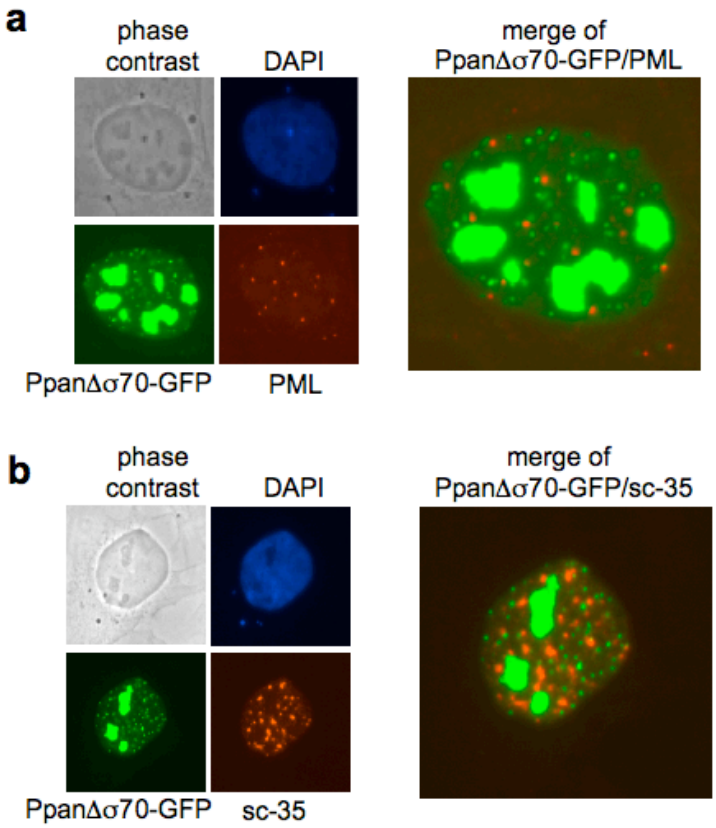

Fig. 21. PpanΔσ70-GFP does not co-localize with PML bodies or nuclear splicing speckles. Immunofluorescence analysis of single cells. PpanΔσ70-GFP was co-stained with PML and nuclear splicing speckles. PpanΔσ70-GFP was expressed in transiently transfected U2OS cells. Staining of paraformaldehyde fixed cells with (a) α-PML or (b) α-sc-35 (splicing speckle protein 35) specific antibodies. Right hand side: merge of the images.

Do the newly formed nucleoplasmic structures represent disrupted nucleoli?

To answer this question several nucleolar factors were co-stained with Ppan and PpanΔσ70 in stably transfected U2OS cells. Nucleophosmin is a highly abundant protein, which locates normally in the granular component of nucleoli. In U2OS cells expressing Ppan, nucleophosmin localizes nucleolar and diffusely in nucleoplasm. Interestingly after expression of PpanΔσ70, nucleophosmin was trapped in the newly formed nucleoplasmic spots and stained in addition in a ring pattern around the nucleoli (Fig. 22a). Another protein, the hRrp6 (human exosome component 10 or PM-Scl100) localizes diffusely in the nucleoplasm and predominately in nucleoli of cells (Schilders *et al*., 2007). The localization of hRrp6 could be confirmed (Fig. 22b).

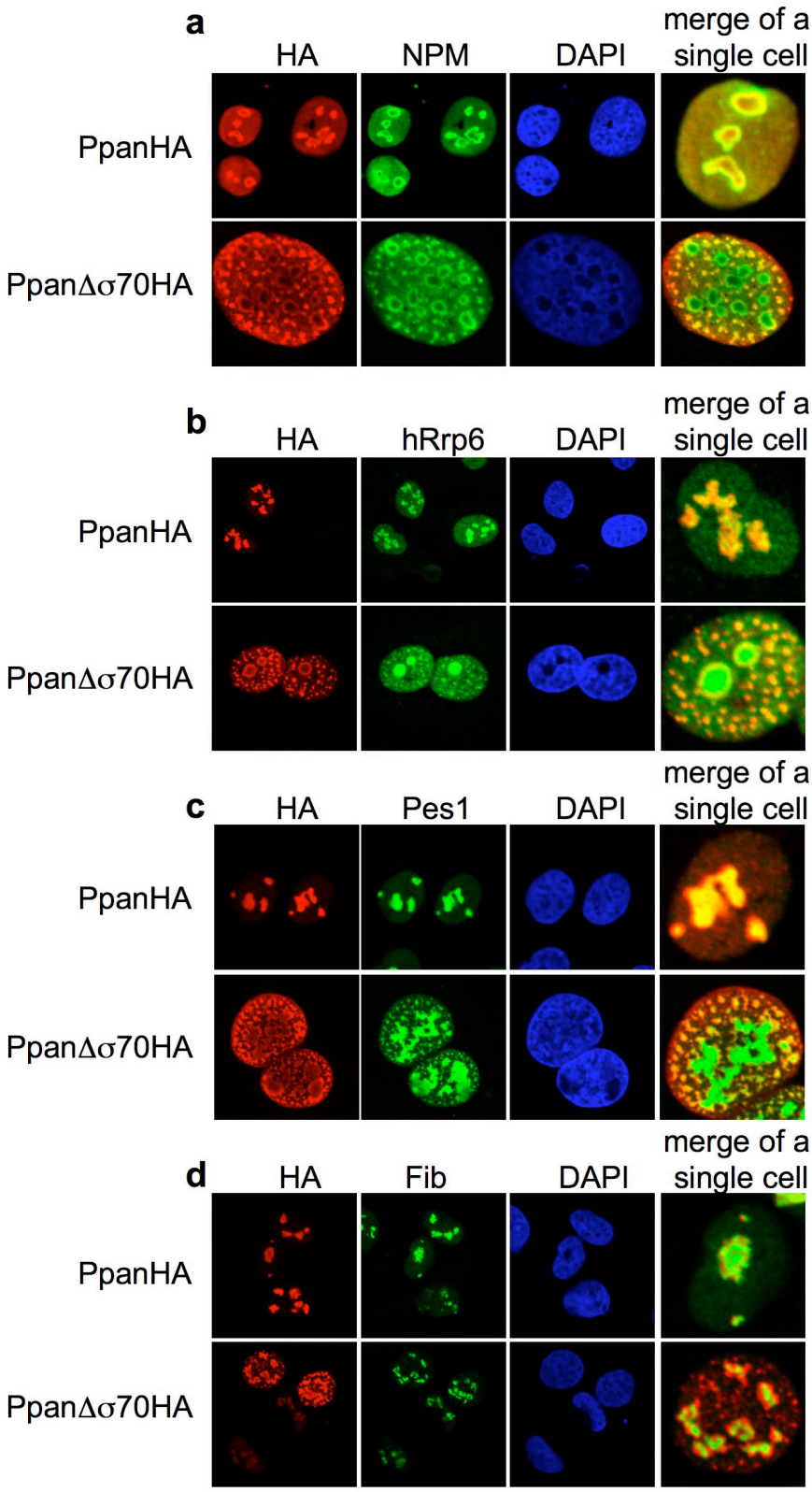

Fig. 22. Ppan lacking the RNA-binding σ70-like motif directs nucleophosmin (a), hRrp6 (b), Pes1 (c), but not fibrillarin (d) in discrete nucleoplasmic foci. Immunofluorescence studies of single nuclei. Ppan or PpanΔσ70 were expressed in stably transfected U2OS cells for 40 hours. Cells were fixed with paraformaldehyde and stained with antibodies for HA, nucleophosmin, hRrp6, Pes1 or fibrillarin, respectively. DNA was counterstained with DAPI. Images were taken with a laser scanning confocal microscope.

Expression of PpanΔσ70 led to a partially redistribution of hRrp6 to nucleoplasmic foci, while the majority of hRrp6 remained in nucleoli (Fig. 22b). Pes1, component of the PeBoW complex, co-localized with Ppan in nucleoli. Like hRrp6, Pes1 was partially attracted to the PpanΔσ70 containing structures in the nucleoplasm, whereas the majority of the protein remained in nucleoli (Fig. 22c). Finally fibrillarin was analyzed as a component of the dense fibrillar component of nucleoli. Fibrillarin co-localized with Ppan in nucleoli of the cells and after expression of PpanΔσ70, fibrillarin did not leave its nucleolar localization to join PpanΔσ70 in nucleoplasmic structures (Fig. 22d)

In summary, the mutation of distinct domains of the Ppan protein showed that the nucleolar localization of the protein requires the σ70 like motif and the coil-coil domain. Deletion of the RNA binding σ70 like motif delocalized the protein to discrete nucleoplasmic foci. PpanΔσ70 showed a dominant phenotype regarding the localization of nucleolar proteins nucleophosmin, hRrp6 and Pes1. These observations indicate a possible role of Ppan in maintaining the structural integrity of some nucleolar components and give hints for possible interactions of PpanΔσ70 with nucleophosmin, hRrp6 and Pes1.

Working with overexpressed Ppan and Ppan mutants causes artificial conditions in the cell. Since a monoclonal antibody against Ppan was available and tested for its specificity, the next goal was to study more explicit the endogenous protein, to approach more the physiological conditions in cultured cells.

3.7 Endogenous Ppan is involved in ribosome biogenesis and cell proliferation

The yeast homolog of Ppan, Ssf1, is involved in ribosome biogenesis by controlling the correct order of rRNA processing. Furthermore, yeast cells with deletion of Ssf1/Ssf2 are not viable. To assess a role for human Ppan, small interfering RNA (siRNA) experiments were performed in human lung carcinoma cells H1299. These cells were chosen, because they can be easily transfected with siRNA and total

cellular RNA of these cells can be isolated in large amounts. H1299 cells were transfected on day 1 and 2 with either control- or *ppan* specific siRNA. The expression of Ppan was reduced, as monitored by Western blot analysis two days after the second siRNA transfection (Fig. 23a). To study a possible effect of *ppan* knock-down on the proliferation of the cells, H1299 cells were transfected with siRNA on days 1 and 2 and the total cell number was counted on days 5 and 8 (Fig. 23b). The proliferation of *ppan* knock-down cells was reduced compared to the control cells.

In an attempt to study the possible involvement of Ppan in mammalian ribosome biogenesis, Northern blot analysis of H1299 cells transfected with siRNA was conducted. Cells were transfected on day 1 and 2 with control or *ppan* specific siRNA and total RNA was isolated 48 hours later. Northern blot analysis was performed with probes specific to the internal transcribed sequences 1 and 2 (ITS-1 and -2) of the rRNA precursors (Fig. 23d). Knock-down of *ppan* revealed a significant reduction of the mature 28S rRNA and more slightly of the 18S rRNA (Fig. 23d, lower pannel). Furthermore, analysis with a probe specific for the ITS-1 sequence showed a slight accumulation of the 47S, 45S and 41S rRNA precursors, compared to control siRNA transfected cells. When applying the probe for the ITS-2 sequence, the cells treated with *ppan* specific siRNA showed a slight increase in the 47S, 45S and 41S rRNA precursors and a decrease of the 12S rRNA precursor. More prominently a new rRNA form of about 25-26S was visible, which did not appear in the control cells.

In conclusion, depletion of the endogenous Ppan protein leads to a reduced proliferation and to reduced levels of mature 18S and 28S rRNA. The processing of the rRNA is affected and an additional rRNA product appears.

3.8 Interaction of Ppan with the PeBoW complex

The yeast homologue of Ppan, Ssf1, interacts with many proteins among them Nop7, Erb1 and Ytm1, the homologues of Pes1, Bop1 and WDR12, components of the PeBoW complex in mammals (Hölzel *et al.*, 2005; Rohrmoser *et al.*, 2007). One interesting phenomenon described earlier in this work was that Ppan$\Delta\sigma$70 protein was able to direct Pes1 to newly formed nuclear foci (Fig. 22). Therefore a possible

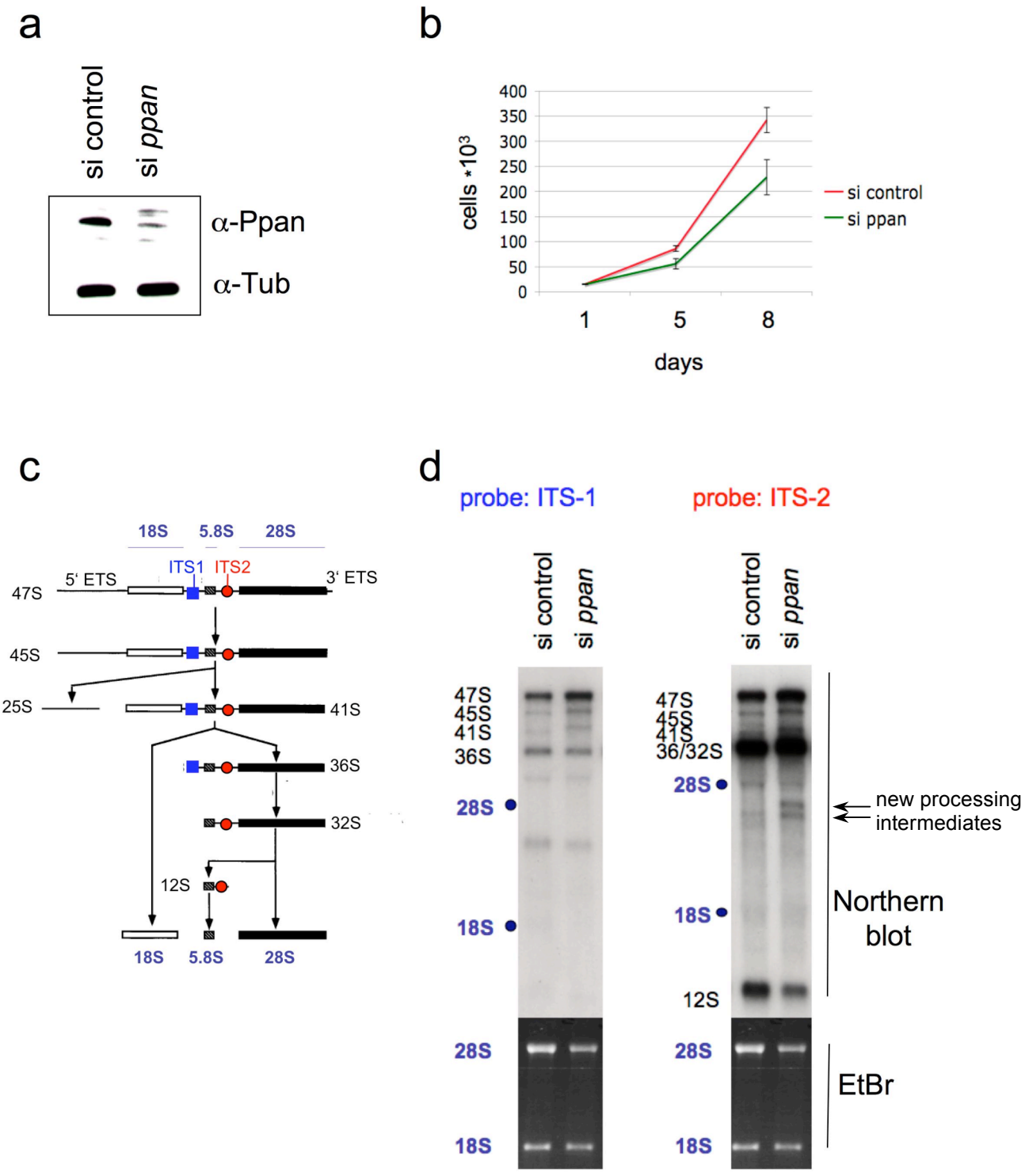

Fig. 23. siRNA knockdown of *ppan* leads to a reduced proliferation, reduction of 28S rRNA, and an additional rRNA product. (a) Immunodetection of Ppan and tubulin in Western blot analysis of cells transfected with control- and *ppan* specific siRNA. (b) Proliferation assay of cells treated with control or *ppan*-siRNA. (c) rRNA processing in mammalian cells with probes for ITS-1 (blue dot) and ITS-2 (red dot). (d) Northern blot analysis with probes ITS-1 and ITS-2 of H1299 cells transfected with control- or *ppan*-siRNA. Lower part: ethidium bromide (EtBr)-staining of the agarose gel.

interaction of Ppan with Pes1 and the two other components of PeBoW, Bop1 and WDR12, was studied in co-immunoprecipitation experiments in U2OS cells.

The antibody 1C3 precipitated only a very small amount of Ppan, approximately 1-2 % of the cellular protein (Fig. 24, lane 2). The Ppan antibody precipitated about 10% of the cellular Pes1 and 1% of Bop1 (lane 2). The antibodies for Bop1, Pes1 and WDR12 precipitated Ppan (Fig. 24, lanes 4,5,6) approximately 1-5% of the cellular protein. Nevertheless, the results of the co-immunoprecipitation of Ppan with Pes1, Bop1 and WDR12 give a hint for a possible interaction. The quantity of the precipitated Ppan protein was very low and the quality of the experiment was not answering satisfactory the question of the interaction between Ppan and Pes1, Bop1 or WDR12. Therefore, a second method was chosen to study the possible interactions, the so called Bimolecular Fluorescence Complementation assay (BiFC).

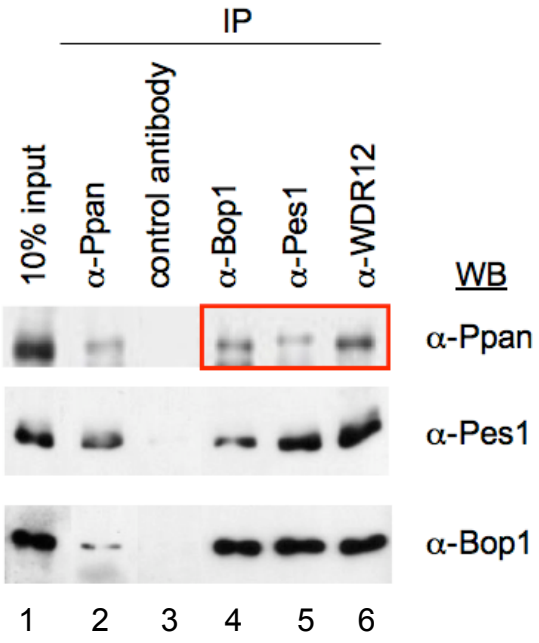

Fig. 24. Ppan interacts with Pes1, Bop1 and WDR12. Western blot analysis of co-immunoprecipitation of endogenous Ppan with Pes1, Bop1 and WDR12 in U2OS cells. Cell lysates were immuno-precipitated with α-Ppan, α-Bop1, α-Pes1 and α-WDR12 antibodies followed by immunoblot detection using α-Ppan, α-Pes1 or α-Bop1 antibodies. The co-immunoprecipitation of Ppan with the PeBoW components is highlighted in the red box. An isotype specific mAb served as control.

The BiFC-assay is very suitable for the visualization of interactions between proteins in living cells (Hu *et al.*, 2002). Non-fluorescent fragments of yellow fluorescent protein (YFP) YN(1-154) and YC(155-238) reconstitute the fluorophore only when brought together by interactions between proteins covalently linked to each fragment of YFP. The complex allows the direct visualization of even a transient and weak interaction as the complex remains stable after formation. As a positive control for BiFC the interaction of Jun with Fos, two members of the basic-region/leucine-zipper (bZIP) family of transcription factors, was investigated (Hu *et al.*, 2002). When plasmids carrying these two factors are co-expressed in cells, a strong BiFC signal is

obtained in nuclei. A leucine zipper deletion in Fos (FosΔZip) that prevents Fos-Jun dimerization (Gentz *et al.*, 1989) eliminates fluorescence complementation. The system was applied to study the interaction of Ppan with Pes1, Bop1 and WDR12.

HepG2 cells were transfected with plasmids YN Ppan and YC Pes1, YC Bop1 or YC WDR12. Twenty-five hours post transfection cells were observed under a laser scanning confocal microscope using excitation at 488 nm and emission between 529-560 nm wavelength to localize the YFP signal after potential interaction. BiFC signals through interaction of Fos and Jun served as a positive control (Fig. 25a). When cells were transfected with empty vectors (pBiFC-YN(1-154)* and pBiFC-YC(155-238)*; simplified YN and YC respectively), no detectable BiFC signal was observed (Fig. 25b). No interaction was detectable in the negative control with Jun and FosΔZip (both gifts from Dr. Andreas Thomae, Helmholtz Centre Munich), from which the zipper domain, shown to be involved in the binding of Jun with Fos, is missing (Fig. 25c). Ppan and Pes1, as well as Ppan and WDR12 interacted in nucleoli of HepG2 cells after co-expression (Fig. 25d,f). The interactions were mainly restricted to the nucleoli. Although immunoprecipitation showed the interaction of Ppan with Bop1, there was no signal detectable in cells co-transfected with Ppan and Bop1 expression vectors (Fig. 25e).

Ppan interacts with Pes1 and WDR12 in the nucleoli of HepG2 cells (Fig. 25). Pes1 and WDR12 exist mainly incorporated in the PeBoW complex in the nucleolus (Rohrmoser *et al.*, 2007). This suggests that Ppan interacts with the PeBoW complex in the nucleolus. The PeBoW complex is involved in the maturation of the 28S rRNA in mammalian cells (Hölzel *et al.*, 2005, Grimm *et al.*, 2006, Rohrmoser *et al.*, 2007). By reducing the levels of the endogenous proteins by siRNA or expression of dominant negative forms of PeBoW components, the processing steps for the 28S rRNA are severely affected. Cells respond to this processing block with stabilization of p53. The exact mechanism how the stalled rRNA processing is signalled to activate p53 is still under investigation.

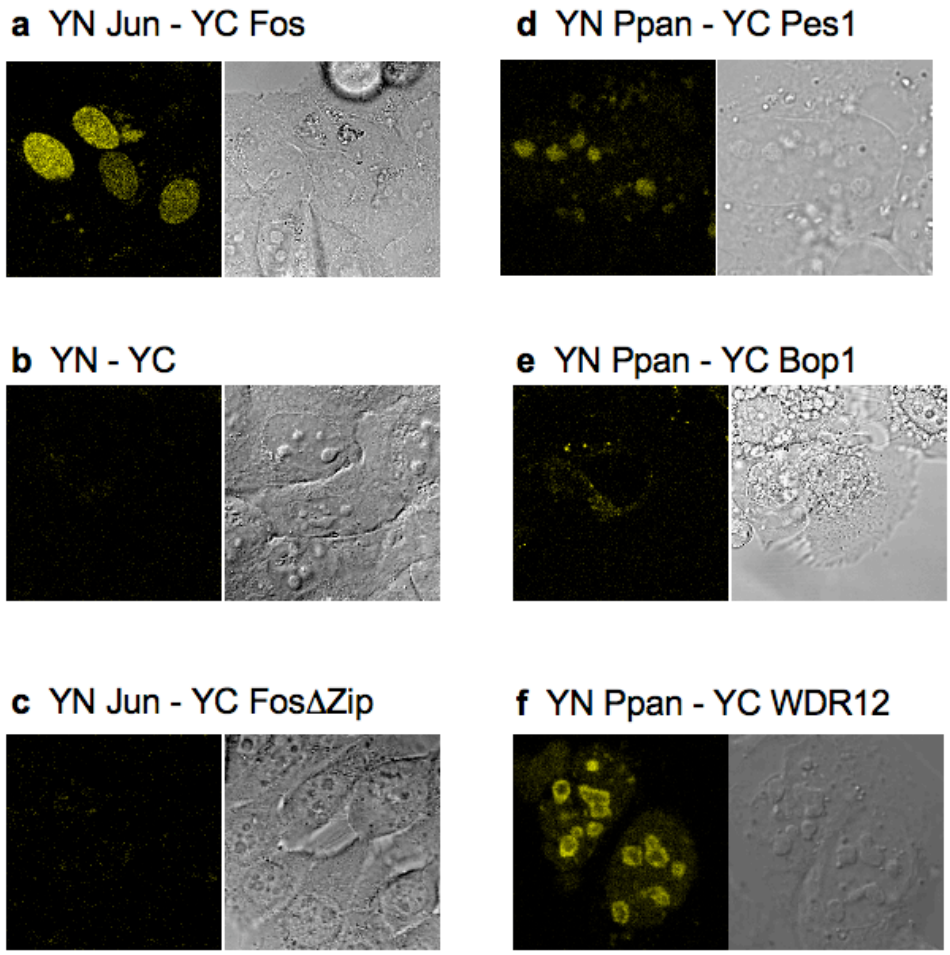

Fig. 25. BiFC analysis of Ppan and Pes1, Bop1 or WDR12. HepG2 cells were co-transfected with plasmids (a) YN Jun with YC Fos (positive control), (b) YN and YC plasmids (negative control) and (c) YN Jun with YC Fos ΔZip (negative control) or YN Ppan with (d) YC Pes1, (e) YC Bop1 or (f) YC WDR12. Twenty-five hours post transfection living cells were analysed with a laser scanning confocal microscope.

In yeast, Ssf1 is needed to prevent premature cleavage of rRNA and is therefore required to maintain the normal order of rRNA processing (Fatica *et al.*, 2002). Preliminary data with siRNA knockdown of *ppan* showed that the mammalian protein shares functional similarities to the yeast homologue Ssf1. When Ppan interacts with the PeBoW complex in the nucleoli of HepG2 cells and controls rRNA processing, what happens to Ppan if rRNA processing is inhibited? To approach this question the cellular localization of Ppan was investigated after inhibition of rRNA processing. This was achieved by three different ways.

3.9 Prominent nucleolar localization of Ppan after inhibition of rRNA processing

Firstly, the processing of rRNA was disturbed by a dominant negative form of Pes1 (dnPes1 M1), which inhibits the maturation of 28S rRNA and promotes the accumulation of the 36S rRNA. DnPes1 M1 is incorporated into the PeBoW complex and blocks its function (Grimm *et al.*, 2006). Stably transfected U2OS cells were incubated with doxycycline to induce the bidirectional promoter for co-expression of dnPes1 M1 and eGFP (Fig. 26). DnPes1 expressing cells showed a prominent nucleolar staining of Ppan, recognized by the specific antibody 1C3. Cells negative for eGFP showed no prominent nucleolar staining for Ppan. It seems that Ppan's localization is very abundant in nucleoli, if rRNA processing is inhibited by the overexpression of the dominant negative form of Pes1.

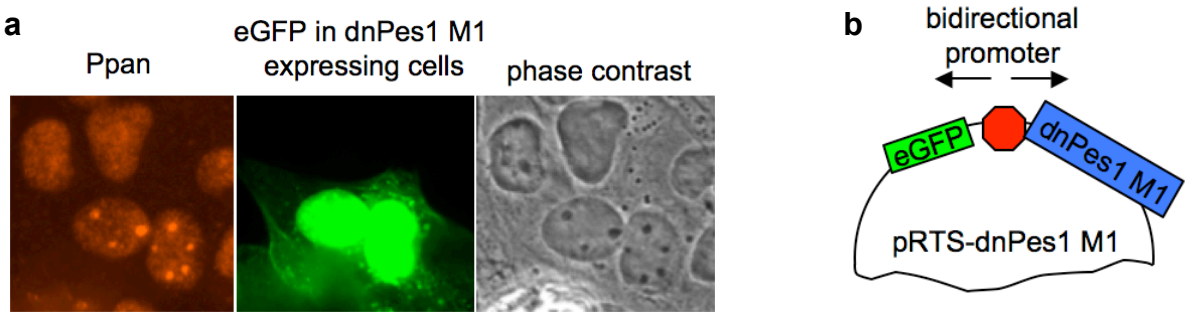

Fig. 26. Inhibition of rRNA processing by a dominant negative form of Pes1 (dnPes1) leads to a prominent nucleolar staining of Ppan. (a) U2OS cells transiently transfected with pRTS-dnPes1 were treated with 1 μg/ml doxycycline to induce expression of dnPes1 M1 and eGFP through the bidirectional promoter. Cells were fixed with paraformaldehyde and stained with the Ppan specific 1C3 antibody. DnPes1 expressing cells are eGFP positive, whereas non-expressing cells are negative for eGFP. (b) Principal function of pRTS-1. Doxycycline induces the bidirectional promoter (in red) for concomitant transcription of *dnpes1 M1* and *egfp*.

In a second approach the processing of rRNA was inhibited by 5-fluorouracil (5-FU) (Ghoshal and Jacob, 1994). 5-FU blocks rRNA processing at concentrations of 100 μM entirely after six hours, while transcription of ribosomal genes remains unaffected (Mühl, 2007).

HeLa, HepG2 and U2OS cells were treated with 5-FU for six hours and the localization of Ppan was examined (Fig. 27 and 28). One hundred cells were carefully examined for statistical evaluation of the localization of Ppan. About 63% of

untreated HeLa cells showed a predominant nucleolar staining of Ppan. After inhibition of rRNA processing by 5-FU, Ppan was detectable in 99 % of the cells (Fig. 27a). Almost identical results were obtained, if U2OS cells were analyzed in similar experiments (Fig. 27b).

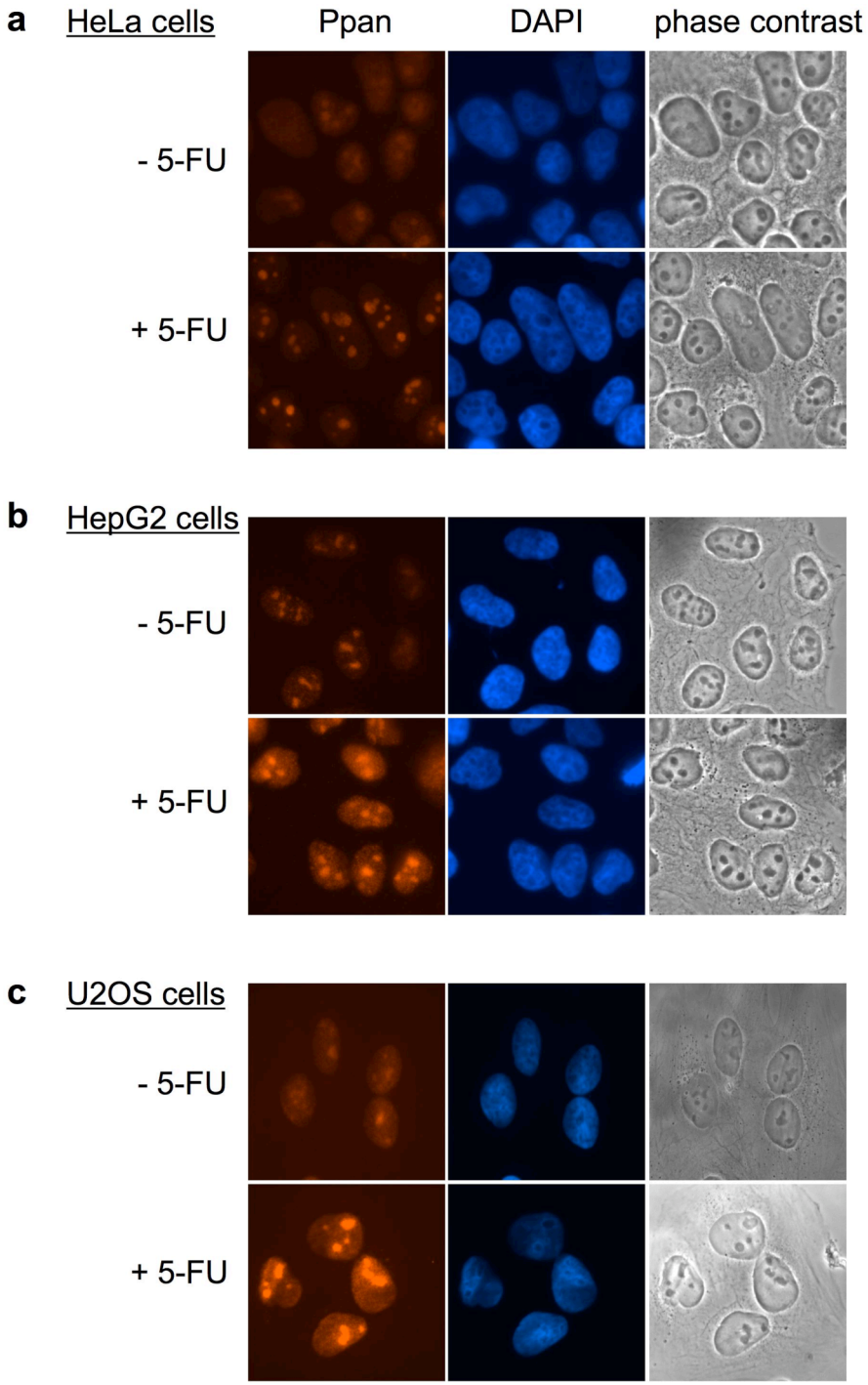

Fig. 27. Nucleolar localization of Ppan after treatment of HeLa, HepG2 and U2OS cells with 5-FU. (a) HeLa, (b) HepG2, and (c) U2OS cells were treated with 100 μM 5-FU for six hours. After paraformadelhyde fixation cells were stained for Ppan with the 1C3 monoclonal antibody. Nuclei were counterstained with DAPI. Pictures were taken with a fluorescence microscope, by applying the same exposure time.

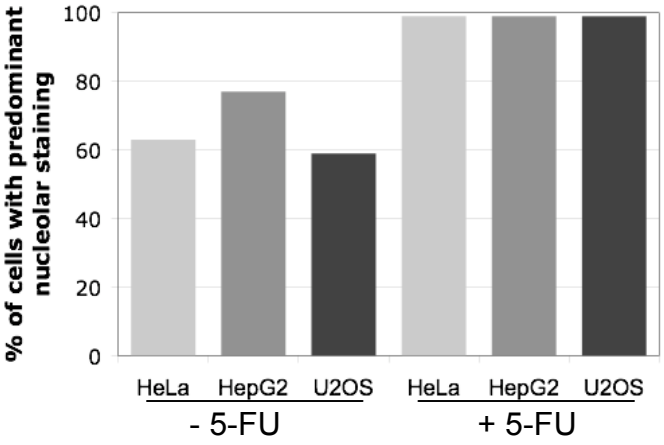

Fig. 28. Statistical analysis of nucleolar localization of Ppan in untreated and 5-FU treated cells. HeLa, HepG2 and U2OS cells were treated with 100 μM 5-FU for six hours. One hundred cells of each cell type were examined for a predominan nucleolar localization of Ppan.

Ppan was co-stained with fibrillarin in HepG2 cells to compare the localization of both proteins before and after 5-FU treatment. In figure 29 a representative cell was chosen for the analysis. Fibrillarin is a nucleolar protein, used widely as a marker for detecting nucleoli in immunofluorescence studies. Untreated cells showed a faint nucleolar staining of Ppan, whereas cells treated with 5-FU showed a strong nucleolar staining. After merging the two different profiles of Ppan and fibrillarin, a RGB profile of the two fluorescent pictures was made (ImageJ, plug in RGB profiler).

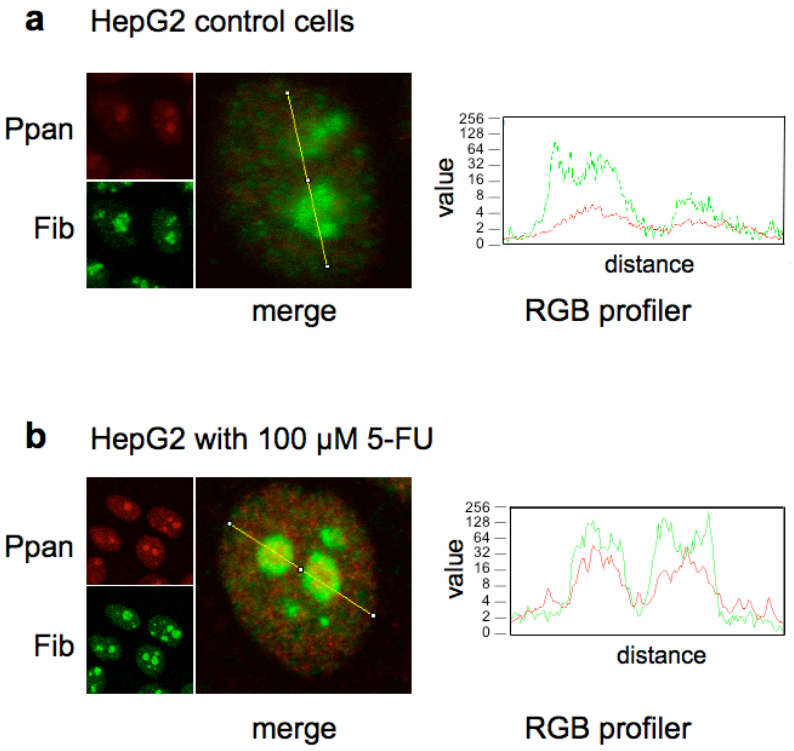

Fig. 29. The signal intensity of Ppan increases in nucleoli of HepG2 cells after treatment with 5-FU. Cells were treated with 100 μM of 5-FU for 6 hours, fixed with paraformaldehyde and stained for Ppan and fibrillarin. Images were captured with the laser scanning confocal micro-scope. Pictures were merged and a RGB profile was drawn to study co-localization. In the y-axis the RGB profiler shows the value of the fluorescence intensity in the logarithmic scale of 2.

The fluorescence intensity of Ppan (red curves) in untreated HepG2 cells had a value

of about 4, whereas in 5-FU treated cells the intensity increased to a value of about 32. The nucleolar fluorescence intensity of Ppan increased in this cell eight-fold after treatment with 5-FU. Fibrillarin (green curves) had a fluorescence intensity value of about 64 in untreated cells, whereas in 5-FU treated cells it had a value of about 128, which indicates a two-fold increase after treatment of cells with 5-FU. In summary the nucleolar staining of Ppan was strongly increased after treatment of the HepG2 cells with 5-FU.

To investigate if the level of Ppan protein in HepG2 cells had changed upon 5-FU treatment, Western blot analysis was performed. Ppan protein levels remained stable after 5-FU treatment (Fig. 30).

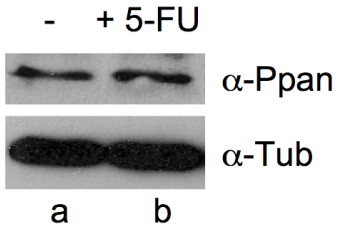

Fig. 30. Ppan protein level is not changed in 5-FU treated cells. Western blot analysis of Ppan in total cell lysates of (a) untreated and (b) 5-FU treated HepG2 cells (100 μM, six hours). Equal cell mounts were lysed and immunoblotted for detection of Ppan and tubulin.

In a third approach, the processing of rRNA was inhibited by the proteasome inhibitor MG-132. Stavrera and colleagues showed that many pre-rRNA processing factors were affected after proteasome inhibition. The proteasome was placed in the list of ribosome biogenesis regulators, because it caused additional ubiquitination of complexes associated with late processing factors, changes in nucleolar morphology and inhibition of pre-rRNA processing (Stavrera *et al*., 2006). Bastian Mühl in our laboratory confirmed that the proteasome inhibitor MG-132 inhibited processing of rRNA within 6 hours (Mühl, 2007).

To study the localization of Ppan under proteasome inhibition, HepG2 cells were treated with MG-132 for six hours (Fig. 31). Over 140 cells were examined for the localization of Ppan (supplementary material). In untreated cells Ppan was nuclear and in about 77 % of the cells fixed with paraformaldehyde, Ppan localized nucleolar. In MG-132 treated cells only 11 % of cells showed a predominan nucleolar staining, if cells were fixed with paraformaldehyde. The immunofluorescence images indicated at a first glance a strong reduction of Ppan levels in the nucleus. To investigate if the level of Ppan protein in HepG2 cells had changed upon MG-132 treatment, western blot analysis was performed. Interestingly, Ppan protein levels remained stable after

MG-132 treatment (Fig. 32).

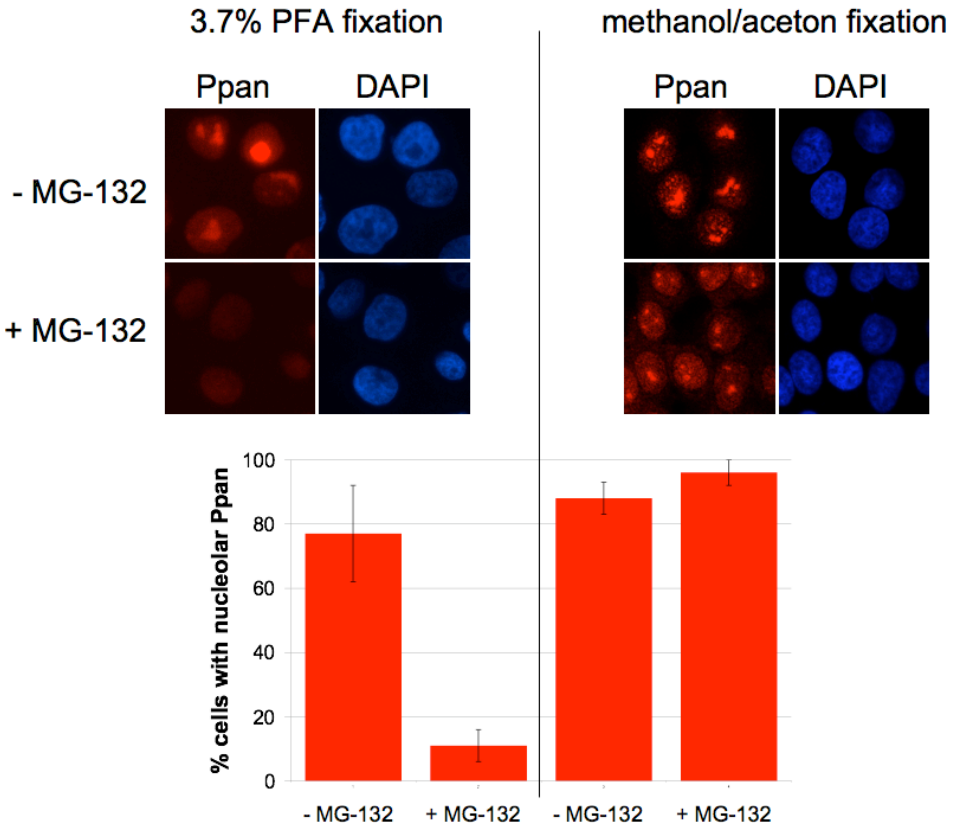

Fig. 31. The N-terminal region of Ppan, recognized by monoclonal antibody 1C3, is masked after MG-132 treatment. HepG2 cells were treated with 10 μM MG-132 for six hours and fixed with paraformaldehyde for structure preservation or alternatively with methanol/aceton. Endogenous Ppan was visualized with the specific 1C3 monoclonal antibody.

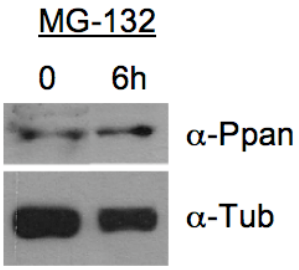

Fig. 32. Ppan protein level is not changed after MG-132 treatment. Western blot analysis of Ppan in total cell lysates of untreated and MG-132 treated HepG2 cells (10 μM, six hours). Equal cell amounts were lysed and immunoblotted for detection of Ppan and tubulin as a loading control.

How can the discrepancy between the results of immunofluorescence and Western blot experiments be explained? Can treatment of cells with MG-132 lead to a masking of the 1C3 antibody epitope in Ppan? And is this mask fixed by paraformalehyde? In fact paraformaldehyde fixation of cells is structure preserving. In contrast, fixation with methanol/aceton destroys substructures and epitopes are

usually better presented than after paraformaldehyde fixation.
When cells were fixed with methanol/aceton, Ppan localized in 88 % of the cells nucleolar (Fig. 31). Intriguingly, when cells were treated with MG-132, Ppan localized nucleolar in 96 % of 199 examined cells. This suggests that the N-terminal sequence of Ppan, which harbours the epitope of 1C3 antibody becomes masked and is no longer accessible for the antibody after MG-132 treatment. Thus, inhibition of rRNA processing probably does not affect the cellular localization of Ppan, but rather the interaction of its N-terminus with other cellular factors.

Inhibition of the rRNA processing by expression of the dominant negative mutant of Pes1 or application of 5-FU, induced an increased signal intensity for Ppan in nucleoli. On the other hand, in the case of the proteasome inhibitor MG-132, the N-terminal epitope of Ppan was not longer visible. However, the protein levels of Ppan did not change after perturbation of rRNA processing.
In the next paragraph, I investigated if inhibition of rDNA gene transcription can induce a similar protection of the N-terminus of Ppan.

3.10 Predominant nucleolar detection of Ppan after inhibition of rDNA transcription

To answer the question of a stress-dependent detection behaviour of Ppan, the transcription of rDNA was disturbed by using the chemotherapeutic drug actinomycinD (ActD). Previous studies done in our laboratory (Mühl, 2007) confirmed that this substance had an effect on the transcription of the 47S precursor by the nucleolus specific RNA polymerase I. In this study ActD was applied at a concentration of 2.5 nM, which inhibits rDNA transcription entirely after 6 hours.
The localization of Ppan was studied in HepG2 cells with the monoclonal antibody 1C3 in untreated and ActD-treated cells (Fig. 33). Approximately one hundred untreated and ActD-treated cells were examined. Ppan localized in 77 % of the untreated cells nucleolar, whereas all ActD-treated cells showed a strong nucleolar staining of Ppan.

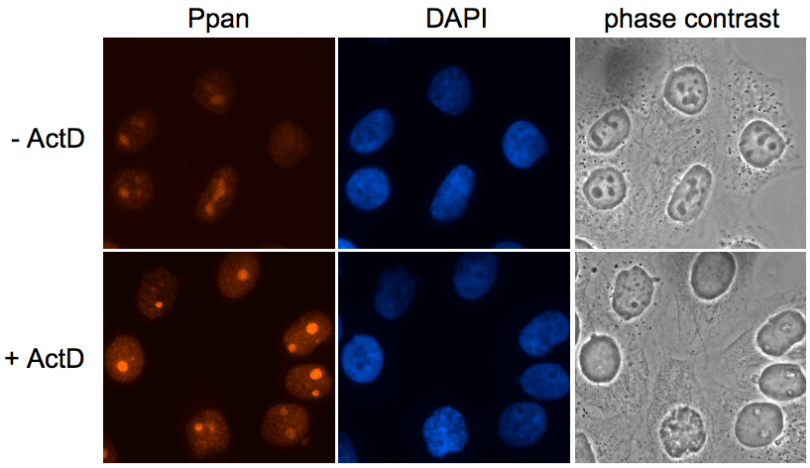

Fig. 33. Treatment of cells with ActD leads to predominant nucleolar detection of Ppan. HepG2 cells were treated with 2.5 nM ActD for 6 hours. After paraformaldehyde fixation cells were stained for Ppan with the 1C3 monoclonal antibody. Nuclear DNA was counterstained with DAPI. Pictures were taken with the same exposure time.

To investigate the protein levels of Ppan, Western blot analysis of protein extracts of untreated and ActD-treated cells was performed (Fig. 34). The protein levels of Ppan were not changed in ActD treated cells.

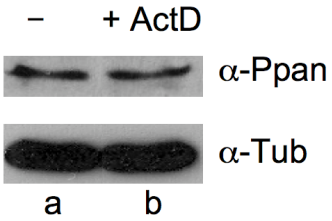

Fig. 34. Ppan protein levels are not changed in ActD treated cells. Western blot analysis of Ppan in total cell lysates of untreated and ActD treated HepG2 cells. 2.5 nM ActD was diluted to the cell culture medium for 6 hours. Equal cell amounts were lysed and immunoblotted for detection of Ppan and tubulin.

To study the nuclear distribution of the Ppan protein, nuclei and nucleoli of untreated and ActD treated HepG2 cells were prepared. Lysates of 1 % of isolated nuclei and 10% of isolated nucleoli were separated in polyacrylamid gels, immunoblotted and analyzed with antibodies detecting RNA polymerase II (as a control for the purity of nucleolar preparations), Ppan, Hdm2 (for reasons explained below), nucleophosmin and fibrillarin (Fig. 35). The RNA polymerase II staining in nuclear preparations in lanes a and c and the lack of signals in isolated nucleoli in lanes b and d confirmed the proper isolation of nucleoli. Ppan was present in nucleoli of untreated and ActD treated cells (Fig. 35, lanes b and d). The levels of Ppan did not change in the nuclear fraction after ActD treatment, while a slight decrease was seen for the nucleolar fraction. Nucleophosmin could be detected in untreated and treated cells.

Fibrillarin was also detected in the nucleoli of untreated and ActD-treated cells (lanes b and d). The levels of nucleophosmin and fibrillarin decreased slightly in the nucleolar fraction of the ActD treated cells, as seen for Ppan (lane d). Treatment of cells with low concentration of ActD (5 nM) has previously been shown to stabilize p53 by disintegrating the p53/Hdm2 complex in the nucleoplasm and delocalizing Hdm2 to nucleoli (Ashcroft *et al.*, 2000). In fact, the levels of Hdm2 were significantly increased in the nucleoli fraction of ActD-treated cells (Fig. 35d), whereas a small increase was seen only for the nuclei fraction (c).

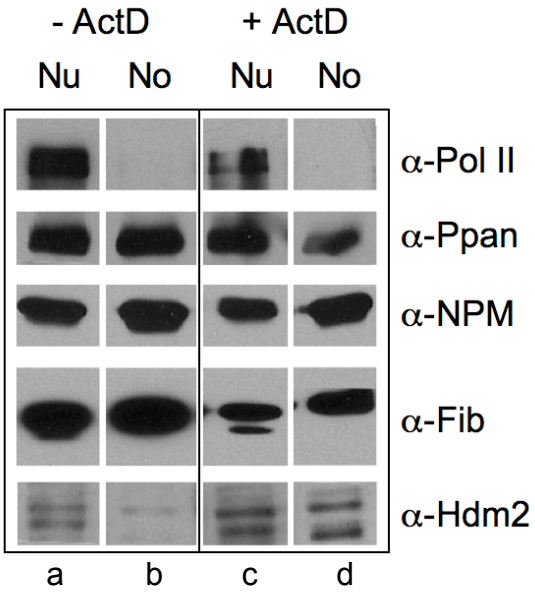

Fig. 35. Hdm2 localizes nucleolar after actinomycinD treatment. Western blot analysis of nuclear and nucleolar preparations from untreated and ActD-treated HepG2 cells. 10 nM ActD was applied for 6 hours. 1% of nuclear (**Nu**) and 10% of nucleolar (**No**) extracts were separated in SDS-PAGE followed by immunoblot using antibodies: α-Pol II (8WG16), α-Ppan (1C3), α-NPM (FC-6), α-fibrillarin and α-Hdm2 (SMP-14).

In summary, Ppan showed a predominant staining of nucleoli, although the entire protein levels did not change in the nuclei and nucleoli of ActD treated cells.

3.11 ActinomycinD causes a structural rearrangement of Ppan and fibrillarin in the nucleoli

Transcriptional arrest after ActD treatment induces the segregation of nucleolar components and the formation of unique structures termed nucleolar caps surrounding a central body (Shav-Tal *et al.*, 2005). Nucleolar caps contain the pre-rRNA and nucleolar proteins like fibrillarin. Other nucleolar factors, like

nucleophosmin, translocate in the nucleoplasm, when the rDNA transcription is inhibited. Until now only two components are known to localize to the central body of segregated nucleoli: p14Arf and the MRP RNA (Shav-Tal *et al.*, 2005). To identify the region in which Ppan locates, double staining of Ppan and fibrillarin was performed in ActD treated HepG2 cells (Fig. 36).

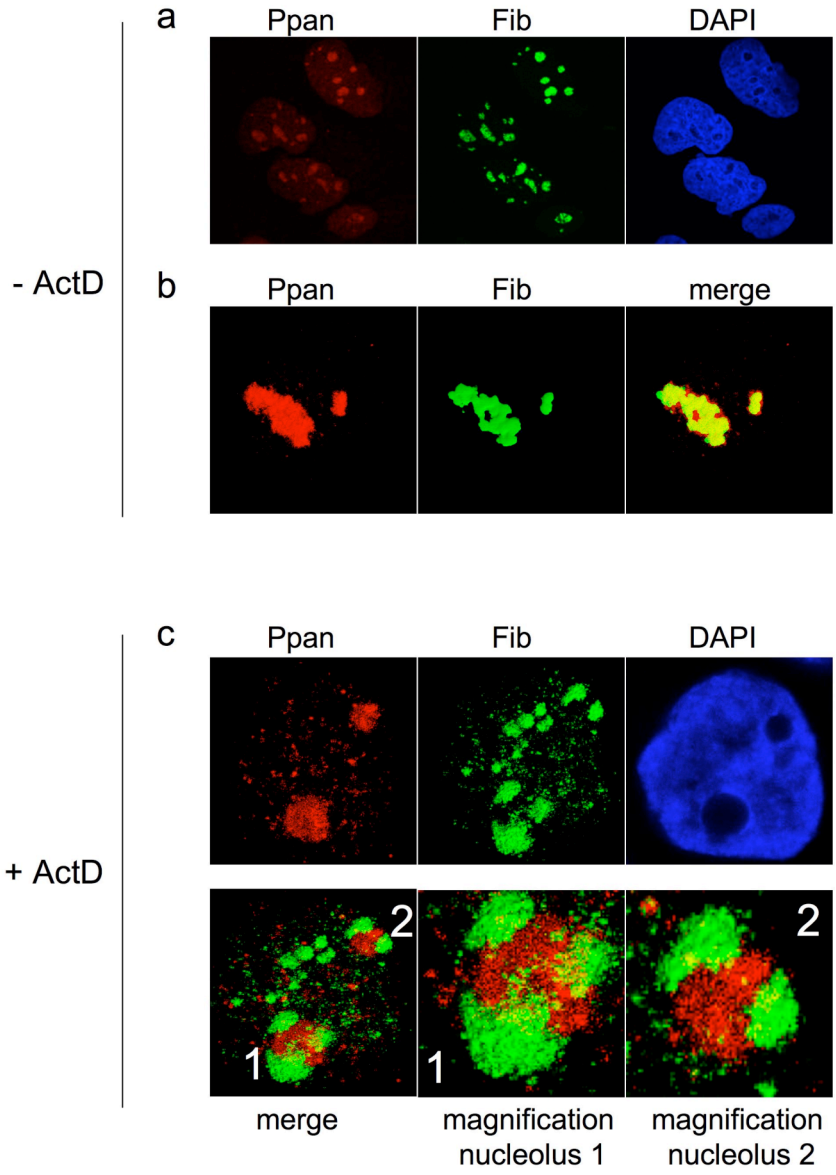

Fig. 36. Localization of Ppan in untreated and ActD treated HepG2 cells. (a) Ppan and fibrillarin localize in nucleoli of untreated cells. (b) Ppan co-localizes with fibrillarin in nucleoli of a single untreated cell. (c) Image of a single cell: Ppan localizes in the central body of segregated nucleoli after inhibition of rRNA transcription by ActD. HepG2 cells were treated with 10 nM ActD for six hours. Cells were fixed with paraformaldehyde and stained for Ppan (red) and fibrillarin (green). Nuclear DNA was counterstained with DAPI. Images were taken with a laser scanning confocal microscope and processed with ImageJ (plug-in VolumeJ). 1,2: magnified nucleoli of the merged image.

In untreated cells Ppan co-localizes with fibrillarin in the nucleoli (Fig. 36a and b). In nucleoli of ActD-treated HepG2 cells Ppan localizes in the nucleolar central body (Fig. 36c), whereas fibrillarin translocated to the nucleolar caps as described in the literature (Shav-Tal *et al.*, 2005).

Although Ppan showed an increased nucleolar detection in ActD treated cells, it differs from that of 5-FU treated cells. In the nucleoli of 5-FU treated cells fibrillarin co-stained with Ppan. Cells treated with ActD clearly showed segregated nucleoli with fibrillarin localizing to newly formed nucleolar caps surrounding the core domain. The core domain was negative for fibrillarin but positive for Ppan. Thus, inhibition of rRNA processing by 5-FU and rDNA transcription by ActD induced the reactivity of Ppan with the 1C3 antibody, albeit the different molecular action of both substances.

3.12 Nucleolar localization of Ppan is independent of p53

Treatment of cells with ActD activates p53 by disintegrating the inhibitory p53/Hdm2 complex in the nucleoplasm (Ashcroft *et al.*, 2000). Additionaly, overexpression of p53 was reported to repress rDNA transcription by RNA pol I by directly interfering with the interaction of the upstream binding factor (UBF) and selectivity factor (SL1) on the human rDNA promoter (Budde and Grummt, 1998; Zhai and Comai, 2000). Ppan localizes in the nucleoli of cells, when cells are treated with ActD. Is this increased nucleolar detection of Ppan a direct effect of transcription inhibition, probably due to recognition of nucleolar stress signals? Or does activated p53 repress rDNA transcription and then as a second action promotes a nucleolar signal-accumulation of Ppan? To answer these questions, two cell lines with and without endogenous p53 were used, namely HCT+/+p53 and HCT-/-p53 (B. Vogelstein, Johns Hopkins University, USA, provided by Dr. H. Gerhard, Helmholtz Centre Munich). Both cell types were treated with 2.5 nM actinomycinD for six hours and stained with Ppan for immunofluorescence studies. Untreated HCT cells showed only a faint nucleolar presence of Ppan (Fig. 37). Ppan localized strongly in the nucleoli of ActD treated cells, both in p53 positive and negative cells. It seems that the epitope was good accessible for the Ppan recognizing antibody after ActD treatment and this phenotype was not dependent on p53.

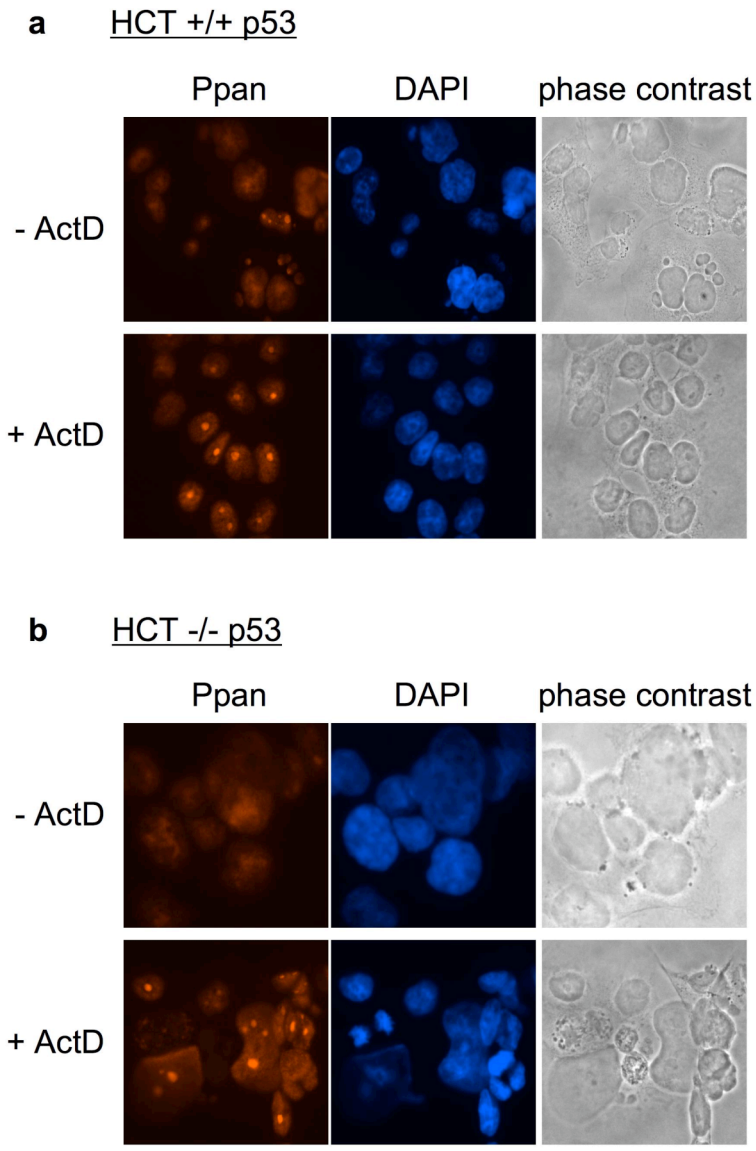

Fig. 37. Predominant nucleolar detection of Ppan ActD treated HCT cells is independent of p53. Immunofluorescence of endogenous Ppan in HCT -/- p53 and HCT +/+ p53 cells treated or not with 2.5 nM ActD for 6 hours. Ppan was stained with monoclonal antibody after fixation of cells. DNA was counterstained with DAPI.

The reactivity of Ppan with the monoclonal antibody 1C3 increased strongly in nucleoli after inhibition of rDNA transcription by ActD in a stress sensitive behaviour. The increase in reactivity was independent of p53, indicating that p53 is not required for the stress-induced detection of Ppan in the nucleoli. On the other hand, it would be interesting to learn whether Ppan is involved in the activation of p53 after inhibition of rDNA transcription and processing of rRNA.

A key factor in the control of p53 is Hdm2, which mediates the rapid degradation of p53. Hdm2 revealed nucleolar accumulation after treatment of cells with ActD (Fig.

35), and could potentially be involved in the unmasking of the 1C3 epitope. Therefore, the functional and physical interaction of Hdm2 and Ppan was studied.

3.13 Stabilization of p53 by overexpression of Ppan

To test whether Ppan is involved in the activation of p53 untransfected or stably transfected HepG2 cells (HepG2 Ppan, -PpanΔσ70 and -PpanΔN) were treated for 72 hours with doxycycline to induce expression of respective proteins. Cellular lysates were separated in polyacrylamide gels and immunoblotted with antibodies to p53, Hdm2, tubulin, HA and Ppan (Fig. 38).

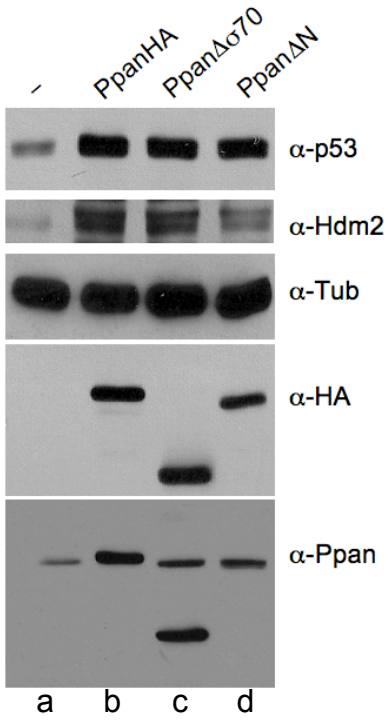

Fig. 38. Ectopic production of Ppan, PpanΔσ70, and PpanΔN activates p53 and Hdm2. Western blot analysis of cellular lysates of non- or stably transfected HepG2 with pRTS-Ppan, -PpanΔσ70 and -PpanΔN. Cells were incubated in medium containing 1 μg/ml doxycycline to allow expression of the genes. 72 hours later, cellular lysates were separated and immunoblotted for detection of p53 (DO-1), Hdm2 (SMP-14), α-tubulin, HA (3F10) and Ppan (1C3). The Ppan antibody recognizes endogenous and overproduced protein (in lanes b and c).

Similar to p53, Hdm2 is an extremely unstable protein and only little amounts are detectable in cells (Fig. 38a). Recombinant Ppan was expressed at least 10-fold higher compared to endogenous Ppan (Fig. 38b). Expression of Ppan, PpanΔσ70 and PpanΔN induced elevated levels of p53 and Hdm2.

To investigate if the increase was due to stabilization of both proteins, the half-life of p53 and Hdm2 was investigated after treatment of cells with cycloheximide (CHX). Expression of Ppan was induced for 68 hours followed by addition of CHX for indicated times. Levels of p53 protein in control cells and cells expressing Ppan were

determined by Western blot analysis (Fig. 39). The half-life of the p53 protein was approximately 60 minutes in control cells, while p53 levels remained stable in Ppan overexpressing cells after addition of CHX.

Overexpression of Ppan led to the stabilization of the p53 protein in U2OS cells. In contrast Hdm2 was destabilized and showed an increased turnover compared to control cells. The half-life of Hdm2 in control cells of about 90 minutes was reduced to about 30 minutes in Ppan overexpressing cells. In conclusion, overexpression of Ppan may stabilize p53 by the concomitant destabilization of the Hdm2 protein. Thus, stabilization of p53 could be a consequence of destabilization of Hdm2.

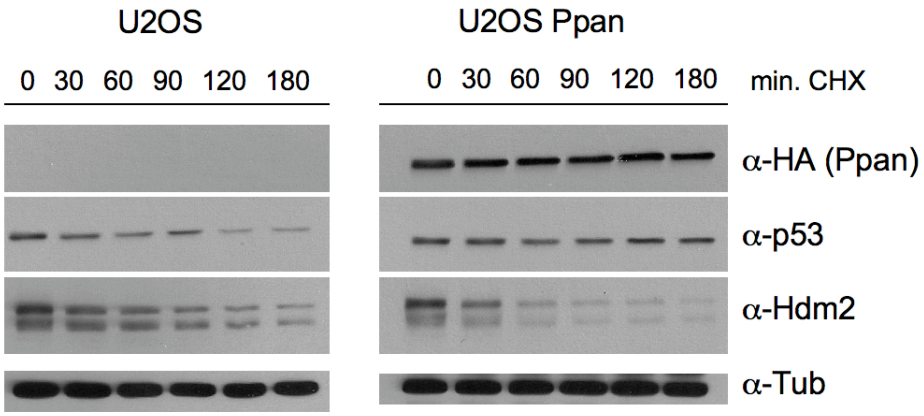

Fig. 39. Overexpression of Ppan stabilizes p53 and destabilizes Hdm2. Expression of recombinant Ppan was induced in U2OS cells (U2OS Ppan) for 68 hours. Subsequently, cycloheximide (CHX, 50 μg/ml) was added for indicated times. Level of Ppan (HA), p53 (DO-1), Hdm2 (SMP14) and tubulin were determined by immunoblot analysis.

If overexpression of Ppan induces destabilization of Hdm2, what could be the mechanism? Does Ppan interact with Hdm2 upon nucleolar stress?

3.14 Activation of p53 and Hdm2, but not Ppan, NPM or Pes1 by MG-132

The study of the interaction of Ppan and Hdm2 is not trivial, since both proteins are not highly abundant in proliferating cells. Treatment of cells with the proteasome inhibitor MG-132 not only inhibits the degradation of proteins with high turnover rates, but also inhibits processing of ribosomal RNA. In fact, treatment of HepG2 cells with

MG-132 strongly increased the levels of Hdm2 and p53, but not Pes1, NPM and Ppan (Fig. 40).

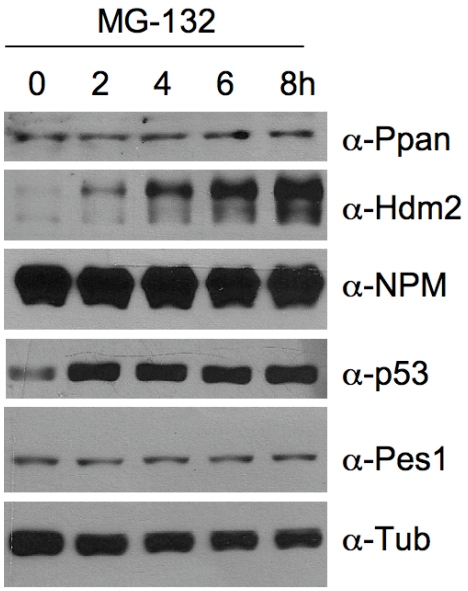

Fig. 40. MG-132 induces and increases the cellular levels of p53 and Hdm2, but not of Ppan, NPM and Pes1. HepG2 cells treated with 10 μM MG-132 were lysed at indicated time points after drug incubation. Western blot analysis of total cell lysates for Ppan (1C3), Hdm2 (SMP-14), NPM (FC-6), p53 (DO-1), Pes1 (8E9) and tubulin (DM1A).

Similar to the nuclei/nucleoli separation experiment after ActD treatment described in Fig. 35, Hdm2 accumulated in the nucleoli of HepG2 cells upon MG-132 treatment, while Hdm2 in unstressed cells was detectable preferentially in the nuclear fraction (Fig. 41).

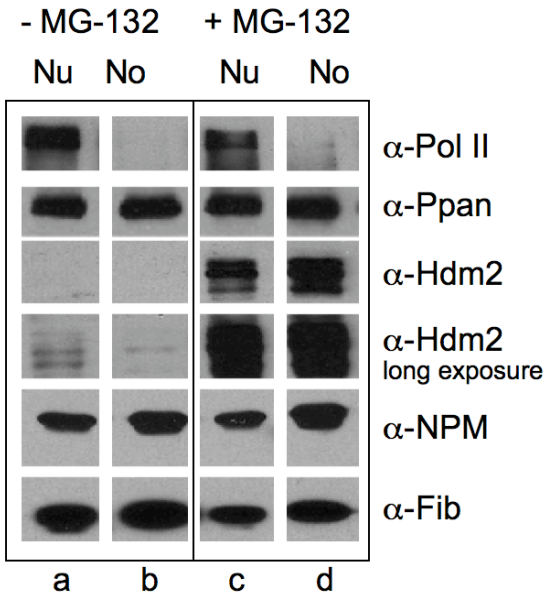

Fig. 41. Stabilization and nucleolar localization of Ppan and Hdm2 after MG-132 treatment. Western blot analysis of nuclear and nucleolar preparations form untreated and MG-132 treated HepG2 cells. 10 μM MG-132 was applied for 6 hours. 1% of nuclear (**Nu**) and 10% of nucleolar (**No**) extracts were separated in SDS-PAGE followed by immunoblot analysis using antibodies: α-Pol II (8WG16), α-Ppan (1C3), α-Hdm2 (SMP-14), α-NPM (FC-6) and α-fibrillarin.

3.15 Interaction of Ppan with Hdm2

Since Hdm2 accumulates after MG-132 treatment of cells and co-localizes with Ppan in nucleoli, the possible interaction of both proteins was studied in co-immunoprecipitation experiments. HepG2 cells were treated with MG-132 for six hours and prepared afterwards for immunoprecipitation with α-Ppan (1C3), α-Hdm2 (SMP14 and D-12) and the isotype control for Ppan (α-Pol II). In extracts of untreated cells Ppan did not co-immunoprecipitate Hdm2 (Fig. 42, lane 2), whereas in extracts of MG-132 treated cells Ppan co-precipitated the stabilized Hdm2 (Fig. 42, lane 4).

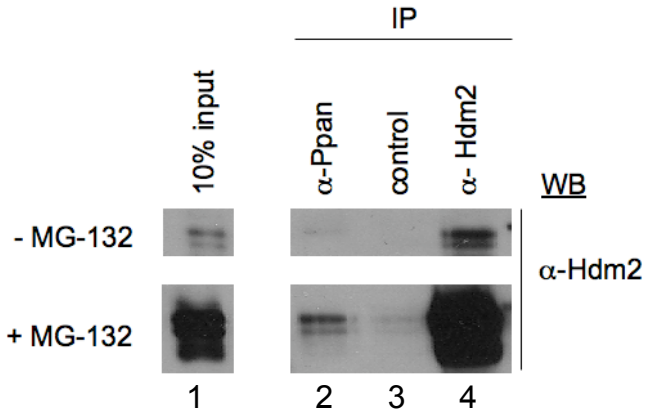

Fig. 42. Ppan interacts with Hdm2 after proteasome inhibition by MG-132. Western blot analysis of co-immunoprecipitations. HepG2 cells were left untreated or treated with 10 μM MG-132 for 6 hours. 10% of total lysate was loaded as input control. Ppan was precipitated by 1C3 monoclonal antibody, Hdm2 by a 1:1 mix of SMP-14 and D-12 antibodies. Control antibody (α-Pol II) with the same isotype to Ppan was used. Western blot was developed for Hdm2.

Ppan thus interacts with Hdm2 after MG-132 treatment in HepG2 cells. Under these conditions, the N-terminal domain of Ppan, recognized by the antibody 1C3 is masked (Fig. 31). To investigate if this domain of Ppan was masked by the interaction with Hdm2, Ppan and the Ppan mutant PpanΔN lacking the N-terminal region were immunoprecipitated in HepG2 cells (Fig. 43). For this, HepG2 cells stably transfected with pRTS-Ppan and -PpanΔN were incubated in medium with doxycycline to express the proteins for 72 hours. Immunoprecipitation of Ppan with the HA antibody co-precipitated Hdm2 (Fig. 43a, lane 1) and vice versa precipitation of Hdm2 co-precipitated Ppan (same figure, lane 3). In cells producing PpanΔN, this truncated form was precipitated by HA and concomitantly co-precipitated Hdm2 (Fig.

43b, lane1). When precipitating Hdm2 in the same cells the PpanΔN was also present in the precipitates (same figure, lane 3). The results suggest that this N-terminal region is not essential for the precipitation of Hdm2 after MG-132 treatment.

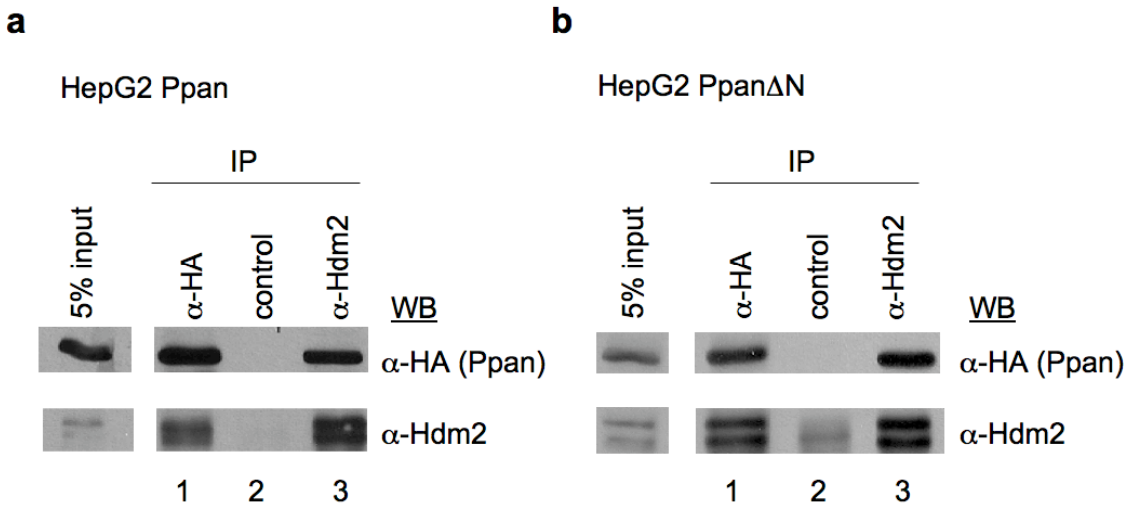

Fig. 43. Ppan and PpanΔN interact with Hdm2 after proteasome inhibition by MG-132. Western blot analysis of co-immunoprecipitations. HepG2 cells, stably transfected with pRTS-Ppan and -PpanΔN were incubated with 1 μg/ml doxycycline for expression of the proteins for 72 hours. Cells were treated with 10 μM MG-132 for 6 hours. 5% of the total lysate was loaded as the input control. Ppan and PpanΔN were precipitated by the HA antibody (12CA5), Hdm2 by 1:1 mix of SMP-14 and D-12 antibodies. As a control immunoprecipitations of the HA antibody (12CA5) in non-transfected HepG2 cells was performed. Antibodies HA (3F10) and Hdm2 (SMP-14) were used for Western blot analysis.

To investigate the occurrence and subcellular localization of Ppan and Hdm2 interaction in living HepG2 cells, the Bimolecular Fluorescence Complementation Assay (BiFC) was used. When cells were transfected with empty vectors (YN and YC), no detectable BiFC signal was observed (Fig. 25). In contrast, when Ppan and Hdm2 were expressed on co-transfected plasmids, BiFC signals mainly in the nucleoli and lower signals in nucleoplasm were noticed (Fig. 44a). Pes1 did not show any interaction with Hdm2 in BiFC analysis (Fig. 44b). Hdm2 interacted with p53 (Fig. 44c) (pBiFC-YN(1-154)*-p53 or simplified YN p53 was a gift from Dr. Michaela Rohrmoser, Helmholtz Centre Munich) in nucleoplasm as expected, whereas Ppan showed with p53 a very weak BiFC signal in cytoplasm (Fig. 44d).

In conclusion, Ppan interacts with Hdm2 and this interaction occurs preferentially in the nucleoli of HepG2 cells. A minor part of the proteins are interacting in the nucleoplasm.

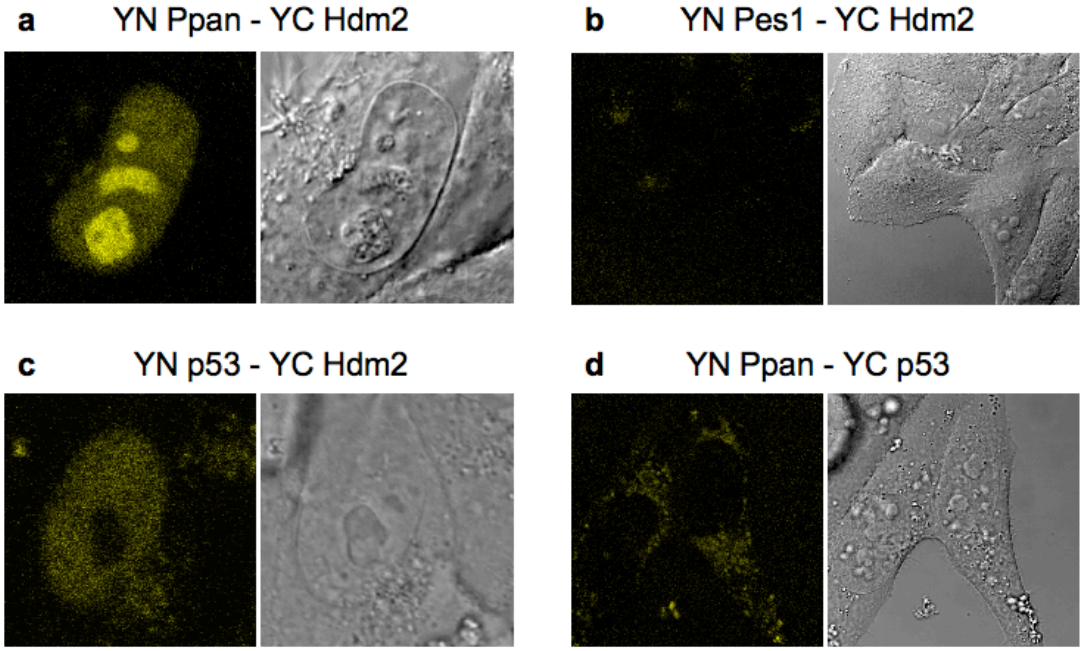

Fig. 44. BiFC analysis of Ppan and Hdm2, p53 and Hdm2, Pes and Hdm2, Ppan and p53. HepG2 cells were co-transfected with plasmids coding for respective proteins. Living cells were examined for BiFC complex formation under a laser scanning confocal microscope twenty-five hours post transfection. Emission of YFP was measured between 529-560 nm.

4. Discussion

The key function of the nucleolus is the synthesis and processing of ribosomal RNAs (rRNAs) and their assembly into ribosomal subunits (r-subunits) (Busch and Smetana, 1970; Hadjiolov, 1985). Control of synthesis of new ribosomes is crucial for the regulation of growth and the process is tightly regulated in response to environmental conditions. One of the most intriguing novel roles of the nucleolus is the participation in sensing cellular stress signals and transmitting them to the p53 stabilization system (Visintin and Amon, 2000; Rubbi and Milner, 2003; Olson, 2004; Mayer and Grummt, 2005). When ribosome biogenesis is blocked or disrupted, immediate signals activate the guardian of the genome p53. The signal transmission from nucleoli to p53 seems to be dependent on the type of stress and is discussed in many ways in the actual literature. In this study the protein Ppan was characterized and added to the list of nucleolar proteins involved in cellular stress response.

4.1 What is the mechanism by which Ppan associates with nucleoli?

The nucleolus is a nuclear compartment without being surrounded by a membrane. The residency of proteins and RNAs in the nucleolus is coordinated through an interaction network. For instance, the nucleolar localization of aprataxin is dependent on its interaction with the nucleolar protein nucleolin and on active rDNA transcription (Becherel *et al.*, 2006). By depleting nucleolin with a specific siRNA, aprataxin delocalizes from the nucleoli. Similarly, the protein Bop1 requires its binding partner Pes1 for stable association with the nucleolus (Rohrmoser *et al.*, 2007).

To answer the question of promoting Ppan's localization in the nucleolus, I firstly performed RNAseA and DNAseI digestion experiments. The nucleolar residency of Ppan was clearly independent of DNA but probably dependent on its binding to RNA. Of course it cannot be excluded under these experimental conditions that Ppan is interacting with another protein, which confers the nucleolar localization. A hypothetical interactor of Ppan could be bound to RNA and translocate highly sensitive after RNAseA treatment out of the nucleolus. To find out if Ppan itself is translocating after loss of RNA binding, I generated a mutant form of Ppan, missing the RNA binding σ70 like motif. Immunofluorescence analysis of Ppan$\Delta\sigma$70

supported the observation that its RNA interaction domain is important to anchor the protein into the nucleolus. More importantly this experiment showed that Ppan itself is bound to RNA and the translocation after RNAseA treatment is probably not a secondary effect promoted by another protein. RNAseA treatment impacts at least two types of RNAs in the nucleolus: small nucleolar RNAs (snoRNAs) and pre-rRNAs. Which type of the RNA is bound to Ppan is still unknown. Studies on the yeast homologue of Ppan, Ssf1, revealed an interaction with the yeast 27S rRNA, the precursor of 5.8S and 25S rRNA (Fatica *et al.*, 2002). The 27S rRNA in yeast corresponds to the 32S rRNA in mammalian cells. This could be a candidate RNA for human Ppan, assuming that it would posses the same role in human cells. This speculation has to be verified by further studies.

The mutant of Ppan lacking the coil-coil domain was excluded from the nucleoli and dispersed throughout the nucleoplasm. The coil-coil domain is a protein-protein interaction domain, which indicates that Ppan needs probably to be bound to another nucleolar protein, additionally to RNA, for residing in the nucleolus. The regulation of nucleolar localization of Ppan seems to be more complex.

The nucleoli are disassembled during mitosis. The localization of nucleolar factors during mitosis can vary. For example, some factors, including several snoRNAs, move toward the nuclear envelope and associate either with the condensing chromosomes forming a layer surrounding the chromosomes called the perichromosomal region (Gautier *et al*., 1992, van Hooser *et al*., 2005) or are found in the cytoplasm and appear to become associated with the spindle apparatus in the cytoplasm (Gassmann *et al.*, 2005; Hernandez-Verdun and Gautier, 1994). During mitosis Ppan was found associated with the perichromosomal region. The localization of proteins in the perichromosomal region has been observed in a variety of plant and animal cells and is suggested to have a role in the equal distribution of proteins to daughter cells required for early nuclear and nucleolar assembly following mitosis (van Hooser *et al*., 2005). This would imply that Ppan might play a role in the early assembly of nuclear and nucleolar structures.

4.2 Binding partners of Ppan

For identification of interaction partners of Ppan, I decided to study its molecular associations with the components of the PeBoW complex, Pes1, Bop1 and WDR12.

The homologues of these three proteins in yeast are interactants of Ssf1. Indeed Ppan interacted with Pes1, Bop1 and WDR12, as did Ssf1 with Nop7, Erb1 and Ytm1 (Fatica *et al.*, 2002).

Two interactions of Ppan in human cells have been described in the past, both are involved in ribosome biogenesis. Nop56p is associated with pre-ribosomal ribonucleoprotein complexes (Hayano *et al*., 2003) and is a component of the box C/D small nucleolar ribonucleoprotein complexes that direct 2'O-methylation of pre-rRNA during its maturation (Gautier *et al.*, 1997). The second protein is the DEAD-box RNA helicase DDX47 (Sekiguchi *et al*., 2006). RNA helicases from the DEAD-box family are present in almost all organisms and have important roles in RNA metabolism (de la Cruz *et al.*, 1999). DDX47 localizes nucleolar and is probably involved in the processing of the primary rRNA transcript and mRNA splicing (Sekiguchi *et al*., 2006). The main role of DDX47 is likely to be in 60S ribosome subunit assembly.

Ppan interacts with Pes1, Bop1, WDR12, Nop56 and DDX47, proteins involved in the processing and maturation of the large subunit 28S rRNA. Ribosome biogenesis in eukaryotes involves a coordinated and sequential assembly of a large number of protein factors in ribonucleoprotein complexes that contain precursors of the rRNAs (Saveanu *et al.*, 2003).

The role of Ppan in the regulation of rRNA processing is not clear. In yeast, deletion of Ssf1 leads to a delay in cleavage at sites A_0, A_1 and A_2 of the pre-rRNA precursor (Fatica *et al.*, 2002). By interacting with rRNA processing factors, Ppan could control the right order of rRNA processing and prevent premature processing, as does Ssf1 in yeast. The siRNA knock-down of *ppan* in this work gave first hints for a similar role in mammalian cells. In the case of stalled ribosome biogenesis, Ppan might form new complexes which are involved in signalling to cell cycle checkpoints.

An intriguing and novel result of this work is the interaction of Ppan with Hdm2. The interaction has been shown for endogenous and overexpressed Ppan under conditions where Hdm2 is stabilized through inhibition of the proteasome. The interaction could be confirmed by BiFC analysis in living cells, and occurred predominantly in the nucleolus. The isolation of nucleoli of HepG2 cells confirmed that Ppan and Hdm2 were present in this nuclear compartment during proteasome inhibition by MG-132. This opens new insights in the function of Ppan in mammalian cells, placing Ppan into the group of nucleolar proteins involved in recognition and

transmission of nucleolar perturbation to the cellular stress response machinery. The implications of this interaction are discussed later in this chapter.

4.3 Nucleolar detection of Ppan changes after nucleolar stress

The N-terminus of Ppan is masked in nucleoli of about 20 % of proliferating cells. Nucleolar stress, like 5-FU or ActD leads to an unmasking of the N-terminus of Ppan, which is then accessible for the 1C3 antibody in all nucleoli of treated cells. In contrast, the N-terminus of Ppan in nucleoli of cells treated with MG-132 was nearly completely inaccessible to the 1C3 antibody in immunofluorescence analysis. However, the 1C3 antibody efficiently binds to denatured Ppan protein from MG-132 treated cells, as evidenced by Western blotting of cellular proteins. Thus, Ppan seems to undergo a conformational change or a protection of the epitope by other factors upon nucleolar stress.

Could the masking of the N-terminus be dependent on the cell cycle phase of the individual cell? For example, the proteasome inhibitor MG-132 leads to a cell cycle arrest in the G2/M phase (Kim *et al.*, 2004) and the N-terminus of Ppan could be masked in a G2/M specific manner, whereas 5-FU synchronizes the cells in the G1 phase (Yoshikawa *et al.*, 2001), where no masking was observed. However doxorubicin (O' Loughlin *et al.*, 2000) and oxaliplatin (William-Faltaos *et al.*, 2006) also lead to a G2/M phase arrest but did not induce a masking of the N-terminus of Ppan. Instead all treated cells showed a clear nucleolar staining of Ppan (data not shown). The observations with MG-132, 5-FU, doxorubicin and oxaliplatin support the notion that the epitope masking of Ppan is probably not dependent on the cell cycle phase, but rather a consequence of the individual stress situation.

4.4 Potential role of Ppan during inhibition of the rRNA processing

A speculated mechanism of 5-FU cytotoxicity features the incorporation of 5-FU into RNA. Evidence comes from experiments showing that co-treatment of cells with uridine, but not thymidine, can relieve the cytotoxic effects of 5-FU (Engelbrecht *et al.*, 1984). 5-FU is rapidly incorporated into pre-rRNA in treated cells, since rRNA is the most abundant class of RNA produced in proliferating cells. Experiments suggest

that 5-FU may cause inhibition of processing at early steps, probably at the primary processing site without affecting ribosomal gene transcription (Cory *et al*., 1979; Greenhalgh and Parish 1989 and 1990; Ghoshal and Jacob, 1994). Goshal and Jacob (1994) proposed, that the drug-induced inhibition of pre-rRNA processing was due to alteration in the activity and/or synthesis of a trans-acting factor rather than inefficient utilization of 5-FU-containing RNA. More recent evidence has refocused attention on rRNA processing being a target for 5-FU, since genome-wide screens in *Saccharomyces cerevisiae* for gene products sensitive to the drug identified components of the rRNA processing pathway (Lum *et al*., 2004). Treatment of a yeast heterozygous deletion pool with 5-FU revealed a drug-induced haploinsufficiency for eight genes, four of them being components of the exosome. Interestingly *ssf1*, the homologue of human *ppan*, was one of these eight target genes, as well as *nop4*, *mak21* and *rrp15*. Ssf1 has been found in a complex with Nop4, Mak21 and Rrp15 (Gavin *et al*., 2002; Fatica *et al*., 2002, Krogan *et al*., 2006), which are required in yeast for processing and maturation of the large ribosomal subunit. Ssf1 seems to be important for the survival of the yeast cells after 5-FU induced ribosomal stress.

Using DNA microarrays to analyze the effect of 5-FU to the yeast transcriptome, it was found that the drug causes firstly the accumulation of polyadenylated fragments of the 27S rRNA precursor and second, that 5-FU antagonized the ability of the exosome to degrade the accumulated polyadenylated rRNAs (Fang *et al*., 2004). In the same study it was shown that production of poly(A)$^+$ 27S rRNA may be a general result of inhibition of rRNA processing. The existence of polyadenylated rRNA was confirmed for human cells (Slomovic *et al*., 2006).

Ppan may be part of a similar surveillance pathway in mammalian cells. Evidence for this assumption comes from the observation that the Ppan$\Delta\sigma$70 mutant can bind and direct the exosome subunit hRrp6 to nuclear spots. This redistribution was observed also for other nucleolar factors. Since the RNA binding motif of the σ70 domain usually retains Ppan in the nucleolus, Ppan (with other factors) might recruit the exosome to polyadenylated rRNA.

Proteasomal regulation has been implicated in many processes, including cell cycle progression, transcription and antigen processing (Hershko and Ciechanover, 1998; Goldberg, 2003; Muratani and Tansey, 2003; Wojcik and DeMartino, 2003). Indirect evidence was given for the participation of the ubiquitin-proteasome system in

ribosome biogenesis. In mammalian cells complexes associated with early and late pre-rRNA processing factors contain ubiquitinated components. Inhibition of the proteasome induces additional ubiquitination of complexes associated with late processing factors, changes in nucleolar morphology and inhibition of pre-rRNA processing (Stavrera *et al*., 2006). MG-132 is a potent inhibitor of the proteasome. In my work, MG-132 treatment led to a stabilization and interaction of Hdm2 with Ppan. Primarily the proteasome inhibitor was used to stabilize Hdm2, in order to detect it and have it in good quantities for the studies. However, MG-132 does not only stabilize proteins, but also inhibits ribosome biogenesis. The mechanims of this inhibition is not yet clear. However, a consequence could be the interaction of Ppan with Hdm2 and the sequestration of Hdm2 in the nucleolus. The nucleolar interaction of Ppan and Hdm2 could be demonstrated in this work by BiFC experiments. Thus, Ppan could be a possible link between inhibition of ribosome biogenesis and p53 stabilization.

Sun et al. (2007) showed that the activation of p53 after 5-FU treatment involves the interactions of Hdm2 with the ribosomal proteins L5, L11 and L23. The stabilization of p53 after inhibition of rRNA processing seems to be more complex regulated, possibly by several nucleolar factors.

Nucleophosmin (NPM) is a multifunctional nucleolar phosphoprotein, which is constantly shuttling between the nucleolus and cytoplasm (Borer *et al.*, 1989). NPM functions as a ribosome assembly and transport protein, binds to proteins containing nuclear localization sequences for their import, acts as a molecular chaperon and is essential in centrosome duplication (Kurki *et al*., 2004). NPM is redistributed from the nucleolus to the nucleoplasm in response to cytotoxic and genotoxic stress (Wu and Yung, 2002; Wu et al., 2002; Yang et al., 2002; Rubbi and Milner, 2003). The interaction of NPM with Hdm2 in the nucleolus after inhibition of the proteasome by MG-132 (Kurki *et al.*, 2004) was extended in this work to Ppan. Since the Ppan $\Delta\sigma$70 mutant attracts NPM to the newly formed nuclear foci, a multiple complex of NPM, Hdm2 and Ppan could be envisaged. Importantly, the N-terminus of Ppan becomes masked after MG-132 treatment, which implicates a new interaction of Ppan with another protein under these conditions. Whether NPM or Hdm2 could be the masking interaction partner has to be studied in future experiments.

4.5 Ppan localizes in the core body of segregated nucleoli

Nucleoli of cells show great variability at different stages of cellular metabolic activity. A special phenotype is the nucleolar segregation, which occurs under physiological circumstances, when transcription is shut down during differentiation and development and can be mimicked by drug-induced transcriptional arrest (Dousset *et al.*, 2000; Shav-Tal *et al.*, 2005). Additionally, nucleolar segregation is observed in quiescent cells (Malatesta *et al.*, 2000) and can be followed by nucleolar reassembly. This mechanism provides flexibility to the cell to maintain a certain degree of nucleolar structure after shut off of rRNA transcription. In segregated nucleoli the fibrillar and granular zones disengage and form separate but juxtaposed structures. These structures show cap-like formations around the core body of the segregated nucleolus. The most nucleolar factors delocalize after transcriptional arrest to newly-formed cap-structures, like fibrillarin (Shav-Tal *et al.*, 2005) or translocate to the nucleoplasm, like nucleophosmin (Shav-Tal *et al*., 2005) and hRrp6 (Brouwer *et al.*, 2001). The presence of Ppan in the core body of the segregated nucleoli is a striking observation. Until now only two components have been reported to reside to this site: the tumor suppressor p14Arf and the MRP RNA. p14Arf activates p53, by sequestration of Hdm2 into the nucleoli after oncogenic stress induced by overexpressed or mutated oncogenes, such as Myc (Weber *et al.*, 1999) or Ras (Palmero *et al.*, 1998). The MRP RNA is involved in the cleavage and maturation of precursor rRNA (van Eenennaam *et al.*, 2000). The residence of Ppan in the core body of stressed nucleoli might indicate that it has a function in retaining the structural integrity of the nucleolus. When the inhibition is abolished, the segregated nucleoli can reshape and Ppan could be involved in this re-establishment, for example by recruitment of other nucleolar factors.

4.6 Ppan co-localizes with Hdm2 in nucleoli when the rDNA transcription is inhibited

The RNA polymerase I activity is responsible for rRNA synthesis and the integrity of the nucleolus. Nucleolar proteins, like nucleophosmin, nucleolin, and many other rRNA binding factors translocate from the nucleolus to the nucleoplasm when the

transciption by the RNA polymerase I is inhibited (Chan, 1992; Kalousek *et al.*, 2005; Shav-Tal *et al.*, 2005). Actinomycin D (ActD) is a chemotherapy drug, which has been used in the treatment of a variety of human cancers for many years. At high concentrations (e.g. >30 nM) ActD causes DNA damage and inhibits transcription of all three classes of RNA polymerases, whereas at low concentrations (e.g. <10 nM) ActD selectively inhibits the RNA polymerase I-dependent transcription and thus ribosomal biogenesis (Perry and Kelley, 1970; Iapalucci-Espinoza and Franze-Fernandez, 1979). Treatment with low levels ActD (5 nM) has previously been shown to stabilize p53 by disintegrating the p53/Hdm2 complex through localization of Hdm2 to nucleoli of treated cells (Ashcroft *et al.*, 2000). In this work I could show the co-localization and interaction of Ppan with Hdm2 after treatment with low doses of ActD in nucleoli of HepG2 cells. Recent studies have shown the interaction of Hdm2 and L11 in nucleoli of ActD treated cells (Lohrum *et al*., 2003). Taken together a stress-signalling complex containing L11 and Ppan can be proposed that sequesters Hdm2 in the nucleolus upon stress. This has to be verified in future studies.

In the studies of Andersen *et al*. (2003) the translocation of Ppan from the nucleolus to the nucleoplasm has been described after transcription inhibition by ActD. This is not consistent with results in my work. However, Andersen and his colleagues used for their study 5 µg/ml (4 µM) ActD, thus about 1000 fold higher concentrations where nucleoli are almost entirely disrupted and may explain why Ppan was found to translocate to the nucleoplasm in the work of Andersen *et al*. (2003).

4.7 Why is Ppan a tumor suppressor?

Ppan has been discussed to be a tumor suppressor in human HF cells (Welch *et al.*, 2000). The HF cells originate from the HeLa cervical cancer cell line, which is infected by the human papillomavirus (HPV). The HPV E6 oncogene targets the p53 protein for ubiquitination and rapid degradation (Huibregtse and Beaudenon, 1996). Interestingly, the HF cells show a stabilization and reactivation of the p53 protein through a reduced binding of the E6 protein to p53 (Athanassiou *et al.*, 1999). Thus, Ppan can act as a tumor suppressor in a p53 positive backround. The mechanism how Ppan functions as a tumor suppressor is unknown.

Tumor suppressors function either by controlling the cell cycle or apoptosis or are involved in DNA damage repair. The major representative is the tumor suppressor

p53. Elevated levels of p53 can inhibit cell growth or induce apoptotic cell death. p53 functions as a sequence-specific transcription factor and regulates the expression of target genes involved in growth arrest, apoptosis, DNA repair, senescence or differentiation (Vogelstein *et al*., 2000; Smeenk *et al*., 2008). The p53 protein levels and activity are under tight control.

Proteins, which can govern the activity of p53 can also act as tumor suppressors, like p14Arf. p14Arf activates p53 directly by interaction with the negative regulator of p53, Hdm2. Hdm2 plays a pivotal role in regulating p53 protein levels and is involved in its degradation (Haupt *et al*., 1997; Kubbutat *et al*., 1997). Hdm2 binds to the N-terminus of p53 and thereby facilitates the ubiquitination and subsequent proteasome-mediated degradation of the p53 protein. Several mechanisms were discussed by which p53 is stabilized. These mechanisms target either p53 or Hdm2 (Ashcroft *et al*., 2000). In the case of Hdm2, Hdm2 can interact with ribosomal proteins S7 (Chen *et al.*, 2007), L5 (Marechal *et al.*, 1994), L11 (Lohrum *et al.*, 2003, Zhang *et al.*, 2003) and L23 (Jin *et al.*, 2004), if these proteins are supplied in excess if ribosome biogenesis is blocked. The fact that Hdm2 interacts with ribosomal proteins suggests a link by which cells can coordinate cell growth with proliferation. The multiple Hdm2-interacting ribosomal proteins may have a synergistic effect to bring about a quick and strong inhibition of Hdm2 when ribosomal damage occurs (Jin *et al.*, 2004). Sequestration of Hdm2 to the nucleolus has also been observed by the tumor suppressor p14Arf (Tao and Levine, 1999).

The above information was integrated to understand a possible role of Ppan in human cells. Ppan interacts with Hdm2 and thereby stabilizes p53. How could this stabilization of p53 be managed? Two possibilities can be considered: the disruption of the nucleoplasmic Hdm2-p53 complex by, for example, sequestration of Hdm2 to the nucleolus or the influence of Ppan on the stability of Hdm2.

Indeed, the Ppan-Hdm2 interaction was mainly nucleolar, as seen by the BiFC analysis. This could indicate a sequestration of Hdm2 into the nucleoli, preventing the nucleoplasmic Hdm2-p53 complex. As a consequence p53 is no longer bound by Hdm2 and therefore not subjected to Hdm2-mediated proteasomal degradation.

Recent studies showed that regulated Mdm2 auto-degradation is an important mechanism by which p53 is activated in cells treated with DNA damaging agents (Stommel and Wahl, 2004). This led to a second proposal for Ppan as a possible activator of p53, by destabilizing Hdm2. Overexpressed Ppan and the truncated

Ppan form PpanΔσ70 showed a clear induction of p53 and also of Hdm2. PpanΔN activated p53 but failed to induce strongly Hdm2. When studying the localization of the PpanΔN, a large part of this protein mislocalized to the cytoplasm, whereas a small part localized nucleolar and slightly nucleoplasmic. This could speculate that the activation of Hdm2 is performed only when Ppan localizes nuclear (nucleoplasmic and nucleolar), thus under normal conditions. Overproduced Ppan could clearly destabilize the activated Hdm2 by reducing the half-life of the protein. The mechanism how it is established is completely unknown. Phosphorylation of Hdm2 is likely to play a role in degradation (Stommel and Wahl, 2004). The phosphorylation is thought to be at multiple sites and by multiple DNA damage-activated kinases of the PI 3-kinase family, such as ATM of ATR (Stommel and Wahl, 2005). In addition to phosphorylation, it was shown that the intrinsic ubiquitin ligase activity is required for Hdm2 destabilization. A specific domain of Hdm2, the RING domain, is involved in this activity. The RING domain binds also accessory proteins that might contribute to the regulation of ubiquitination. MdmX might be the most interesting candidate for this role. MdmX interacts and stabilizes Hdm2 through its ring domains (Tanimura *et al.*, 1999; Sharp *et al.*, 1999). MdmX was found to be an important regulator of p53 activation after ribosomal stress (Gilkes *et al.*, 2006). It sequesters p53 to inactive Mdmx-p53 complexes, preventing the p53 activation through inhibiting of its DNA binding activity. Taken the data together, Ppan could lead to a destabilization of Hdm2, possibly by recruiting kinases to phosphorylate Hdm2. Furthermore an interaction with Hdm4 (human homologue of MdmX) could lead to the destabilization of Hdm2. These speculations are open to be investigated in future studies.

It would be also possible that Ppan can stabilize p53 in conditions other than nucleolar stress. c-Myc can elevate the expression of Ppan and other nucleolar proteins, such as Pes1, Bop1 and WDR12, suggesting that Ppan could also play a role in mediating induction of p53 in response to Myc. The preliminary results showing that Ppan is able to stabilize p53 could explain the role as a postulated tumor suppressor.

Hdm2 has been extensively studied as a regulator of p53. Nevertheless, there is considerable evidence that Hdm2 has p53-independent functions (Ganguli and Wasylyk, 2003). Hdm2 has been shown to interact with a large number of proteins besides p53. The retinoblastoma protein (pRB) is a tumor suppressor that functions

similar to p53 in cell cycle inhibition and apoptosis. Hdm2 interacts with pRB and modulates its activity, the pRB mediated G1 arrest (Xiao *et al.*, 1995). The Mdm2 binding protein (MTBP) induces a G1 arrest in a p53-independent manner and this arrest can be inhibited by interaction of MTBP with Hdm2 (Boyd *et al.*, 2000). Hdm2 binds and promotes the degradation of Numb, a protein involved in differentiation (Juven-Gershon *et al.*, 1998). The DNA polymerase ε is involved in DNA repair, recombination, replication, damage sensing and chromatin remodelling and interacts with Hdm2 (Vlatkovic *et al.*, 2000).

The p53-independent functions of Hdm2 could have implications on the Ppan-Hdm2 interaction. Ppan could act as a tumor suppressor independently on p53. The unmasking of the N-terminus of Ppan after ActD treatment was independent of p53 in HCT cells. This implicates that the unmasking of Ppan is an action before, and possibly needed for the activation and stabilization of p53 or the function of Ppan is independent on p53 in these cells. The observation that overexpression of Ppan is followed by activation and stabilization of p53 suggests, that Ppan may regulate the p53 pathway. Nevertheless other mechanisms have to be considered in future studies.

4.8 Model for action of Ppan in human cells

The results obtained during this thesis led me propose the following models (Fig. 45a-c):

Ppan localizes in the nucleolus in an RNA- and protein-interaction dependent manner (Fig. 45a). It interacts with factors involved in the processing of rRNA. After nucleolar perturbation most nucleolar factors delocalize from the nucleolus to the nucleoplasm. Ppan remains in nucleoli of cells with defects in rRNA processing or rDNA transcription and this implicates that it has probably a function in retaining the structural integrity of the nucleolus.

The inhibition of rDNA transcription causes the segregation of nucleoli, which form a core component (or central body) surrounded by nucleolar caps (Fig. 45b). The majority of the nucleolar factors translocate to the nucleoplasm (like nucleophosmin (NPM) or hRrp6) or to the nucleolar caps (like fibrillarin). Ppan localizes intriguingly in the core component. Since Ppan interacts with Hdm2 in the nucleoli and L11 interacts with Hdm2 after ActD treatment, a multimeric complex of L11-Hdm2-Ppan

could be discussed.

The inhibition of rRNA processing leads to polyadenylated rRNAs, which are degraded by the exosome (Fig. 45c). Since Ppan interacts with nucleolar RNA and binds to the exosome component hRrp6, it could sequester the latter to polyadenylated rRNA. The N-terminus of nucleolar Ppan is masked after treatment of cells with the proteasome inhibitor MG-132 implicating changes in interactions. Ppan interacts under rRNA processing inhibition with Hdm2 in nucleoli, liberating p53 from nucleoplasmic p53-Hdm2 complexes, which leads to activation of p53. Ppan attracts probably NPM in a multimeric complex for the coordination of nucleolar malfunction and cellular response.

4.9 Outlook

The studies of this thesis reveal a mechanism for the inhibition of Hdm2 and activation of p53 through an interaction of Hdm2 with Ppan. Many questions are still open to investigate. Ppan has two nucleic acid binding domains. Firstly, the σ70 domain is important for binding to nucleolar RNA and the nucleolar localization of Ppan. Secondly, Ppan possesses two AT-hook domains, which bind probably to AT-rich sequences in DNA. The nature of bound nucleic acid would give more information for the stress regulated function of Ppan.

The interaction of Ppan and Hdm2 has to be studied in more detail. Many questions are open: Is the interaction direct or mediated by other factors? Which are the domains responsible for the interaction of the proteins? Is there a competition between p53 and Ppan for binding to Hdm2? And more important: Does Ppan possibly interact with p53? Further interaction partners, which play a role in sensing cellular stress have to be investigated. It would be interesting to know if Ppan could interact with the ribosomal proteins S7, L5, L11 and L23, the main signal agents of stress-disrupted nucleoli and contribute to a complex of stress-regulated proteins, a “stressosome”. Preliminary results show that the mutant PpanΔσ70 is able to translocate NPM and hRrp6 from nucleoli to the nucleoplasm. Are NPM and hRrp6 binding partners of Ppan in the nucleolus? What would be the relevance of an interaction of Ppan with the exosome component hRrp6? Is Ppan needed to position the exosome at aberrant rRNA intermediates?

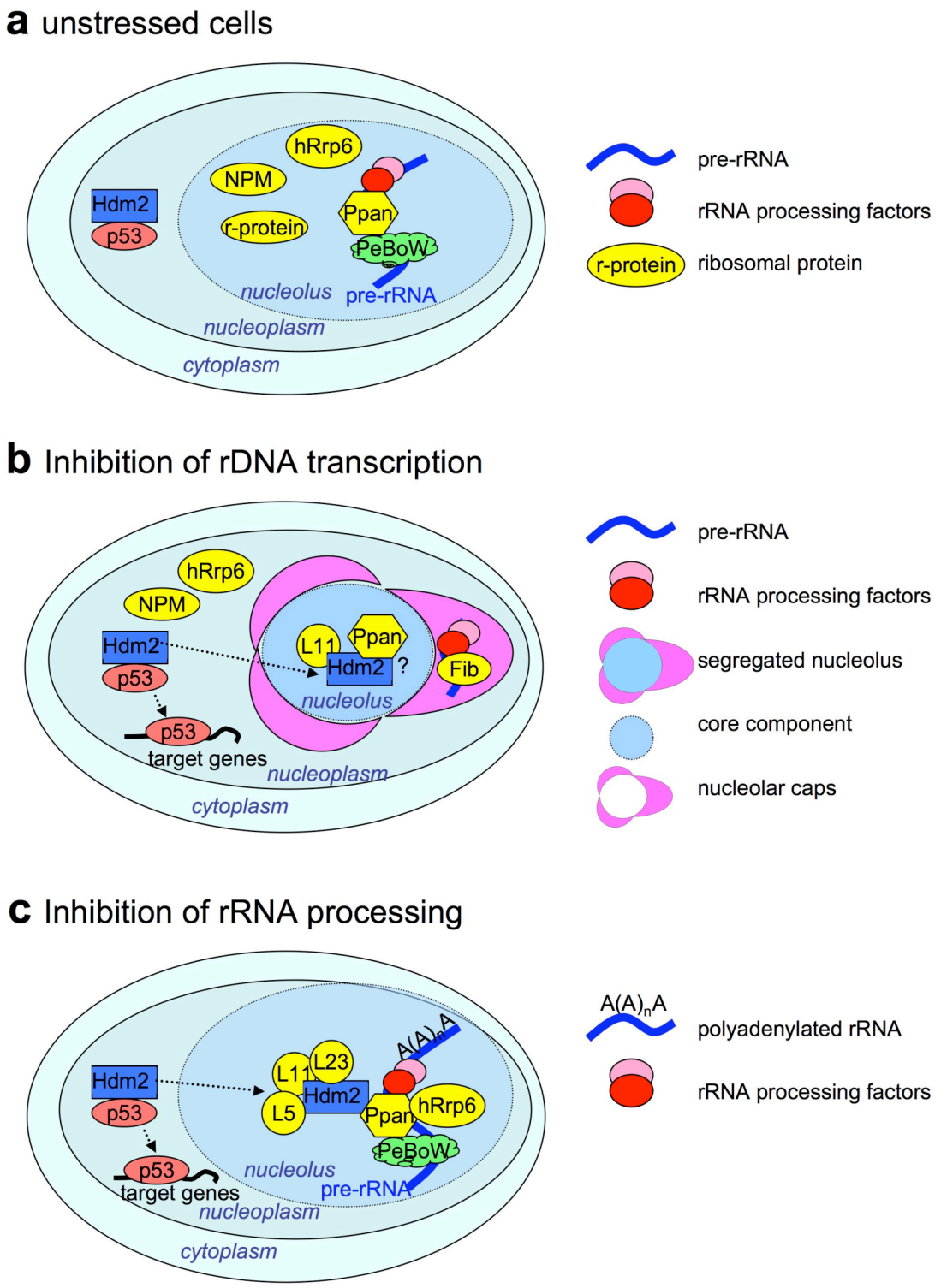

Fig. 45. Models for Ppan action in unstressed cells (a) and after inhibition of rDNA transcription (b) or rRNA processing (c) (for details see text).

Can p53 be stabilized after inhibition of rRNA processing of even rDNA transcription in a *ppan* negative backround? Which morphology would have the segregated nucleoli after ActD in cells treated with *ppan*-specific siRNA? Is Ppan needed for the re-establishment of the normal nucleolar structure after the inhibition of transcription has been removed?

The mechanism of Ppan to stabilize p53 may play a role in the response to abnormalities in ribosomal biogenesis that could occur during tumor development. Preventing the Ppan-Hdm2 interaction may therefore contribute to cancer development by inhibition or decrease of p53 activation in response to these types of stress signals. A more complete understanding of how Ppan is serving the cell could reveal novel targets for the development of therapies, aiming a reactivation of p53.

5. References

Andersen JS, Lyon CE, Fox AH, Leung AKL, Lam YW Steen H, Mann M and Lamond AI. 2002. Directed proteomic analysis of the human nucleolus. *Curr. Biol*. **12**: 1-11.

Arabi A, Wu S, Ridderstrale K, Bierhoff H, Shiue C, Fatyol K, Fahlen S, Hydbring P, Söderberg O, Grummt I, Larsson LG and Wright APH. 2005. c-Myc associates with ribosomal DNA and activates RNA polymerase I transcription. *Nat. Cell Biol.* **7**: 303-310.

Ashcroft M, Taya Y and Vousden KH. 2000. Stress signals utilize multiple pathways to stabilize p53. *Mol. Cell. Biol*. **20**: 3224-3233.

Athanassiou M, Hu Y, Jing L, Houle B, Zarbl H and Mikheev AM. 1999. Stabilization and reactivation of the p53 tumor suppressor protein in nontumorigenic revertants of HeLa cervical cancer cells. *Cell Growth Differ.* **10**: 729-737.

Bassler J, Kallas M and Hurt E. 2006. The NUG1 GTPase reveals and N-terminal RNA-binding domain that is essential for association with 60 S pre-ribosomal particles.
J. Biol. Chem. **281**: 24737-23744.

Beausoleil SA, Jedrychowski M, Scwartz D, Elias JE, Villén J, Li X, Cohn MA, Cantley L and Gygi S. 2004. Large-scale characterization of HeLa cell nuclear phosphoproteins. *Proc. Natl. Acad. Sci.* **101**: 12131-12135.

Becherel OJ, Gueven N, Birrell GW, Schreiber V, Suraweera A, Jakob B, Taucher-Scholz G and Lavin MF. 2006. Nucleolar localization of Aprataxin is dependent on interaction with nucleolin and on active ribosomal DNA transcription. *Hum. Mol. Genet.* **15**: 2239-2249.

Bernardi R, Scaglioni PP, Bergmann S, Horn H, Vousden KH and Pandolfi PP. 2004. PML regulates p53 stability by sequestering Mdm2 to the nucleolus. *Nat. Cell Biol.* **6**: 665-672.

Boisvert FM, van Koningsbruggen S, Navascués J and Lamond AI. 2007. The multifunctional nucleolus. *Mol. Cell. Biol.* **8**: 574-585.

Borer RA, Lehner CF, Eppenberger HM and Nigg EA. 1989. Major nucleolar proteins shuttle between the nucleolus and cytoplasm. *Cell* **56**: 379-390.

Boyd M, Vlatkovic N and Haines DS. 2000. A novel cellular protein (MTBP) binds to MDM2 and induces a G1 arrest that is suppressed by MDM2. *J. Biol. Chem.* **275**: 31883-31890.

Boxer LM and Dang CV. Translocations involving c-myc and c-myc function. Oncogene **20**: 5595-5610.

Boylan MO, Athanassiou M, Houle B, Wang Y and Zarbl H. 1996. Activation of tumor suppressor genes in non-tumorigenic revertants of HeLa cervical carcinoma cell line. *Cell Growth Differ.* **7**: 725-735.

Boyne JR and Whitehouse A. 2006. Nucleolar trafficking is essential for nuclear export of intronless herpesvirus mRNA. *Proc. Natl. Acad. Sci.* **103**: 15190-15195.

Brouwer R, Pruijn GJ and van Venrooij WJ. 2000. The human exosome: an autoantigenic complex of exoribonucleases in myositis and scleroderma. *Arthritis Res.* **3**: 102-106.

Budde A. and Grummt I. 1998. p53 represses ribosomal gene transcription. *Oncogene* **19**: 1119-1124.

Burger F, Daugeron MC and Linder P. 2000. Dbp10p, a putative RNA helicase from *Saccharomyces cerevisiae*, is required for ribosome biogenesis. *Nucleic Acids Res.* **28**: 2315-23.

Burkhard P, Stetefeld J and Strelkov SV. 2001. Coiled coils: a highly versatile protein folding motif. *Trends Cell Biol*. **11**: 82-88.

Busch H and Smetana K. 1970. The nucleolus. New York: Academic Press

Chan PK. 1992. Characterization and cellular localization of nucleophosmin/B23 in HeLa cells treated with selected cytotoxic agents (studies of B23-translocation mechanism). *Exp. Cell Res.* **203**: 174-181.

Chen D, Zhang Z, Li M, Wang W, Li Y, Rayburn ER, Hill DL, Wang H and Zhang R. 2007. Ribosomal protein S7 as a novel modulator of p53-Mdm2 interaction: binding to Mdm2, stabilization of p53 protein, and activation of p53 function. *Oncogene* **26**: 5029-5037.

Chen X, Ko LJ, Jayaraman L and Prives C. 1996. p53 levels, functional domains, and DNA damage determine the extent of the apoptotic response of tumor cells. *Genes Dev* **10**: 2438-2451.

Cohen PT. 2002. Protein phosphatase 1--targeted in many directions. *J. Cell Sci.* **115**: 241-56.

Colombo E, Marine JC, Danovi D, Falini B and Pelicci PG. 2002. Nucleophosmin regulates the stability and transcriptional activity of p53. *Nat. Cell Biol.* **4**: 529-533.

Communi D, Suarez-Huerta N, Dussossoy D, Savi P and Boeynaems JM. 2001. Cotranscription and intergenic splicing of human P2Y11 and SSF1 genes. *J. Biol. Chem.* **276**: 16561-16566.

Cory JG, Breland JC and Carter GL. 1979. Effect of 5-fluorouracil on RNA metabolism in Novikoff hepatoma cells. *Cancer Res*. **39**: 4905-4913.

Daniely Y, Borowiec JA. 2000. Formation of a complex between nucleolin and replication protein a after cell stress prevents initiation of DNA replication. *J. Cell Biol.* **149**: 799-809.

Da Rocha AB, Lopes RM and Schwartsmann G. 2001. Natural in anticancer therapy. *Curr. Opin. Pharmacol.* **1:** 364–369.

David-Pfeuty T and Nouvian-Dooghe Y. 2002. Human p14(Arf): an exquisite sensor of morphological changes and of short-lived perturbations in cell cycle and in nucleolar function. *Oncogene* **21**: 6779–6790.

Dephoure N, Zhou C, Villén J, Beausoleil SA, Bakalarski CE, Elledge SJ and Gygi SP. 2008. A quantitative atlas of mitotic phosphorylation. *Proc. Natl. Acad. Sci. USA* **105**: 10762-10767.

Dousset T, Wang C, Verheggen C, Chen D, Hernandez-Verdun D and Huang S. 2000. Initiation of nucleolar assembly is independent of RNA polymerase I transcription. *Mol. Biol. Cell* **11**: 2705-2717.

Dubaele S and Chène P. 2007. Cellular studies of MrDb (DDX18). *Oncol. Res.* **16**: 549-556.

Dundr M and Olson MOJ. 1998. Partially processed pre-rRNA is preserved in association with processing components in nucleolus derived foci during mitosis. *Mol. Biol. Cell* **9**: 2407-2422.

Dundr M, Misteli T and Olson MOJ. 2000. The dynamics of postmitotic reassembly of the nucleolus. *J. Cell Biol.* **150**: 433-446.

Edskes HK, Ohtake Y and Wickner RB. 1998. Mak21p of Saccharomyces cerevisiae, a homolog of human CAATT-binding protein, is essential for 60 S ribosomal subunit biogenesis. *J. Biol. Chem.* **273**: 28912-28120.

Eisenhaber F, Wechselberger C and Kreil G. 2001. The Brix domain protein family, a key to ribosomal biogenesis pathway? *Trends Biochem. Sci.* **26**: 345-347.

Engelbrecht CI, Ljungquist I, Lewn L and Yngner T. 1984. Modulation of 5-fluorouracil metabolism by thymidine. In vivo and in vitro studies on RNA-directed effects in rat liver and hepatoma. *Biochem. Pharmacol.* **33**: 745-750.

Esquela-Kerscher A and Slack FJ. 2006. Oncomirs - microRNAs with a role in cancer. *Nat. Rev. Cancer* **6**: 259-269.

Fang F, Hoskins J and Butler JS. 2004. 5-Fluorouracil enhances exosome-dependent accumulation of polyadenylated rRNAs. *Mol. Cell. Biol*. **24**: 10766-10776.

Feng ZH, Wilson SE, Peng ZY, Schlender KK, Reimann EM and Trumbly RJ. 1991. The yeast GLC7 gene required for glycogen accumulation encodes a type 1 protein phosphatase. *J. Biol. Chem.* **266**: 23796-801.

Fatica A, Cronshaw AD, Dlakic M and Tollervey D. 2002. Ssf1p prevents premature processing of an early pre-60S ribosomal particle*. Mol. Cell* **9**: 341-351.

Fontoura BM, Sorokina EA, David E and Carroll RB. 1992. p53 is covalently linked to 5.8S rRNA. *Mol. Cell. Biol.* **12**: 5145-5151.

Fontoura BM, Atienza CA, Sorokina EA, Morimoto T and Carroll RB. 1997. Cytoplasmic p53 polypeptide is associated with ribosomes. *Mol. Cell. Biol.* **17**: 3146-3154.

Gallagher JE, Dunbar DA, Granneman S, Mitchell BM, Osheim Y, Beyer AL and Baserga SJ. 2004. RNA polymerase I transcription and pre-rRNA processing are linked by specific SSU processome components. *Genes Dev.* **18**: 2506-2517.

Ganguli G and Wasylyk B. 2003. p53-independent functions of MDM2. *Mol. Cancer Res.* **1**: 1027-1035.

Gassmann R, Henzing AJ and Earnshaw WC. 2005. Novel components of human mitotic chromosomes identified by proteomic analysis of the chromosome scaffold fraction. *Chromosoma* **113**: 385–397.

Gautier T, Bergès T, Tollervey D and Hurt E. 1997. Nucleolar KKE/D repeat proteins Nop56p and Nop58p interact with Nop1p and are required for ribosome biogenesis. *Mol. Cell. Biol.* **17**:

7088-7098.

Gautier T, Robert-Nicoud M, Guilly MN and Hernandez-Verdun D. 1992. Relocation of nucleolar proteins around chromosomes at mitosis. A study by confocal laser scanning microscopy. *J. Cell. Sci.* **102**: 729-737.

Gavin AC, Bosche M, Krause R, Grandi P, Marzioch M, Bauer A, Schultz J, Rick JM, Michon AM, ... and Superti-Furga G. 2002. Functional organization of the yeast proteome by systematic analysis of protein complexes. *Nature* **415**: 141-147.

Gentz R, Rauscher FD, Abate C., Curran T and Rauscher FJ. 1989. Parallel association of Fos and Jun leucine zippers juxtaposes DNA binding domains. *Science* **243**: 1695-1699.

Gilkes DM, Chen L and Chen J. 2006. Mdmx regulation of p53 response to ribosomal stress. *EMBO J*. **25**: 5614-5625.

Goldberg Al. 2003. Protein degradation and protection against misfolded or damaged proteins. *Nature*: **426**: 895-899.

Ghoshal K. and Jacob ST. 1994. Specific Inhibition of pre-ribosomal RNA processing in extracts from the lymphosarcoma cells treated with 5-fluorouracil. *Cancer Res.* **54**: 632-636.

Grandori C, Gomez-Roman N, Felton-Edkins ZA, Ngouenet C, Galloway DA, Eisenman RN and White RJ. 2005. c-Myc binds to human ribosomal DNA and stimulates transcription of rRNA genes by RNA polymerase I. *Nat. Cell Biol.* **7**: 311-318.

Granneman S and Baserga SJ. 2005. Crosstalk in gene expression: coupling and co-regulation of rDNA transcription, pre-ribosome assembly and pre-rRNA processing. *Curr. Opin. Cell Biol.* **17**: 281-286.

Greenhalgh DA and Parish JH. 1989. Effects of 5-fluorouracil on cytotoxicity and RNA metabolism in human colonic carcinoma cells. *Cancer Chemother. Pharmacol*. **25**: 37-44.

Greenhalgh DA and Parish JH. 1990. Effects of 5-fluorouracil combination therapy on RNA processing in human colonic carcinoma cells. *Br. J. Cancer* **61**: 415-419.

Grimm T, Hölzel M, Rohrmoser M, Harasim T, Malamoussi A, Gruber-Eber A, Kremmer E and Eick D. 2006. Dominant-negative Pes1 mutants inhibit ribosomal RNA processing and cell proliferation via incorporation into the PeBoW-complex. *Nucleic Acids Res.* **34**: 3030-3043.

Gu W and Roeder RG. 1997. Activation of p53 sequence-specific DNA binding by acetylation of the p53 C-terminal domain. *Cell* **90**: 595-606.

Guo QM, Malek RL, Kim S, Chiao C, He M, Ruffy M, Sanka K, Lee NH, Dang CV and Liu ET. 2000. Identification of c-myc responsive genes using rat cDNA microarray. *Cancer Res.* **60**: 5922–5928.

Gustafson WC, Taylor CW, Valdez BC, Henning D, Phippard A, Ren Y, Busch H and Durban E. 1998. Nucleolar protein p120 contains an arginine-rich domain that binds to ribosomal RNA. *Biochem. J.* **331**: 387-393.

Hadjiolov AA. 1985. The nucleolus and ribosome biogenesis. Cell Biology Monographs. A.M. Beermann, L. Goldstein, K.R. Portrer, and P. Sitte, editors. New York. 1–263.

Haupt Y, Maya R, Kazaz A and Ohren M. 1997. Mdm2 promotes the rapid degradation of p53. *Nature* **387**: 296-299.

Hayano T, Yanagida M, Yamauchi Y, Shinkawa T, Isobe T and Takahashi N. 2003. Proteomic analysis of human Nop56p-associated pre-ribosomal ribonucleoprotein complexes. *J. Biol. Chem.* **278**: 34309-343919.

Henriksson M, Lüscher B. 1996. Proteins of the Myc network: essential regulators of cell growth and differentiation. *Adv. Cancer Res.* **68**: 109-82.

Hernandez-Verdun D. 2006. Nucleolus: from structure to dynamics. *Histochem. Cell Biol.* **125**: 127-137.

Hernandez-Verdun D and Gautier T. 1994. The chromosome periphery during mitosis. *Bioessays* **16**: 179–185.

Hershko A and Ciechanover A. 1998. The ubiquitin system. *Ann. Rev. Biochem.* **67**: 425-479.

Ho Y, Gruhler A, Heilbut A, Bader GD, Moore L, Adams SL, Millar A, Taylor P, Bennett K, ... and Tyers M. 2002. Systematic identification of protein complexes in *Saccharomyces cerevisiae* by mass spectrometry. **Nature 415**: 180-183.

Hölzel M, Rohrmoser M, Schlee M, Grimm T, Harasim T, Malamoussi A, Gruber-Eber A, Kremmer E, Hiddemann W, Bornkamm GW and Eick D. 2005. Mammalian WDR12 is a novel member of the Pes1-Bop1 complex and is required for ribosome biogenesis and cell proliferation. *J. Cell. Biol.* **170**: 367-378.

Hong B, Brockenbrough JS, Wu P and Aris JP. 1997. Nop2p is required for pre-rRNA processing and 60S ribosome subunit synthesis in yeast. *Mol. Cell. Biol.* **17**: 378-388.

Horsey EW, Jakovljevic J, Miles TD, Harnpicharnchai P and Woolford JL Jr. 2004. Role of the yeast Rrp1 protein in the dynamics of pre-ribosome maturation. *RNA* **10**: 813-827.

Hu CD, Chinenov Y and Kerrpola T. 2002. Visualization of interactions among bZIP and Rel family proteins in living cells using bimolecular fluorescence complementation. *Mol. Cell* **9**: 789-798.

Huibregtse JM and Beaudenon S. 1996. Mechanism of HPV E6 proteins in cellular transformation. *Semin. Cancer Biol.* **7**: 317-326.

Iapalucci-Espinoza S and Franze-Fernandez MT. 1979. Effect of protein synthesis inhibitors and low concentrations of actinomycin D on ribosomal RNA synthesis. *FEBS Lett*. **107**: 281-284.

Iida S, Akiyama Y, Nakajima T, Ichikawa W, Nihei Z, Sugihara K and Yusua Y. 2000. Alterations and hypermethylation of the p14(ARF) gene in gastric cancer. *Int. J. Cancer* **87**: 654-658.

Iyer VR, Eisen MB, Ross DT, Schuler G, Moore T, Lee JCF, Trent JM, Staudt LM, Hudson J Jr., Boguski MS, Lashkari D, Shalon D, Botstein D and Brown PO. 1999. The transcriptional program in the response of human fibroblasts to serum. *Science* **283**: 83-86.

Jacobson MR and Pederson T. 1998. Localization of signal recognition particle RNA in the nucleolus of mammalian cells. *Proc. Natl. Acad. Sci. USA* **95**: 7981-7986.

Jin A, Itahana K, O'Keefe K and Zhang Y. 2004. Inhibition of Hdm2 and activation of p53 by ribosomal protein L23. *Mol. Cell. Biol.* **24**: 7669-7680.

Juven-Gershon T, Shifman O, Unger T, Elkeles A, Haupt Y and Oren M. 1998. The Mdm2 oncoprotein interacts with the cell fate regulator Numb. *Mol. Cell. Biol.* **18**: 3974-3982.

Kallstrom G, Hedges J and Johnson A. 2003. The putative GTPases Nog1p and Lsg1p are required for 60S ribosomal subunit biogenesis and are localized to the nucleus and cytoplasm, respectively. *Mol. Cell. Biol.* **23**: 4344-4355.

Kass S, Tyc K, Steitz JA and Sollner-Webb B. 1990. The U3 small nucleolar ribonucleoprotein functions in the first step of preribosomal RNA processing.
Cell **60**: 897-908.

Kim J and Hirsch JP. 1998. A nucleolar protein that affects mating efficiency in *Saccharomyces cerevisiae* by altering the morphological response to pheromone. *Genetics* **149**: 795–805.

Kim OH, Lim JH, Woo KJ, Kim YH, Jin IN, Han ST, Park JW, Kwon TK. 2004. Influence of p53 and p21Waf1 expression on G2/M phase arrest of colorectal carcinoma HCT116 cells to proteasome inhibitors. *Int. J. Oncol.* **24**: 935-41.

Klibanov SA, O'Hagan HM and Ljungman M. 2001. Accumulation of soluble and nucleolar-associated p53 proteins following cellular stress. *J. Cell. Sci*. **114**: 1867-73.

Kopp K, Gasiorowski JZ, Chen D, Gilmore R, Norton JT, Wang C, Leary DJ, Chan EK, Dean DA and Huang S. 2007. Pol I transcription and pre-rRNA processing are coordinated in a transcription-dependent manner in mammalian cells. *Mol. Biol. Cell.* **18:** 394-403.

Krogan NJ, Cagney G, Yu H, Zhong G, Guo X, Ignatchenko A, Li J, Pu S, Datta N, Tikuisis AP,... and Greenblatt JF. 2006. Global landscape of protein complexes in the yeast *Saccharomyces cerevisiae*. *Nature* **440**: 637-643.

Kuai L, Fang F, Butler JS and Sherman F. 2004. Polyadenylation of rRNA in *Saccharomyces cerevisiae*. *Proc. Natl. Acad. USA* **101**: 8581-8586.

Kubbutat MH, Jones SN and Vousden KH. 1997. Regulation of p53 stability by Mdm2. *Nature* **387:** 299-303.

Kurki S, Petronen K, Latonen L, Kiviharju T, Ojala PM, Meek D and Laiho M. 2004. Nucleolar protein NPM interacts with HDM2 and protects tumor suppressor p53 from HDM2 mediated degradation. *Cancer Cell* **5**: 465-475.

Lafontaine DLJ, Preiss T and Tollervey D. 1998. Yeast 18S rRNA dimethylase Dim1p: a quality control mechanism in ribosome biogenesis? *Mol. Cell. Biol.* **18**: 2360-2370.

Lapik YR, Misra JM, Lau LF and Pestov DG. 2007. Restricting conformational flexibility of the switch II region creates a dominant-inhibitory phenotype in Obg GTPase Nog1. *Mol. Cell. Biol.* **27**: 7735-7744.

Leary DJ and Huang S. 2001. Regulation of ribosome biogenesis within the nucleolus. *FEBS Lett.* **509**: 145-150.

Lebreton A, Saveanu C, Decourty K, Rain JC, Jacquier A and Fromont-Racine M. 2006. A functional network involved in the recycling of nucleocytoplasmic pre-60S factors. *J. Cell Biol.* **173**: 349-360.

Leung AK, Gerlich D, Miller G, Lyon C, Lam YW, Lleres D, Daigle N, Zomerdijk J, Ellenberg J and Lamond AI. 2004. Quantitative kinetic analysis of nucleolar breakdown and reassembly during mitosis in live human cells. *J. Cell. Biol.* **166**: 787-800.

Levine AJ. 1997. p53, the cellular gatekeeper for growth and division. *Cell* **88**: 323-331.

Lewis JD and Tollervey D. 2000. Like attracts like: getting RNA processing together in the nucleus. *Science* **288**: 1385–1389.

Li Z, Van Calcar S, Qu C, Cavenee WK, Zhang MQ and Ren B. 2000. A global transcriptional regulatory role for c-Myc in Burkitt's lymphoma cells. *Proc Natl Acad Sci USA* **100**: 8164-9.

Liang XH and Fournier MJ. 2006. The helicase Has1p is required for snoRNA release from pre-rRNA. *Mol. Cell. Biol.* **26**: 7437-7450.

Ljungman M. 2000. Dial 9-1-1 for p53: Mechanisms of p53 activation by cellular stress. *Neoplasia* **2**: 208-225.

Lohrum MA, Ludwig RL, Kubbutat MH, Hanlon M and Vousden KH. 2003. Regulation of HDM2 activity by the ribosomal protein L11. *Cancer Cell* **3:** 577–587.

Ludwig RL, Bates S and Vousden KH. 1996. Differential activation of target cellular promoters by p53 mutants with impaired apoptotic function. *Mol. Cell Biol.* **16**: 4952-4960.

Lum PY, Armour CD, Stepaniants SB, Cavet G, Wolf MK, Butler JS, Hinshaw JC, Garnier P, Prestwich GD, Leonardson A, Garrett-Engele P, Rush CM, Bard M, Schimmack G, Phillips JW, Roberts CJ and Shoemaker DD. 2004. Discovering modes of action for therapeutic compounds using a genome-wide screen of yeast heterozygotes. *Cell* **116**: 121-137.

Malatesta M, Gazzanelli G, Battistelli S, Martin TE, Amalric F and Fakan S. 2000. Nucleoli undergo structural and molecular modifications during hibernation. *Chromosoma* **109**: 506-513.

Marechal V, Elenbaas B, Piette J, Nicolas JC and Levine AJ. 1994. The ribosomal protein L5 is associated with Mdm-2 and Mdm2-p53 complexes. *Mol. Cell. Biol.* **14:** 7414–7420.

Marinkovic D, Marinkovic T, Kokai E, Barth T, Möller P and Wirth T. 2004. Identification of novel Myc target genes with a potential role in lymphomagenesis. *Nucleic Acids Res.* **32**: 5368-5378.

Mayer C and Grummt I. 2005. Cellular stress and nucleolar function. *Cell Cycle* **4**: 1036-1038.

Migeon JC, Garfinkel MS and Edgar BA. 1999. Cloning of *peter pan*, a novel Drosophila gene required for larval growth. *Mol. Biol. Cell* **10**: 1733-1744.

Mühl B. 2007. Wirkung von Chemotherapeutika auf die Ribosomenbiogenese. Diploma thesis. Helmholtz Centre Munich and Ludwig-Maximilians-University Munich (LMU), Germany.

Muratani M and Tansey WP. 2003. How the ubiquitin-proteasome system controls transcription. *Nat. Rev. Mol. Cell. Biol.* **4**: 192-201.

O'Louglin C, Heenan M, Coyle S and Clynes M. 2000. Altered cell cycle response of drug-resistant lung carcinoma cells to doxorubicin. *Eur. J. Cancer* **36**: 1149-1160.

Olson MOJ. 2004. Sensing cellular stress: another new function for the nucleolus? *Science STKE* pe10.

Olson MOJ and Dundr M. 2005. The moving parts of the nucleolus. *Histochem. Cell Biol.* **123**: 203-216.

Olson MOJ, Hingorani K and Szebeni A. 2002. Conventional and non-conventional roles of the nucleolus. *Int. Rev. Cytol.* **219**: 199-266.

Palmero I, Pantoja C and Serrano M. 1998. p19ARF links the tumour suppressor p53 to Ras. *Nature* **395**: 125-126.

Pederson T. 1998. The plurifunctional nucleolus. *Nucleic Acids Res.* **26**: 3871–3876.

Perry RP and Kelley DE. 1970. Inhibition of RNA synthesis by actinomycin D: characteristic dose-response of different RNA species. *J. Cell. Physiol*. **76**: 127-139.

Phair RD and Misteli T. 2000. High mobility of proteins in the mammalian cell nucleus. *Nature* **404**: 604-605.

Ramji DP and Foka P. 2002. CCAAT/enhancer-binding proteins: structure, function and regulation. *Biochem. J.* **365**: 561-575.

Raska I, Shaw PJ and Cmarko D. 2006. New insights into nucleolar architecture and activity. *Int. Rev. Cytol.* **255**: 177-235.

Reeves R and Nissen MS. 1990. The AT-DNA-binding domain of mammalian high mobility group I chromosomal proteins. A novel peptide motif for recognizing DNA structure. *J. Biol. Chem.* **265**: 8573-8582.

Rohrmoser M, Hölzel M, Grimm T, Malamoussi A, Harasim T, Orban M, Pfisterer I, Gruber-Eber A, Kremmer E and Eick D. 2007. Interdependence of Pes1, Bop1, and WDR12 controls nucleolar localization and assembly of the PeBoW complex required for maturation of the 60S ribosomal subunit. *Mol. Cell. Biol.* **27**: 3682-3694.

Roussel P, Andre C, Comai L and Hernandez-Verdun D. 1996. The rDNA transcription machinery is assembled during mitosis in active NORs and absent in inactive NORs. *J. Cell. Biol.* **133**: 235-246.

Rubbi CP and Milner J. 2000. Non-activated p53 co-localizes with sites of transription within both the nucleoplasm and the nucleolus. *Oncogene* **19**: 85-97.

Rubbi CP and Milner J. 2003. Disruption of the nucleolus mediates stabilization of p53 in response to DNA damage and other stresses. *EMBO J*. **22**: 6068-6077.

Sakaguchi K, Herrera JE, Saito S, Miki T, Bustin M, Vassilev A, Anderson CW and Appella E. 1998. DNA damage activates p53 through a phosphorylation-acetylation cascade. *Genes Dev.* **12**: 2831-2841.

Saveanu C, Namane A, Gleizes PE, Lebreton A, Rousselle JC, Noaillac-Depeyre J, Gas N, Jacquier A and Fromont-Racine. 2003. Sequential protein association with nascent 60S ribosomal particles. *Mol. Cell. Biol.* **23**: 4449-4460.

Savino TM, Bastos R, Jansen E and Hernandez-Verdun D. 1999. The nucleolar antigen Nop52, the human homologue of the yeast ribosomal RNA processing RRP1, is recruited at late stages of nucleologenesis. *J. Cell Sci.* **112**: 1889-1900.

Savino TM, Gébrane-Younès J, De Mey J, Sibarita JB and Hernandez-Verdun D. 2001. Nucleolar assembly of the rRNA processing machinery in living cells.
J. Cell. Biol. **153**: 1097-110.

Schilders G, van Dijk E and Pruijn GJM. 2007. C1D and hMtr4p associate with the human exosome subunit PM/Scl-100 and are involved in pre-rRNA processing. *Nucleic Acids Res.*: 1-9.

Schimmang T, Tollervey D, Kern H, Frank R and Hurt EC. 1989. A yeast nucleolar protein related to mammalian fibrillarin is associated with small nucleolar RNA and is essential for viability**.** *EMBO J.* **8**: 4015-24.

Schlosser I, Hölzel M, Murnseer M, Burtscher H, Weidle UH and Eick D. 2003. A role for c-Myc in the regulation of ribosomal RNA processing. *Nucleic Acids Res.* **31**: 6148–6156.

Schuhmacher M, Kohlhuber F, Hölzel M, Kaiser C, Burtscher H, Jarsch M, Bornkamm GW, Laux G, Polack A, Weidle UH and Eick D. 2001. The transcriptional program of a human B cell line in response to Myc. *Nucleic Acids Res.* **29**: 397–406.

Sekiguchi T, Hayano T, Yanagida M, Takahashi N and Nishimoto T. 2006. NOP132 is required for proper nucleolus localization of DEAD-box RNA helicase DDX47. *Nucleic Acid Res*. **34**: 4593-4608.

Sharp DA, Kratowicz SA, Sank MJ and George DL. 1999. Stabilization of the MDM2 oncoprotein by interaction with the structurally related MDMX protein. *J. Biol. Chem.* **274**: 38189-38196.

Shav-Tal Y, Blechman J, Darzacq X, Mantagna C, Dye BT, Patton JG, Singer RH Zipori D. 2005. Dynamic sorting of nuclear components into distinct nucleolar caps during transcriptional inhibition. *Mol. Biol. Cell* **16**: 2395-2413.

Shaw P and Doonan J. 2005. The nucleolus: Playing by different rules? *Cell Cycle* **4**: 102-105.

Sherr CJ. 2004. Principles of tumor suppression. *Cell* **11**: 235-246.

Sherr CJ and Weber JD. 2000. The ARF/p53 pathway. *Curr. Opin. Genet. Dev*. **10**: 94-99.

Shire K, Ceccarelli DF, Avolio-Hunter TM and Frappier L. 1999. EBP2, a human protein that interacts with sequences of the Epstein-Barr virus nuclear antigen 1 important for plasmid maintenance. *J. Virol.* **73**: 2587-95.

Siliciano JD, Canman CE, Taya Y, Sakaguchi K, Appella E and Kastan MB. 1997. DNA damage induces phosphorylation of the amino terminus of p53. *Genes Dev.* **11:** 3471–3481.

Sirri V, Roussel P and Hernandez-Verdun D. 2000. In vivo release of mitotic silencing of ribosomal gene transcription does not give rise to precursor ribosomal RNA processing. *J. Cell. Biol.* **148**: 259-270.

Sirri V, Hernandez-Verdun D and Russel P. 2002. Cyclin-dependent kinases govern formation and maintentance of the nucleolus. *J. Cell Biol.* **156**: 969-981.

Slomovic S, Laufer D, Geiger D and Schuster G. 2006. Polyadenylation of ribosomal RNA in human cells. *Nucleic Acids Res.* **34**. 2966-2975.

Smeenk L, van Heeringen SJ, Koeppel M, van Driel MA, Bartels SJJ, Akkers RC, Denissov S, Stunnenberg HG and Lohrum M. 2008. Characterization of genome-wide p53-binding sites upon stress response. *Nucleic Acids Res*. Advance online Acces May 2008: 1-16.

Stavrera DA, Kawasaki M, Dundr M, Koberna K, Müller WG, Tsujimura-Takahashi T, Komatsu W, Hayano T, Isobe T, Raska I, Misteli T, Takahashi N and McNally JG. 2006. Potential roles for ubiquitin and the proteasome during ribosome biogenesis. *Mol. Cell. Bio*l. **26**: 5131-5145.

Stommel JM and Wahl GM. 2004. Accelerated Mdm2 auto-degradation induced by DNA-damage kinases is required for p53 activation. *EMBO J.* **23**: 1547-1556.

Stommel JM and Wahl GM. 2005. A new twist in the feedback loop: Stress-activated Mdm2 destabilization is required for p53 activation. *Cell Cycle* **4**: 411-417.

Sun XX, Dai MS and Lu H. 2007. 5-Fluorouracil activation of p53 involves an Mdm2-ribosomal protein interaction. *J. Biol. Chem*. **282**: 8052-8059.

Sweet T, Yen W, Khalili K and Amini S. 2008. Evidence for involvement of NFBP in processing of ribosomal RNA. *J. Cell. Physiol.* **214**: 381-388.

Tanimura S, Ohtsuka S, Mitsui K Shirouzu K, Yoshimura A and Ohtsubo M. 1999. MDM2 interacts with MDMX through their RING finger domains. *FEBS Lett.* **447**: 5-9.

Tao W and Levine AJ. 1999. $p19^{ARF}$ stabilizes p53 by blocking nucleocytoplasmic shuttling of Mdm2. *Proc. Natl. Acad. Sci. USA* **96**: 6937-6941.

Tomlinson RL, Ziegler TD, Supakorndej T, Terns RM and Terns MP. 2006. Cell cycle-regulated trafficking of human telomerase to telomeres. *Mol. Biol. Cell* **17**: 955-965.

Tsai RYL and McKay RDG. 2002. A nucleolar mechanism controlling cell proliferation in stem cells and cancer cells. *Gene Dev.* **16**: 2991–3003.

Tsujii R, Miyoshi K, Tsuno A, Matsui Y, Toh-e A, Miyakawa T and Mizuta K. 2000. Ebp2p, yeast homologue of a human protein that interacts with Epstein-Barr virus nuclear antigen 1, is required for pre-rRNA processing and ribosomal subunit assembly. *Genes Cells* **5**: 543-53.

van Eenennaam H, Jarrous N, van Venrooij WJ, Pruijn GJ. 2000. Architecture and function of the human endonucleases RNase P and RNase MRP. *IUBMB Life* **49**: 265-72.

van Hooser AA, Yuh P and Heald R. 2005 The perichromosomal layer. *Chromosoma* **114**: 377-388.

Venema J and Tollervey D. 1996. RRP5 is required for formation of both 18S and 5.8S rRNA in yeast. *EMBO J.* **15**: 5701-5714.

Venema J and Tollervey D. 1999. Ribosome synthesis in *Sacchyromyces cerevisiae*. *Annu. Rev. Genet.* **33**: 261-311.

Visintin R and Amon A. 2000. The nucleolus: the magician's hat for cell cycle tricks. *Curr. Opin. Cell Biol.* **12**: 372-377.

Visintin R, Craig K, Hwang ES, Prinz S, Tyers M and Amon A. 1998. The phosphatase Cdc14 triggers mitotic exit by reversal of Cdk-dependent phosphorylation. *Mol. Cell* **2**: 709-718.

Vlatkovic N, Guerrera S, Li Y, Linn S, Haines DS and Boyd MT. 2000. MDM2 interacts with the C-terminus of the catalytic subunit of DNA polymerase ε. *Nucleic Acids Res.* **28**: 3581-3586.

Vogelstein B, Lane D and Levine AJ. 2000 Surfing the p53 network. *Nature* **408**: 307–310.

Weber JD, Taylor LJ, Roussel MF, Sherr CJ and Bar-Sagi D. 1999. Nucleolar Arf sequesters Mdm2 and activates p53. *Nat. Cell Biol*. **1**: 20-26.

Weber JD, Kuo ML, Bothner B, DiGiammarino EL, Kriwacki RW, Roussel MF, Sherr CJ. 2000. Cooperative signals governing ARF-Mdm2 interaction and nucleolar localization of the complex. *Mol. Cell. Biol.* **20**: 2517–2528.

Wehner KA and Baserga SJ. 2002. The σ70-like motif: A eukaryotic RNA binding domain unique to a superfamily of proteins required for ribosome biogenesis. *Mol. Cell* **9**: 329-339.

Weinstein JN, Myers TG, O'Connor PM, Friend SH, Fornace AJ Jr, Kohn KW, Fojo T, Bates SE, Rubinstein LV, Anderson NL, Buolamwini JK, van Osdol WW, Monks AP, Scudiero DA, Sausville EA, Zaharevitz DW, Bunow B, Viswanadhan VN, Johnson GS, Wittes RE, Paull KD. 1997. An information-intensive approach to the molecular pharmacology of cancer. *Science* **275**: 345-349.

Welch PJ, Marcusson EG, Li QX, Beger C, Krüger M, Zhou C, Leavitt M, Wong-Staal F and Barber JR. 2000. Identification and validation of a gene involved in anchorage-independent cell growth control using a library of randomized hairpin ribozymes. *Genomics* **66**: 274-283.

William-Faltaos S, Rouillard D, Lechat P, Bastian G. 2006. Cell cycle arrest and apoptosis induced by oxaliplatin (L-OHP) on four human cancer cell lines. *Anticancer Res.* **26**: 2093-9.

Wojcik C and DeMartino GN. 2003. Intracellular localization of proteasomes. *Int. J. Biochem. Cell Biol.* **35**: 579-589.

Wu MH and Yung BYM. 2002. UV stimulation of nucleophosmin/B23 expression is an immediate-early gene response induced by damaged DNA. J. Bio. Chem. **277:** *48234-48240*.

Wu MH, Chang JH and Yung BYM. 2002. Resistance to UV-induced cell-killing in nucleophosmin/NMP overexpressed NIH 3T3 fibroblasts: enhancement of DNA repair and up-regulation of PCNA is association with nucleophosmin/B23 overexpression. *Carcinogenesis* **23**: 93-100.

Xiao Z, Chen J, Levine AJ, Modjtahedi N, Xing J, Sellers WR and Livingston DM. 1995. Interaction between the retinoblastoma protein and the oncoprotein MDM2. *Narure* 375: 694-698.

Yang C, Maiguel DA and Carrier F. 2002. Identification of nucleolin and nucleophosmin as genotoxic stress-responsive RNA-binding proteins. *Nucleic Acids Res.* **30**: 2251-2260.

Yoshikawa R, Kusunoki M, Yanagi H, Noda M, Furuyama JI, Yamamura T, Hashimoto-Tamaoki T. 2001. Dual antitumor effects of 5-fluorouracil on the cell cycle in colorectal carcinoma cells: a novel target mechanism concept for pharmacokinetic modulating chemotherapy. *Cancer Res.* **61**: 1029-37.

Yu Y and Hirsch JP. 1995. An essential gene pair in Saccharomyces cerevisiae with a potential role in mating. *DNA Cell Biol.* **14**: 411-418.

Zhai W and Comai L. 2000. Repression of RNA polymerase I transcription by the tumor suppressor p53. *Mol. Cell. Biol*. **20**; 5930-5938.

Zhang B, Pan X, Cobb GP and Anderson TA. 2007. MicroRNAs as oncogenes and tumor suppressors. *Dev. Biol.* **302**: 1-12.

Zhang Y, White Wolf G, Bhat K, Jin A, Allio T, Burrkhart WA and Xiong Y. 2003. Ribosomal protein L11 negatively regulates oncoprotein MDM2 and mediates a p53-dependent ribosomal-stress checkpoint pathway. *Mol. Cell. Biol*. **23**: 8902-8912.

Zhao R, Gish K, Murphy M, Yin Y, Notterman D, Hoffman WH, Tom E, Mack DH and Levine AJ. 2000. Analysis of p53-regulated gene expression patterns using oligonucleotide arrays. *Genes Dev.* **14**: 981-993.

6. Appendix

A. Supplementary material

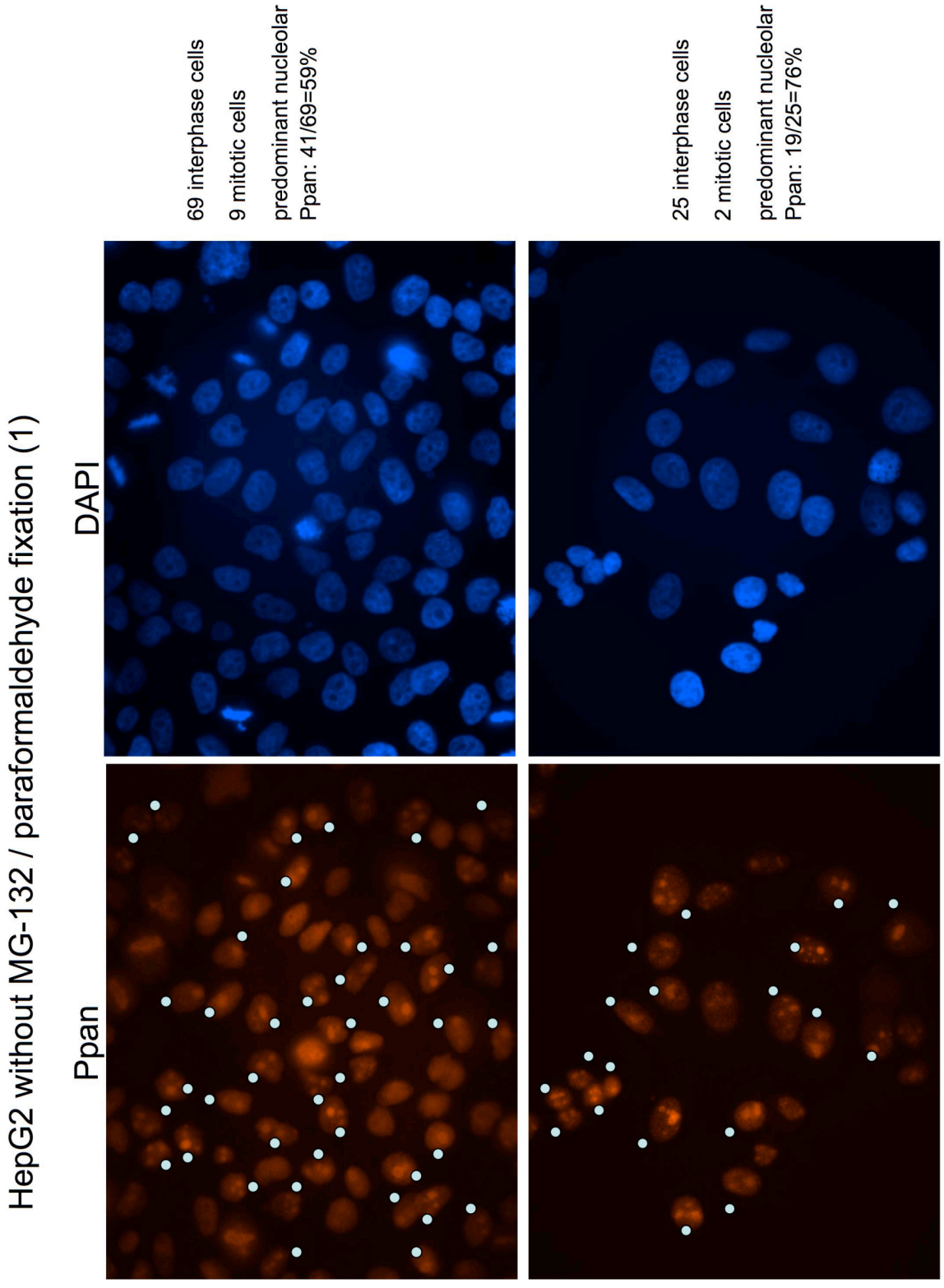

HepG2 without MG-132 / paraformaldehyde fixation (2)

Ppan DAPI

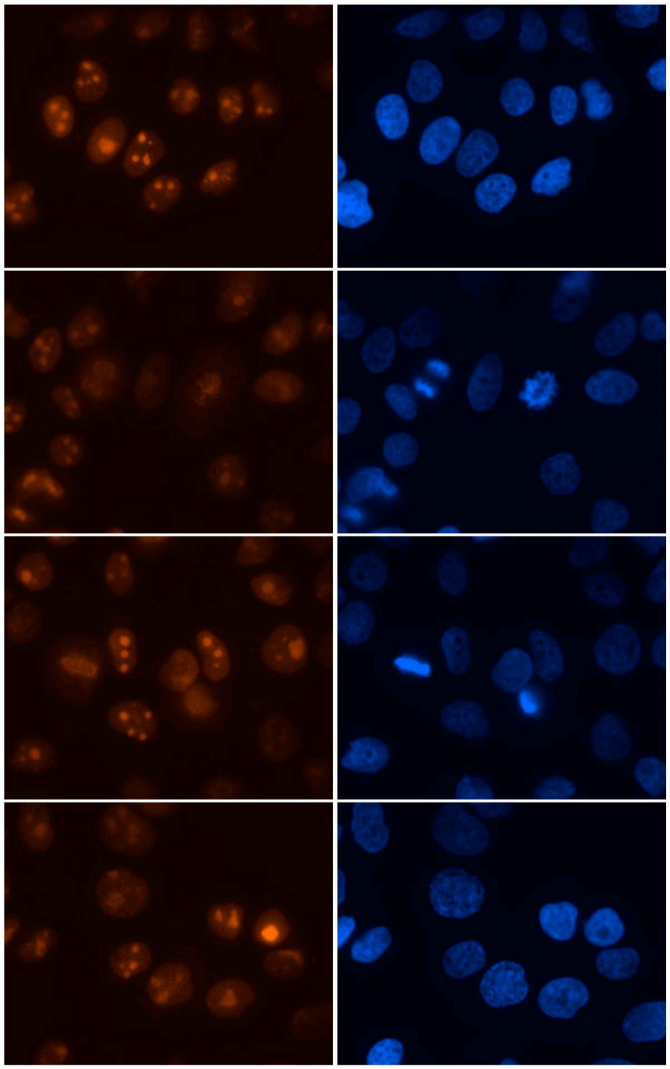

14 interphase cells

0 mitotic cells

predominant nucleolar Ppan: 14/14=100%

11 interphase cells

4 mitotic cells

predominant nucleolar Ppan: 8/11=72%

12 interphase cells

2 mitotic cells

predominant nucleolar Ppan: 8/12=67%

9 interphase cells

1 mitotic cells

predominant nucleolar Ppan: 8/9=89%

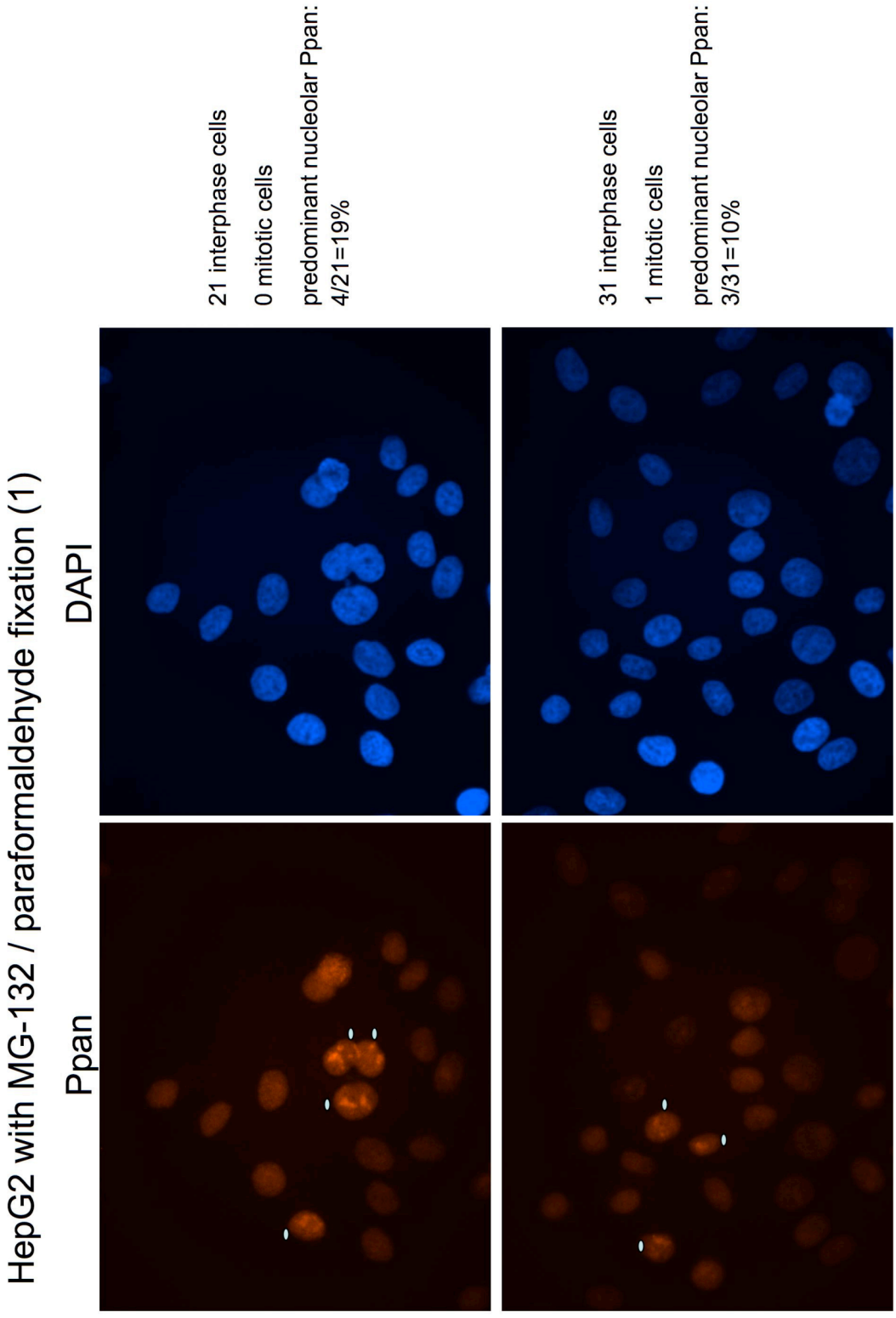
HepG2 with MG-132 / paraformaldehyde fixation (1)
Ppan
DAPI
21 interphase cells
0 mitotic cells
predominant nucleolar Ppan:
4/21=19%
31 interphase cells
1 mitotic cells
predominant nucleolar Ppan:
3/31=10%

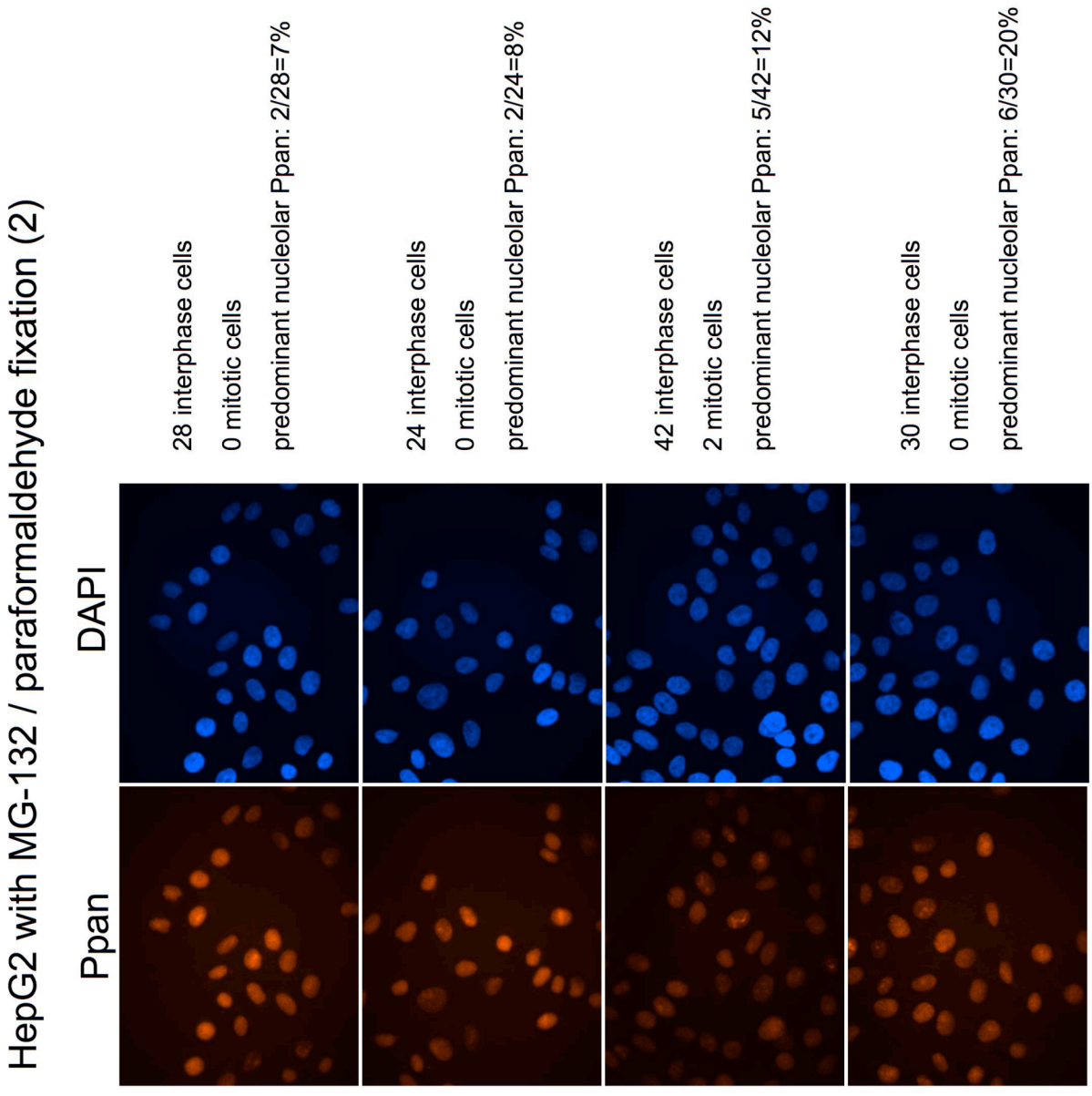
HepG2 with MG-132 / paraformaldehyde fixation (2)
Ppan
DAPI
28 interphase cells
0 mitotic cells
predominant nucleolar Ppan: 2/28=7%
24 interphase cells
0 mitotic cells
predominant nucleolar Ppan: 2/24=8%
42 interphase cells
2 mitotic cells
predominant nucleolar Ppan: 5/42=12%
30 interphase cells
0 mitotic cells
predominant nucleolar Ppan: 6/30=20%

HepG2 with MG-132 / paraformaldehyde fixation (3)

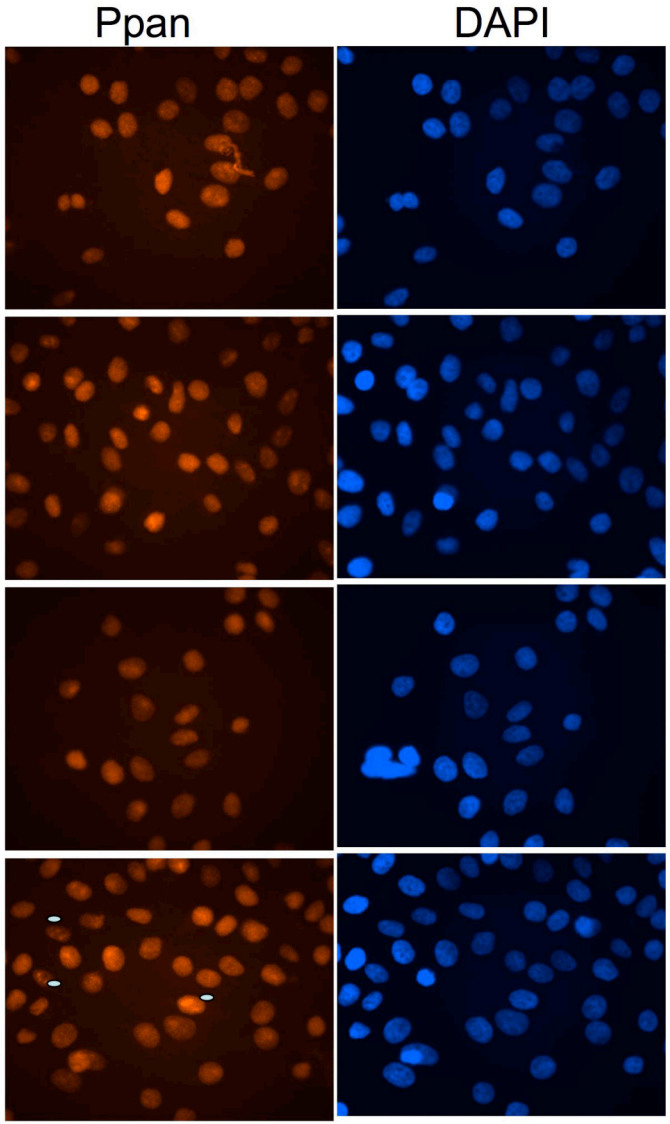

21 interphase cells

2 mitotic cells

predominant nucleolar Ppan: 1/21=5%

38 interphase cells

4 mitotic cells

predominant nucleolar Ppan: 5/38=13%

17 interphase cells

1 mitotic cells

predominant nucleolar Ppan: 2/17=12%

51 interphase cells

2 mitotic cells

predominant nucleolar Ppan: 3/51=6%

SUMMARY
HepG2 without and with MG-132 / paraformaldehyde fixation

without MG-132			with MG-132	
	out of			out of
41	69		4	21
8	12		3	51
8	9		2	24
14	14		2	28
8	11		3	31
19	25		5	42
			6	30
Sum: 98	140		1	21
In %	77 %		5	38
standard deviation	15 %		2	17
			Sum: 33	303
			In %	11 %
			standard deviation	5 %

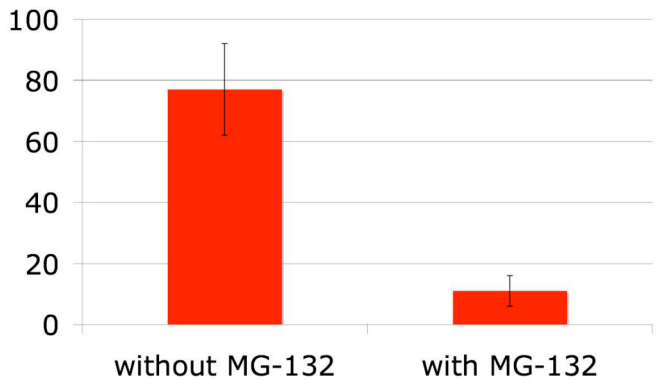

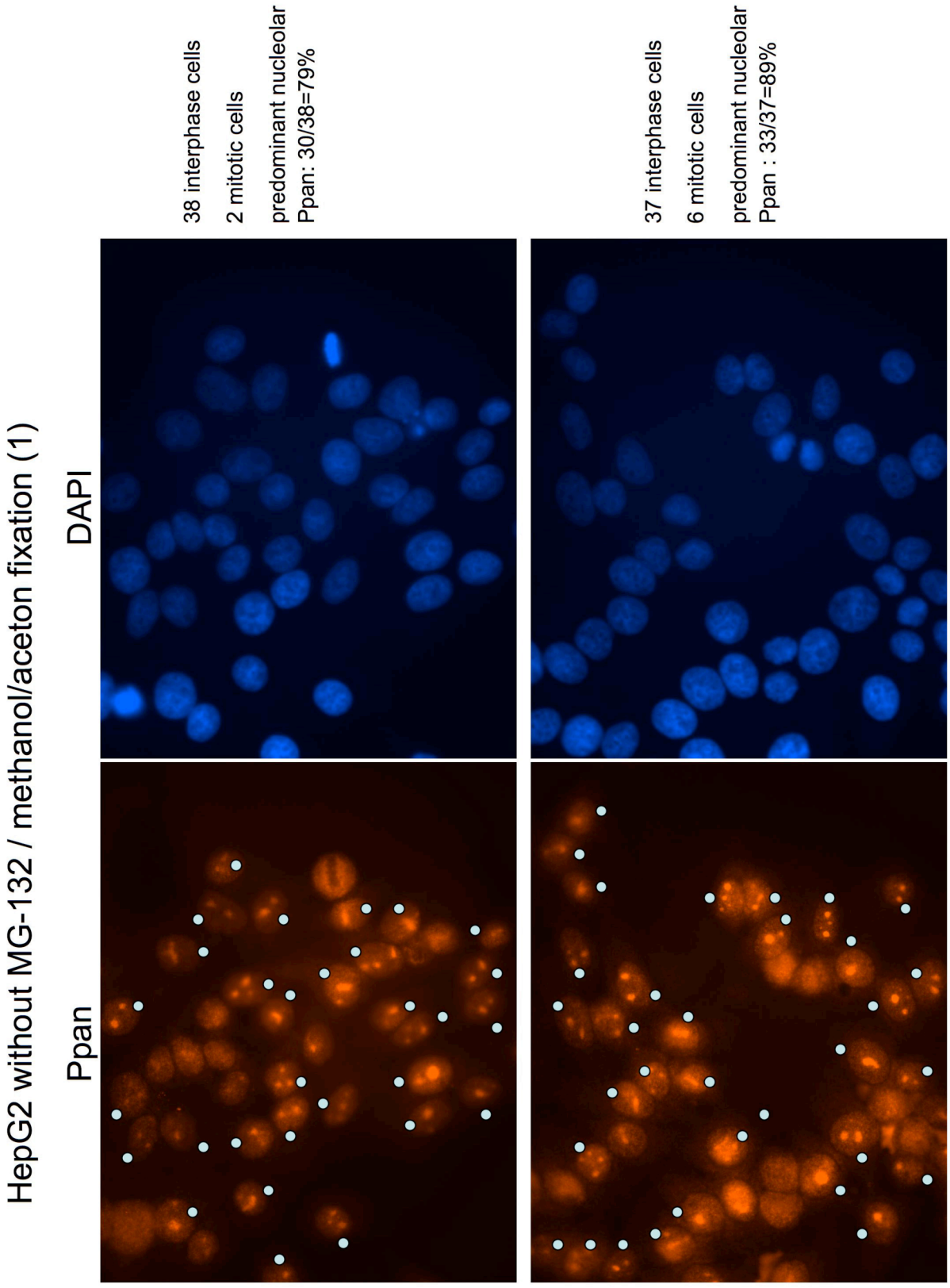
HepG2 without MG-132 / methanol/aceton fixation (1)
Ppan
DAPI
38 interphase cells
2 mitotic cells
predominant nucleolar
Ppan: 30/38=79%
37 interphase cells
6 mitotic cells
predominant nucleolar
Ppan : 33/37=89%

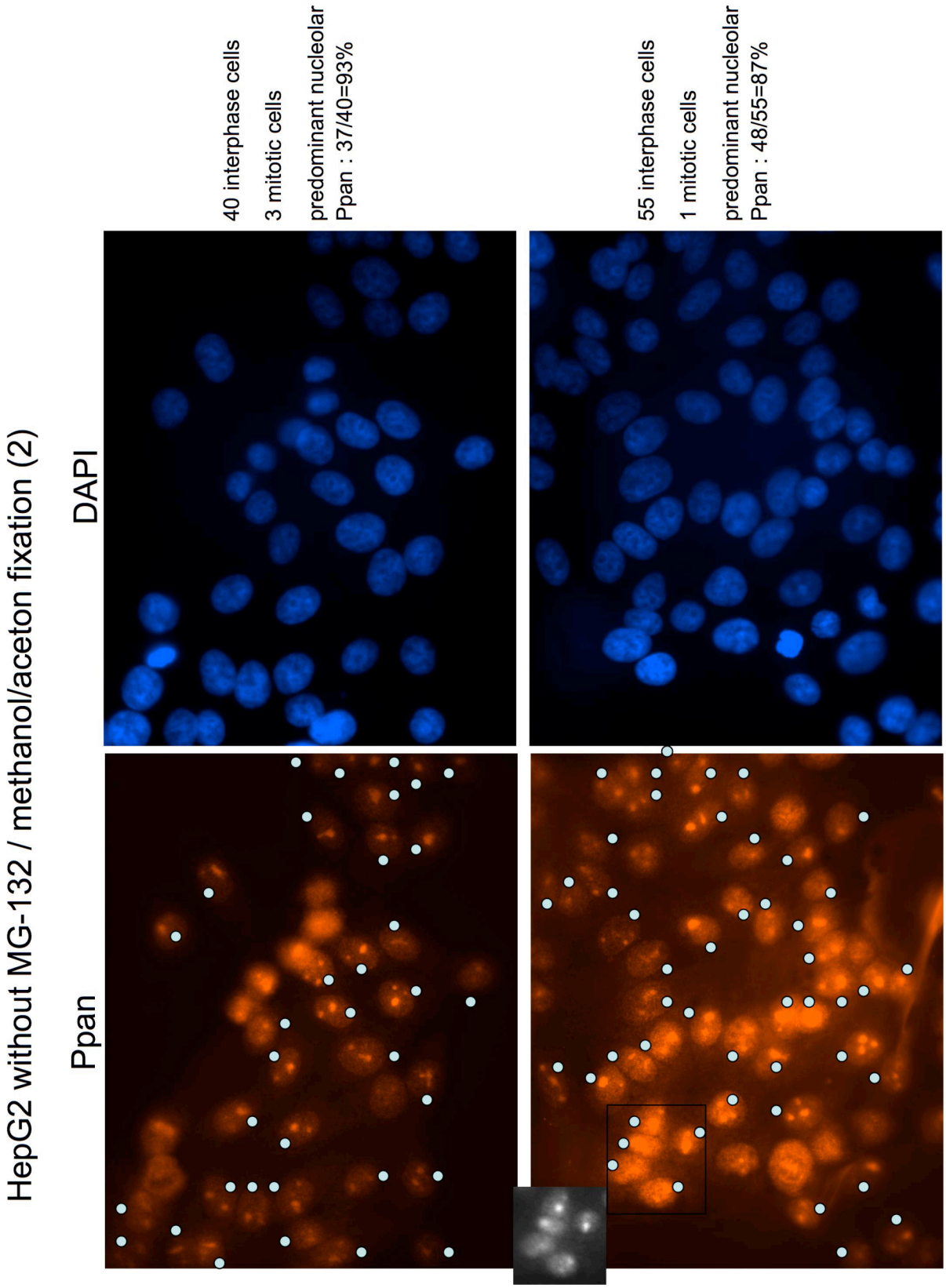
HepG2 without MG-132 / methanol/aceton fixation (2)
Ppan
DAPI
40 interphase cells
3 mitotic cells
predominant nucleolar
Ppan : 37/40=93%
55 interphase cells
1 mitotic cells
predominant nucleolar
Ppan : 48/55=87%

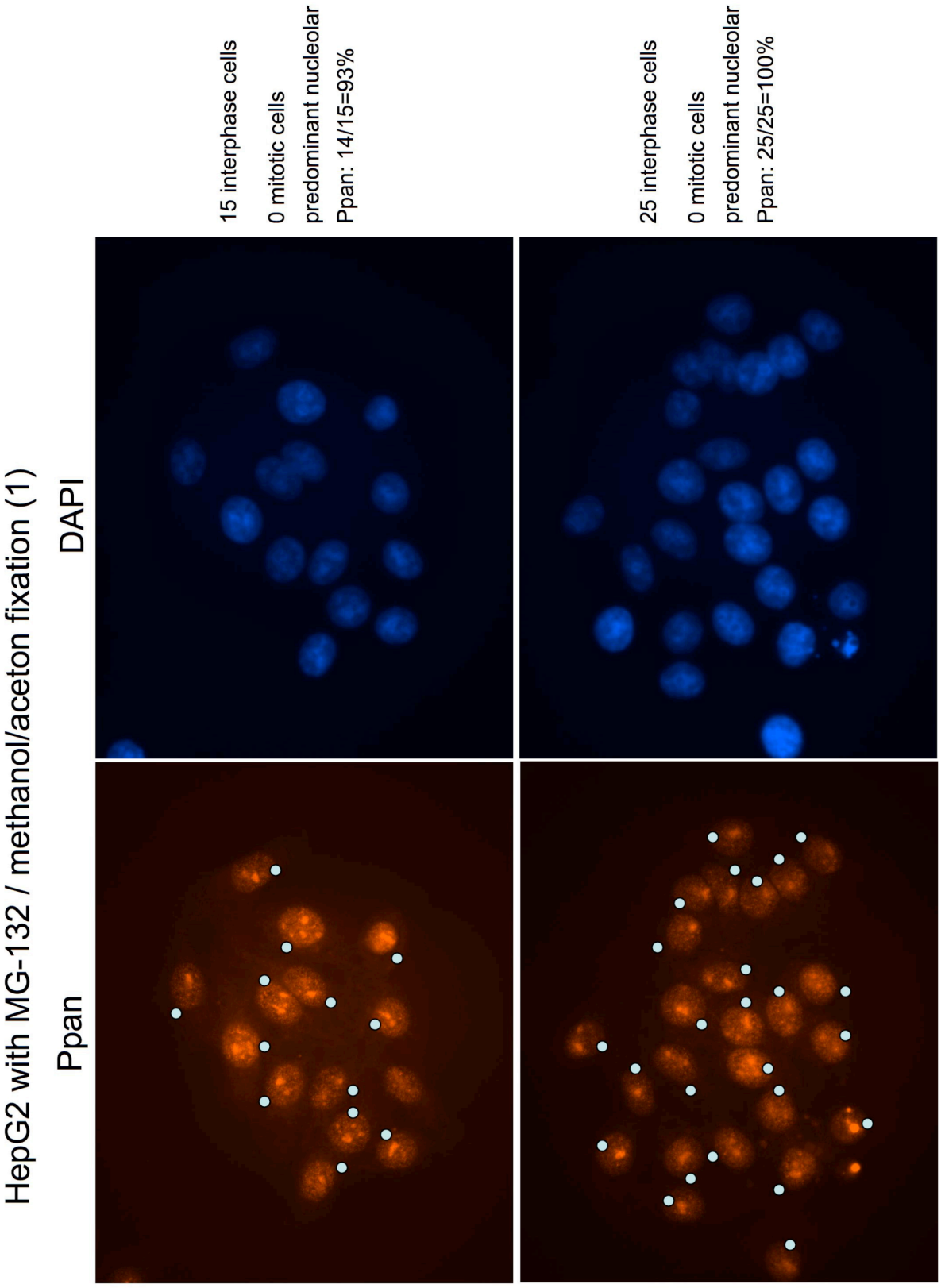
HepG2 with MG-132 / methanol/aceton fixation (1)
Ppan
DAPI
15 interphase cells
0 mitotic cells
predominant nucleolar
Ppan: 14/15=93%
25 interphase cells
0 mitotic cells
predominant nucleolar
Ppan: 25/25=100%

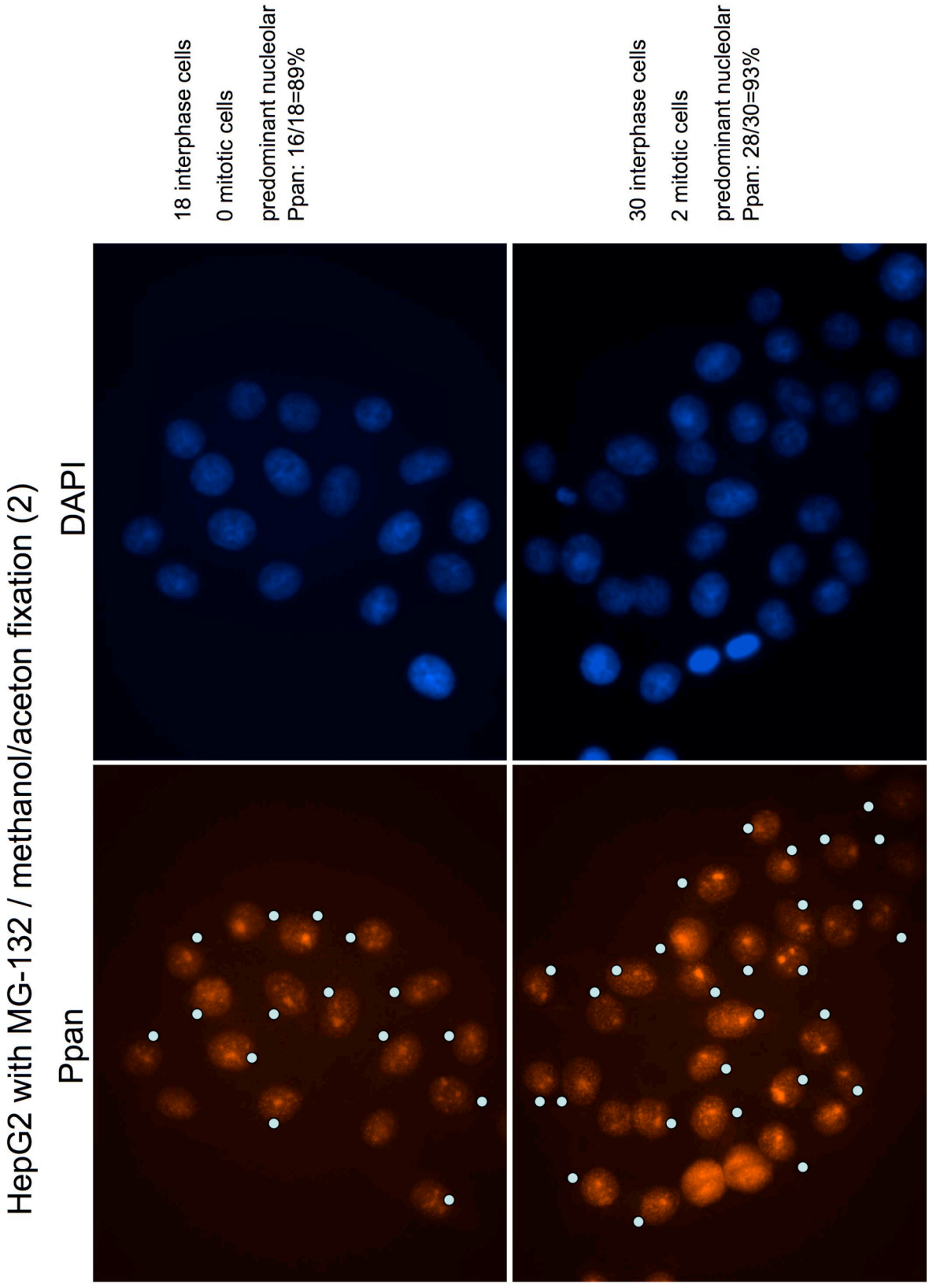
HepG2 with MG-132 / methanol/aceton fixation (2)
Ppan
DAPI
18 interphase cells
0 mitotic cells
predominant nucleolar
Ppan: 16/18=89%
30 interphase cells
2 mitotic cells
predominant nucleolar
Ppan: 28/30=93%

HepG2 with MG-132 / methanol/aceton fixation (3)

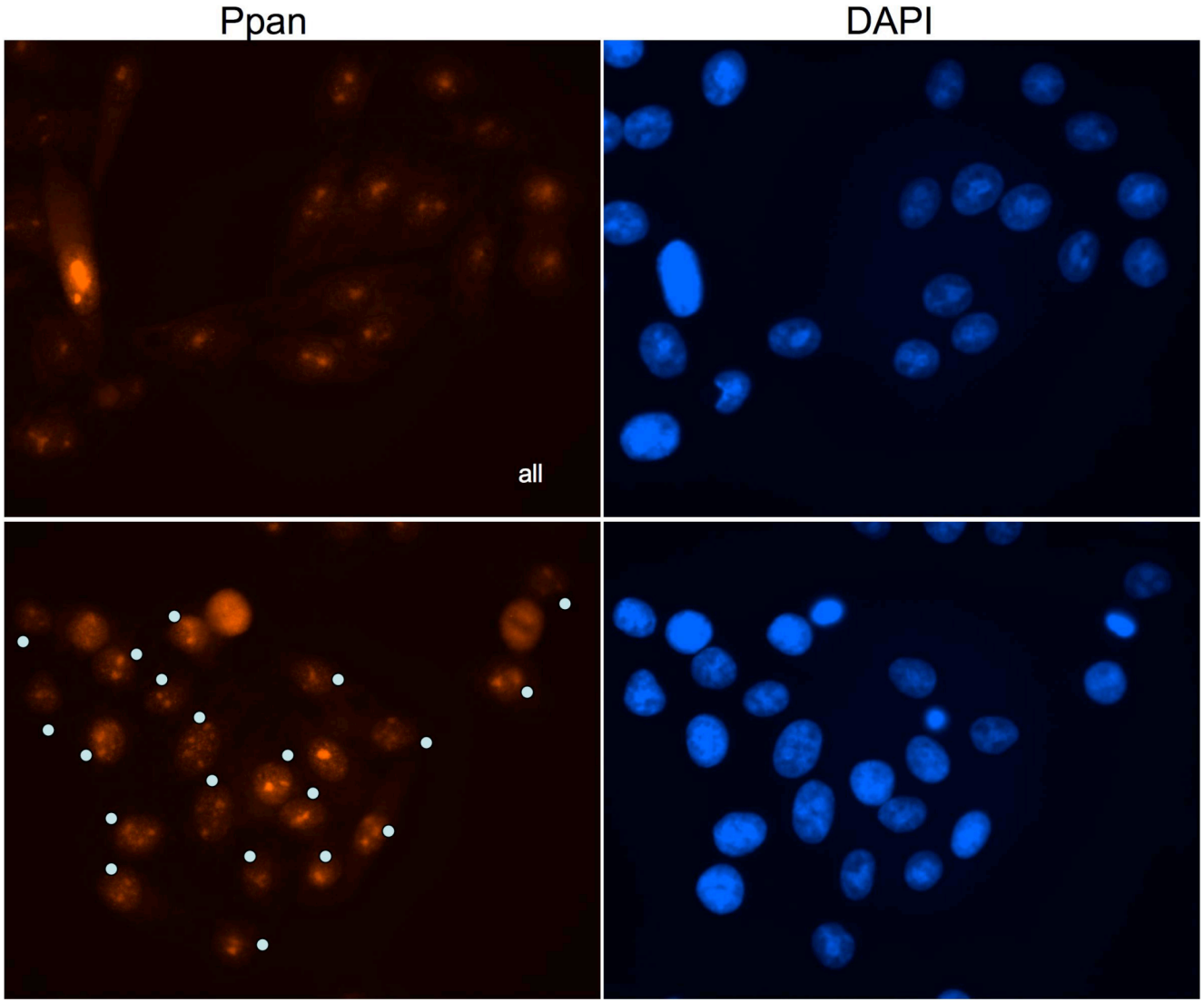

19 interphase cells

0 mitotic cells

predominant nucleolar
Ppan: 19/19=100%

22 interphase cells

2 mitotic cells

predominant nucleolar
Ppan: 21/22=95%

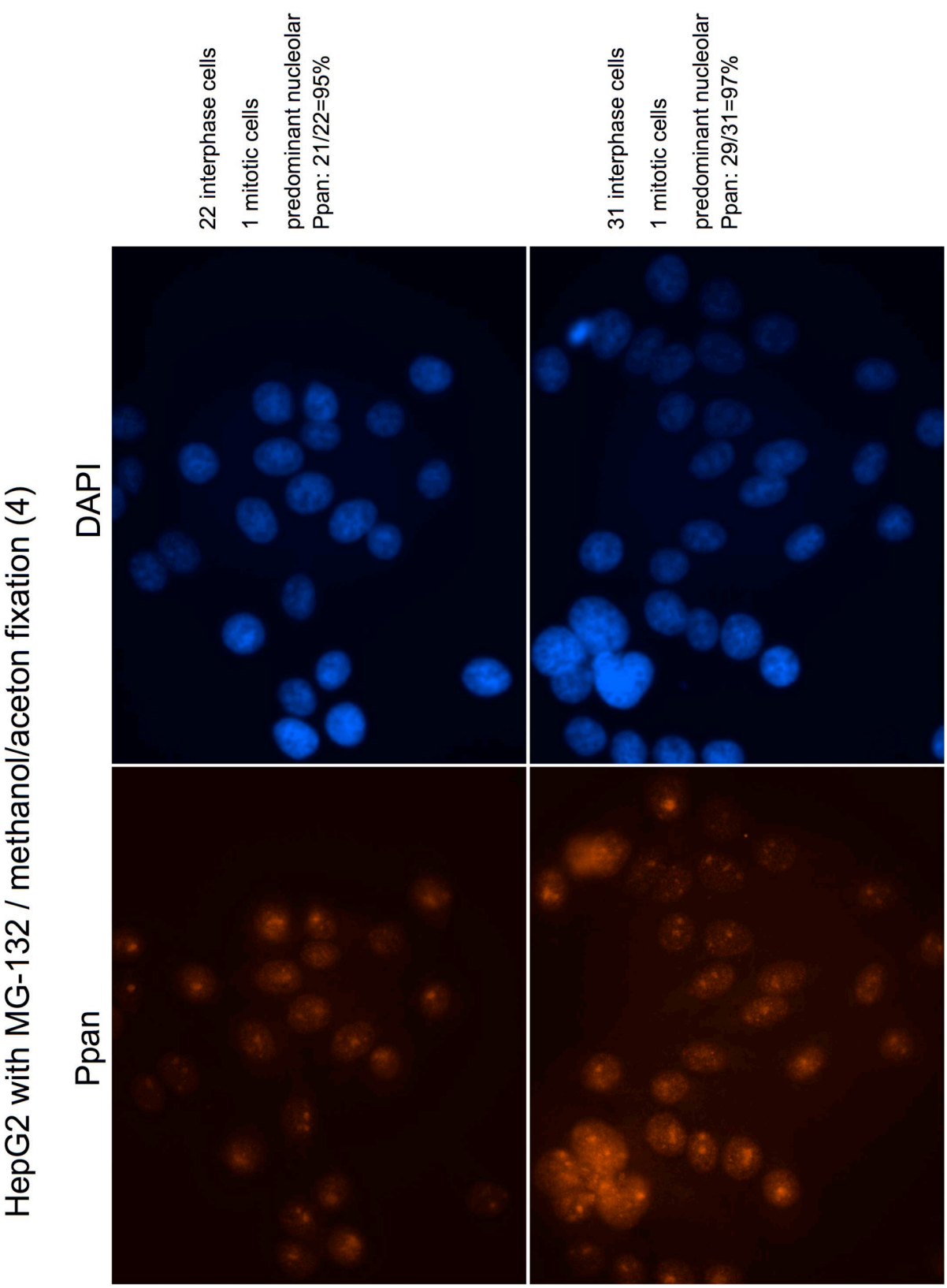
HepG2 with MG-132 / methanol/aceton fixation (4)
DAPI
Ppan
22 interphase cells
1 mitotic cells
predominant nucleolar
Ppan: 21/22=95%
31 interphase cells
1 mitotic cells
predominant nucleolar
Ppan: 29/31=97%

HepG2 with MG-132 / methanol/aceton fixation (5)

Ppan

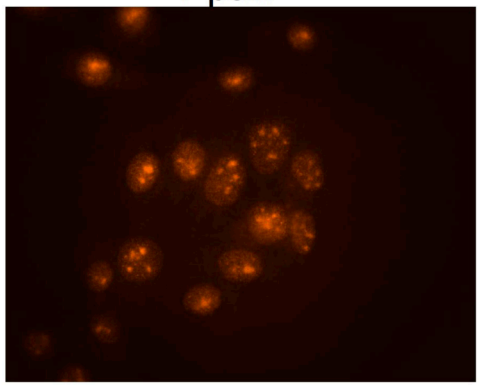

DAPI

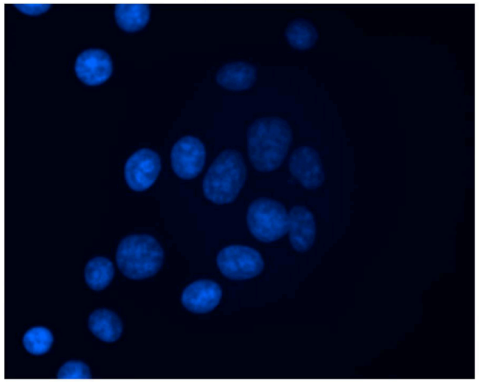

17 interphase cells

0 mitotic cells

predominant nucleolar Ppan: 17/17=100%

SUMMARY
HepG2 without and with MG-132 / methanol/aceton fixation

without MG-132			with MG-132	
	out of			out of
31	38		17	17
37	40		29	31
33	37		21	22
48	55		19	19
Sum: 149	170		21	22
In %	88 %		16	18
standard deviation	5 %		28	30
			14	15
			25	25
			Sum: 190	199
			In %	96 %
			standard deviation	4 %

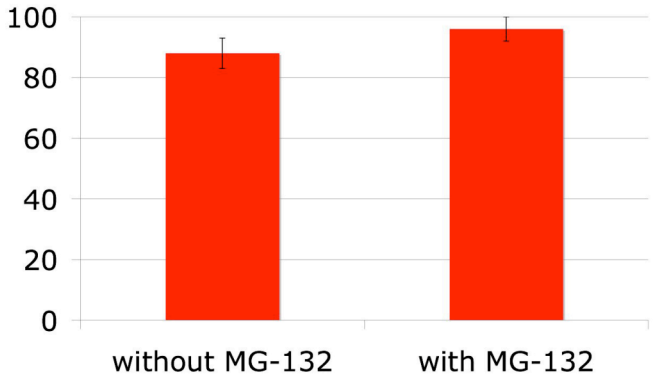

B. Curriculum vitae

Personal Data

Name:	Anastassia Malamoussi
	married, one child (5 years old)
Date of birth:	18.09.1978
Place of birth:	Munich, Germany

School education

1984-1996	Greek Private Primary School, Gymnasium and Lyceum, Munich

Academic education

1997-2003	Studies of biology at the Ludwig-Maximilians-University (LMU) in Munich, Germany
2001-2002	Diploma thesis at the Institute of Microbiology (Prof. Dr. A. Böck) at the LMU, Munich, Germany Topic: „Amino acid specificity of the translation factor SelB" (german)
2004-2008	Doctoral thesis at the Helmholtz Centre in Munich, at the Institute of Clinical Molecular Biology and Tumor Genetics (Prof. Dr. D. Eick) Topic: „Ppan, a new link between ribosome biogenesis and the cell cycle control"

C. Publications

Malamoussi A, Mühl B, Rohrmoser M, Harasim T, Orban M, Burger K, Gruber-Eber A, Hölzel M, Kremmer E, Eick D. (2008). Ppan, a new link between ribosome biogenesis and cell cycle control. In preparation.

Rohrmoser M, Hölzel M, Grimm T, Malamoussi A, Harasim T, Orban M, Pfisterer I, Gruber-Eber A, Kremmer E, Eick D. 2007. Interdependence of Pes1, Bop1 and WDR12 controls nucleolar localization and assembly of the PeBoW complex required for maturation of the 60S ribosomal subunit. *Mol Cell Biol*. **27**: 3682-94.

Hölzel M, Grimm T, Rohrmoser M, Malamoussi A, Harasim T, Gruber-Eber A, Kremmer E, Eick D. 2007. The BRCT domain of mammalian Pes1 is crucial for nucleolar localization and rRNA processing. *Nucleic Acids Res.* **35**: 789-800.

Hölzel M, Rohrmoser M, Orban M, Hömig C, Harasim T, Malamoussi A, Gruber-Eber A, Heissmeyer V, Bornkamm G, Eick D. 2007. Rapid conditional knock-down-knock-in system for mammalian cells. *Nucleic Acids Res.* **35**: e17.

Grimm T, Hölzel M, Rohrmoser M, Harasim T, Malamoussi A, Gruber-Eber A, Kremmer E, Eick D. 2006. Dominant-negative Pes1 mutants inhibit ribosomal RNA processing and cell proliferation via incorporation into the PeBoW-complex. *Nucleic Acids Res.* **34**: 3030-43.

Bornkamm GW, Berens C, Kuklik-Roos C, Bechet JM, Laux G, Bachl J, Korndoerfer M, Schlee M, Hölzel M, Malamoussi A, Chapman RD, Nimmerjahn F, Mautner J, Hillen W, Bujard H, Feuillard J. 2005. Stringent doxycycline-dependent control of gene activities using an episomal one-vector system. *Nucleic Acids Res.* **33**: e137.

Hölzel M, Rohrmoser M, Schlee M, Grimm T, Harasim T, Malamoussi A, Gruber-Eber A, Kremmer E, Hiddemann W, Bornkamm GW, Eick D. 2005. Mammalian WDR12 is a novel member of the Pes1-Bop1 complex and is required for ribosome biogenesis and cell proliferation. *J Cell Biol.* **170**: 367-78.

D. Oral presentations

Presentation

Peter Pan: a new link between ribosome biosynthesis and cell cycle
„RNA Pol I transcription 2007“, Regensburg, Germany

Poster

Malamoussi A, Mühl B, Rohrmoser M, Harasim T, Orban M, Hölzel M, Burger K, Gruber-Eber A, Kremmer E and Eick D. Peter Pan: a new link between ribosome biosynthesis and cell cycle.
„RNA Pol I transcription 2007“, Regensburg, Germany

Malamoussi A, Hölzel M, Rohrmoser M, Grimm T, Harasim T, Gruber-Eber A, Orban M, Kremmer E and Eick D. Mammalian Peter Pan is required for ribosome biogenesis and cell proliferation.
„Ribosome Synthesis 2006“, Warrenton / Virginia, USA

Rohrmoser M, Malamoussi A, Hölzel M, Grimm T, Harasim T, Gruber-Eber A, Schlee M, Kremmer E, Hiddemann W, Bornkamm GW and Eick D. Role of nucleolar Myc-target genes in cell cycle and growth control.
„EMBO/FEBS Conference on Nuclear Structure and Dynamics 2005”, La Grande Motte, France

E. Acknowledgements

In this section I would like to thank all the people who were involved in the successful completion of this thesis:

Prof. Dr. Dirk Eick for the great opportunity to develop a Ph.D. thesis under his supervision and to work on this interesting project, as well as for his permanent support and help during the entire Ph.D. project.

Dr. Elisabeth Kremmer and Andrew Flatley for the generation of the monoclonal antibody, without which some experiments would not have been possible.

The microscope expert **Manuel Deutsch** for the excellent introduction of the confocal microscope.

Dr. Tom Kerppola and Dr. Andreas Thomae for providing the BiFC plasmids and introduction to the method.

Dr. Inge Röckelein for proofreading of the thesis.

My colleagues, Dr. Michaela Rohrmoser, Corinna Hintermair, Anita Gruber-Eber, Thomas Harasim, Martin Heidemann, Mathias Orban, Bastian Mühl, Kaspar Burger, Roland Schüller and Markus Kellner and the former colleagues Dr. Michael Hölzel, Dr. Rob Chapman, Dr. Thomas Grimm and Dr. Martin Schlee for fruitful discussions, the great atmosphere and team work in the laboratory and tasty coffee and cakes.

My **friends** and **family** indirectly contributed to this thesis by showing their interest and understanding.

A special thanks to my **parents** and **parents-in-law** for their unlimited dedication, love and support and taking care of Vassilia.

My husband **Grigorios** for his love, support and his company.

My wonderful daughter **Vassilia**, who often missed me during the last years.